

**Resveratrol slows cell growth by targeting the Warburg effect and stimulating
mitochondria metabolism**

João Fonseca, MSc

Biotechnology

Submitted in partial fulfillment
of the requirements for the degree of

Doctor of Philosophy

Faculty of Mathematics and Science, Brock University

St. Catharines, Ontario

© 2019

Abstract

Resveratrol (RES) is a plant-derived polyphenol that has been widely studied due to its health promoting effects, which are associated with RES ability to positively impact mitochondria function. Here, I investigated the interaction between RES's effects on growth and metabolism in PC3 prostate cancer cells and demonstrated that RES-mediated growth inhibition is coincidental with an increase in mitochondrial network fusion, biogenesis and cellular respiration. This indicates that a metabolic reprogramming towards oxidative phosphorylation might be essential for RES antiproliferative effects. Indeed, when RES-induced metabolic reprogramming was prevented either by growing cells in galactose or stabilizing hypoxia inducible factor-1 α (HIF-1 α) expression, RES effects on growth and metabolism were attenuated or even abolished. Furthermore, consistent with RES ability to reduce HIF-1 α levels, I observed that RES's cell growth inhibitory effects were enhanced under hypoxia. This denotes the importance of conducting *in vitro* studies under conditions that better represent the physiological environment. However, , most *in vitro* studies are performed at supraphysiological levels of oxygen (O₂) (18% O₂; compared to the usual 1-5% O₂ range observed *in vivo*) and glucose (25mM, which is close to five-times higher than normal plasma (glucose) in a healthy human). This artificial environment can affect a wide variety of cellular activities that may compromise *in vitro* studies' reliability. It is therefore important to determine how cell culture conditions might affect RES *in vitro* effects. This was achieved by growing PC3 human prostate cancer and C2C12 mouse myoblasts cells under different culture conditions: physiological O₂ (here considered 5% O₂) and glucose levels (5mM); physiological O₂ and high glucose (25mM); supraphysiological O₂ (18% O₂) and high glucose (25mM). Overall, RES effects on cell proliferation and mitochondrial network were less effective when cells were grown at 5% O₂ and 5mM glucose (media condition that best resembles the

physiological environment). In conclusion, these findings demonstrate the importance of oxygen and glucose levels as key determinants of RES *in vitro* antiproliferative effects, which may contribute to the discrepancy observed for resveratrol's effects both *in vivo* and *in vitro*.

Acknowledgments

This work would not have been possible without the support of several individuals to whom I have a great feel of gratitude.

First and foremost, I am extremely thankful to Doctor Jeff Stuart for giving me the opportunity to pursue my PhD studies in his laboratory. I will always be grateful for his support and insight, as well as his continuous guidance through my entire PhD studies, which turned my journey less turbulent and painful.

I am very thankful to my supervisory committee members, Doctor Glenn Tattersall and Doctor Jeffrey Atkinson. Their insightful critiques were of extreme importance to better develop my PhD research.

I am also grateful to my friends and colleagues at Stuart's lab. A special thanks to Lucas Maddalena and Max Merilovich for their companionship and support during my initial adaptation to the lab, Brock community and, in a more broadly sense, to Canada. I always be grateful for our shared moments inside and outside the lab. I also would like to thank Fereshteh Moradi, Mohamed Rezk, Holt Messner, Andrew Valente, Shehab Selim and Bruna Ferreira-Tollstadius for their unconditional support and help during my PhD journey. I also would like to thank Val Fajardo for his expertise and mentorship during my final stages of my PhD studies.

I would like to extend my warmest thanks to friends and colleagues at the biological and chemistry departments, which contributed to my life's enrichment of outside of the lab. I have a huge gratitude for Paulo Cazares, Min Pyo, Mikel Ghelfi, Nicholas Vesprini, Mark Lukewich, Kiel Ormerod and Deron Britt. I will always remember with great fondness our soccer games. Most

importantly, during these past years, our shared moments and stories were of extreme importance to my personal growth.

Finally, this journey would not be possible without the help, care and love of my family. You are the reason why I always try to give my best and never give up on my life goals. Above all, I am extremely grateful to my wife Marina Marcolin. I will always remember the day that we met as the most important day in my life. I am thankful for your wisdom, enthusiasm and constant support. This journey would not be complete without your presence.

Table of contents

Abstract.....	ii
Acknowledgments.....	iv
List of figures.....	ix
List of tables.....	xii
List of abbreviations	xiii
Chapter 1 – Literature review	1
1.1 General overview.....	1
1.2 Resveratrol.....	2
1.3 <i>In vivo and in vitro</i> targets of resveratrol.....	3
1.3.1 Mitochondria.....	5
1.3.1.1 Mitochondrial biogenesis.....	5
1.3.1.2 Mitophagy.....	6
1.3.1.3 Mitochondrial morphology.....	8
1.3.1.3.1 Mitochondrial Network Analysis.....	10
1.3.1.4 Mitochondrial reactive oxygen species.....	12
1.3.1.5 Mitochondrial antioxidant defense systems.....	13
1.3.2 Warburg effect.....	16
1.3.3 Hypoxia inducible factor.....	18
1.3.3.1 Cell metabolic regulation by HIF-1.....	20
1.3.3.2 PHD downstream targets.....	21
1.3.4 NADPH oxidases.....	22
1.4 Redox signaling.....	24
1.4.1 Hydrogen peroxide.....	24
1.4.1.1 Cysteine.....	25
1.4.1.2 Transitional metal centers.....	26
1.4.2 Hydrogen peroxide detection.....	27
1.5 Cell culture.....	31
1.5.1 Background.....	31
1.5.2 Influence of O ₂ levels in cell culture.....	33
1.5.3 Influence of glucose levels in cell culture.....	37
1.5.4 Caveats of resveratrol's <i>in vitro</i> studies.....	38

1.6	<i>In vitro</i> manipulation of cellular energy metabolism	39
1.7	Study aims and general hypothesis	40
Chapter 2. Resveratrol stimulates a shift toward oxidative metabolism that underlies the growth its growth inhibition effects on PC3 prostate cancer cells		43
	Hypothesis	43
	Objectives	43
	Publication of results	43
	Contributions	43
2.1	Introduction	44
2.2	Material and Methods	45
2.2.1	Materials	45
2.2.2	Cell lines and culture conditions	47
2.2.3	Hypoxia conditions	47
2.2.4	Preparation of whole cell lysates	48
2.2.5	Preparation of nuclear lysates	48
2.2.6	Lactate Dehydrogenase activity	49
2.2.7	Western blots	49
2.2.8	Glucose oxidase activity	50
2.2.9	Plasmid DNA transfections	51
2.2.10	Fluorescence microscopy and image analysis	51
2.2.11	Cell cycle analysis	52
2.2.12	Cellular respiration measurements	53
2.2.13	Statistics	53
2.3	Experimental design	54
2.4	<i>In vitro</i> models	55
2.5	Results	56
2.6	Discussion	67
Chapter 3. Oxygen and glucose levels in cell culture media determine resveratrol's effects on growth, hydrogen peroxide production, and mitochondria dynamics		71
	Hypothesis	71
	Objectives	71
	Publication of results	72
	Contributions	72
3.1	Introduction	73

3.2	Experimental Procedures	75
3.2.1	Materials	75
3.2.2	Cell Lines and Culture Conditions	76
3.2.3	Cell Cycle Analysis.....	77
3.2.4	Hydrogen Peroxide Efflux Determination	77
3.2.5	Stable C2C12 and PC3 Emerald Fluorescent Protein-Labelled Mitochondria	78
3.2.6	Fluorescence Microscopy	79
3.2.7	Quantitative Analysis of Mitochondrial Morphology.....	80
3.2.8	Statistics	80
3.3	Experimental design	81
3.4	<i>In vitro</i> models	82
3.5	Results.....	82
3.6	Discussion.....	93
Chapter 4 General Discussion and Conclusions		96
4.1	Cancer therapy	96
4.2	Mitochondria as a resveratrol target	98
4.3	Cell culture caveats.....	99
4.4	Study limitations and future work	101
4.5	Conclusion	103
Appendix.....		106
S.1	Supplementary information to chapter 2	106
I.	Intracellular H ₂ O ₂ detection.....	106
II.	HIF-1.....	109
III.	Pentose phosphate pathway	110
V.	Mitochondrial ROS.....	113
S.2	Supplementary information to chapter 3	116
I.	NADPH oxidases.....	116
II.	Nitric oxide synthases.....	122
References		125

List of figures

Figure 1.1	Chemical structure of trans-resveratrol.	2
Figure 1.2	Estrogen receptors signaling pathway	4
Figure 1.3	Mitochondria dynamics and cell cycle regulation	9
Figure 1.4	Mitochondria morphology	11
Figure 1.5	Metabolic reprogramming of cancer cells	17
Figure 1.6	HIF-1 α regulation by PHD	19
Figure 1.7	Genetically encoded fluorescent biosensor Hyper for H ₂ O ₂ measuring	29
Figure 1.8	Gas phase composition in a typical cell culture incubator	33
Figure 1.9	Chapter 2 hypothesis	41
Figure 1.10	Chapter 3 hypothesis	42
Figure 2.1	Experimental design	54
Figure 2.2	Chapter 2 <i>In vitro</i> models, hypothesis and predicted results	55
Figure 2.3	RES stimulates PC3 cell respiration and mitochondrial fusion while slowing cell growth	57
Figure 2.4	Growth in galactose medium abolishes effects of RES	59
Figure 2.5	Effects of RES were diminished in PC3 cells expressing a stable HIF-1 α mutant	61
Figure 2.6	Inhibition of prolyl hydroxylase activity with IOX2 abolished RES effects on cellular respiration, mitochondrial network features, cell growth and cell cycle distribution	63

Figure 2.7	IOX2 inhibition of prolyl hydroxylase activity abolishes RES's effects on growth in PC3 and LNCaP, but not C2C12 or SHSY5Y cells	64
Figure 2.8	RES strongly inhibits PC3 cell growth under hypoxic conditions	66
Figure 3.1	Experimental design	81
Figure 3.2	Media oxygen and glucose levels determine RES's effects on cell growth	84
Figure 3.3	Media oxygen and glucose levels determine RES's effects on cellular hydrogen peroxide production	86
Figure 3.4	RES effects on mitochondrial network parameters are subtly affected by media glucose and oxygen levels in C2C12 cells	88
Figure 3.5	RES effects on mitochondrial network parameters are mostly unaffected by media glucose and oxygen levels in PC3 cells	91
Figure S1.1	RES effects on cytosolic H ₂ O ₂ levels	106
Figure S1.2	RES effects on cell doubling time were abolished when HIF-1 α is stabilized both with cobalt chloride (CoCl ₂) and IOX2	109
Figure S1.3	RES decreased G6PDH activity in PC3 cells growing at hypoxic conditions (≤ 0.4 % O ₂ , but had no effect when cells were grown at normoxic (18% O ₂) conditions or treated with IOX2	111
Figure S1.4	RES cell growth inhibitory effects under hypoxic conditions are cell type dependent	112

Figure S1.5	RES cell growth inhibitory effects under hypoxic conditions are dependent on MnSOD expression (a) and superoxide (b)	113
Figure S2.1	NOX 1 and 4 inhibition by GKT137831 modulates RES effects on H ₂ O ₂ production in C2C12 cells	117
Figure S2.2	RES effects on NOX 1 and 4 protein expression in C2C12 cells were different at 5% O ₂ versus 18% O ₂	118
Figure S2.3	At the most physiological conditions (5% O ₂ and 5mM glucose) NOX1/4 specific inhibition does not influence RES effects on H ₂ O ₂ production	119
Figure S2.4	In low glucose media [5mM glucose], RES effects on NOX4 protein expression in C2C12 cells were oxygen-dependent. RES effects on NOX1 expression were not influenced by oxygen levels	120
Figure S2.5	RES effects on H ₂ O ₂ production are independent of NOS inhibition with L-NAME	123

List of tables

Table 1	pO ₂ values observed in various human tissues	34
----------------	--	-----------

List of abbreviations

AFU	arbitrary fluorescence units
ANOVA	analysis of variance
ARNT/HIF-1 β	aryl hydrocarbon nuclear translocator
ATP	adenosine triphosphate
BSA	bovine serum albumin
CLAHE	contrast limited adaptive histogram equalization
CREB	cAMP response element binding protein
Cys	cysteine
DMEM	Dulbecco's modified eagle medium
DMSO	dimethylsulfoxide
DRP1	dynammin-related protein 1
DTT	DL-dithiothreitol
EDTA	ethylenediaminetetraacetic acid
ER	estrogen receptor
ERR α	estrogen-related receptor α
ETC	electron transport chain
FA	fatty acid
FBS	fetal bovine serum
FCCP	carbonylcyanide-p-trifluoromethoxyphenylhydrazone
FIH	factor inhibiting HIF
FIJI	FIJI is just ImageJ
FMN	flavin mononucleotide
FOXO1	forkhead box class-O
G418	geneticin
GPx	glutathione peroxidase
GR	glutathione reductase
GRx	glutaredoxin
GSH	glutathione

H ₂ O ₂	hydrogen peroxide
HEPES	(4-(2-hydroxyethyl)-1-piperazineethanesulfonic acid
HIF-1 α	hypoxia inducible factor-1 α
HRE	hypoxia response elements
HRP	horseradish peroxidase
IMM	inner mitochondrial membrane
LDH	lactate dehydrogenase
mEFP	modified emerald fluorescent protein
MEM	modified eagle medium
MiNA	mitochondrial network analysis toll
MPP	mitochondrial processed peptidase
NAD ⁺	nicotinamide adenine dinucleotide (oxidized)
NADH	nicotinamide adenine dinucleotide (reduced)
NADPH	nicotinamide adenine dinucleotide phosphate
NO	nitric oxide
NOX	NADPH oxidase
NRF	nuclear respiratory factor
Nrf2	nuclear factor (erythroid-derived 2) related factor 2
O ₂	oxygen
O ₂ ⁻	superoxide onion
•OH	hydroxyl radical
OMM	outer mitochondrial membrane
ONOO ⁻	peroxynitrite
OPA1	optic trophic 1
OXPHOS	oxidative phosphorylation
PARL	presenilin-associated rhomboid-like protein
PBS	phosphate-buffered saline
PBS-t	phosphate-buffered saline with Tween-20
PDH	pyruvate dehydrogenase
PGC-1 α	peroxisome proliferator-activated γ receptor coactivator 1 α
PHD	prolyl hydroxylase domain

PINK1	PTEN-induced putative protein kinase
PKM2	pyruvate kinase M2
PPP	pentose phosphate pathway
PRC	PGC-1 α related activator
Prx	peroxiredoxin
PTPs	protein tyrosine phosphatases
RES	resveratrol
RET	reverse electron transfer
ROS	reactive oxygen species
RSO ₂ H	sulfinic acid
RSO ₃ H	sulfonic acid
RSOH	sulfenic acid
SDS-PAGE	sodium dodecyl sulfate polyacrylamide gel electrophoresis
SEM	standard error of the mean
SIRT1	NAD ⁺ -dependent protein deacetylase sirtuin 1
SOD	superoxide dismutase
SOD2/MnSOD	manganese superoxide dismutase
TCA	tricarboxylic acid
TFAM	transcription factor A mitochondrial
Trx	thioredoxin
TrxR	thioredoxin reductase
VHL	von Hippel-Lindau
Ψ_m	mitochondrial membrane potential

Chapter 1 – Literature review

1.1 General overview

RES is a plant-derived polyphenol that has been widely studied for its health promoting effects. In many cell types and tissues, RES has been shown to slow cell cancer growth, promote mitochondrial biogenesis, fusion, and oxidative phosphorylation (OXPHOS) (Lagouge et al., 2006; Robb et al., 2017; Stuart and Robb, 2013). Therefore, in the first data chapter I investigated how a metabolic switch from glucose fermentation towards oxidative phosphorylation is required for RES to mediate slow growth in a prostate cancer cell line (PC3).

There is a growing body of literature describing the use of RES as a nutraceutical compound in human health (reviewed in (De Paepe and Van Coster, 2017)). However, many of the RES health promoting effects are observed *in vitro*, where O₂ and glucose levels do not mimic *in vivo* conditions. Therefore, in the second data chapter I assessed how supra-physiological levels of O₂ and glucose influence RES *in vitro* effects on reactive oxygen species (ROS) metabolism, cell growth, as well as mitochondrial network characteristics.

This thesis uncovers an important cellular and molecular mechanism involved in RES's antiproliferative effects, while shedding light on the importance of using physiologically relevant cell culture conditions (e.g. O₂ and glucose levels).

1.2 Resveratrol

Since the 1970s, oxidative stress has been described as being the cause of several pathological conditions, such as cancer, diabetes, neurodegenerative diseases and cardiovascular diseases. RES was first studied for its antioxidant properties, as a molecule with the potential capacity to quench and thus inactivate the excessive levels of ROS that can occur in some disease contexts. RES is a member of a class of polyphenolic compounds called polyhydroxystilbenes, which is found in a wide variety of plants including grapes, cocoa, berries and peanuts. The pathway of stilbene synthesis, leading to RES production, is stimulated by biotic and abiotic stresses, including fungal infection and excessive UV radiation. The basic structure of RES comprises two phenolic rings joined by a *trans*-double bond, forming the 3, 5, 4'-trihydroxystilbene. This double bond is responsible for RES *cis*- and *trans*-isomers. However, only the *trans*-isomer (**Figure 1.1**) has been associated with the putative cardioprotective (Wu and Hsieh, 2011), anti-tumor (Athar et al., 2007), anti-aging (Kasiotis et al., 2013), anti-diabetes (Szkudelska and Szkudelski, 2010) and antimicrobial (Chalal et al., 2014) effects of RES. From now on, for simplicity I will use the term RES and *trans*-RES interchangeably.

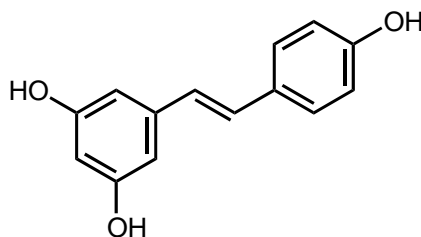


Figure 1.1 Chemical structure of *trans*-resveratrol.

1.3 *In vivo and in vitro* targets of resveratrol

Initially, the chemical antioxidant activity of RES was considered its main mechanism of action. Indeed, several of RES's effects are due to its ability to act either directly or indirectly on ROS production (e.g. NADPH oxidases, mitochondria) and scavenging mechanisms (e.g. free radical scavenger and antioxidant enzymes) (reviewed in (Truong et al., 2018)).

RES is an effective scavenger of a variety of oxidants (e.g. superoxide anion ($O_2^{\bullet-}$), hydrogen peroxide (H_2O_2) and hydroxyl radical ($\bullet OH$)) and its antioxidant properties are associated with the presence of phenolic hydroxy groups. RES can also act as a chelating agent of transition metals, such as iron (Fe) and copper (Cu), thereby reducing their prooxidant activity (Gülçin, 2010). On the other hand, in a dose-dependent manner RES can act as a pro-oxidant (Procházková et al., 2011). For example, RES can form a complex with oxidized copper ions (i.e. Cu (II)), leading to its reduction to Cu (I). This will increase ROS production (e.g. through a Fenton Reaction; normal Fe-based but it can also occur with Cu (Pham et al., 2013)), causing cellular DNA breakage (Fukuhara et al., 2006; de la Lastra and Villegas, 2007). Interestingly, this prooxidant pathway has been shown to induce apoptosis and growth inhibition in cancer cells (Khan et al., 2014; León-González et al., 2015), and therefore may be an important mechanism by which RES exerts its anticancer properties.

In addition to its direct effects, RES can exert its effects indirectly. For example, RES can act as an antioxidant molecule is by increasing the expression and activity of antioxidant enzymes, such as superoxide dismutase (SOD), catalase, glutathione reductase (GR) and glutathione peroxidase (GPx), which neutralize ROS (reviewed in (Truong et al., 2018)). Some of these effects are mediated by RES ability to modulate estrogen receptors (ERs) signaling (reviewed in

(Cipolletti et al., 2018; Stuart and Robb, 2013)). ERs participate in the regulation of different biological processes including cell growth, survival and differentiation. ERs are comprised of two distinct receptors, ER α and ER β (Leitman et al., 2010), which show a unique expression profile across tissues and cell types (Ascenzi et al., 2006). For example, ER α is highly expressed in reproductive tissues, while ER β is expressed in a wide variety of tissues, such as brain, lung and prostate (**Figure 1.2**).

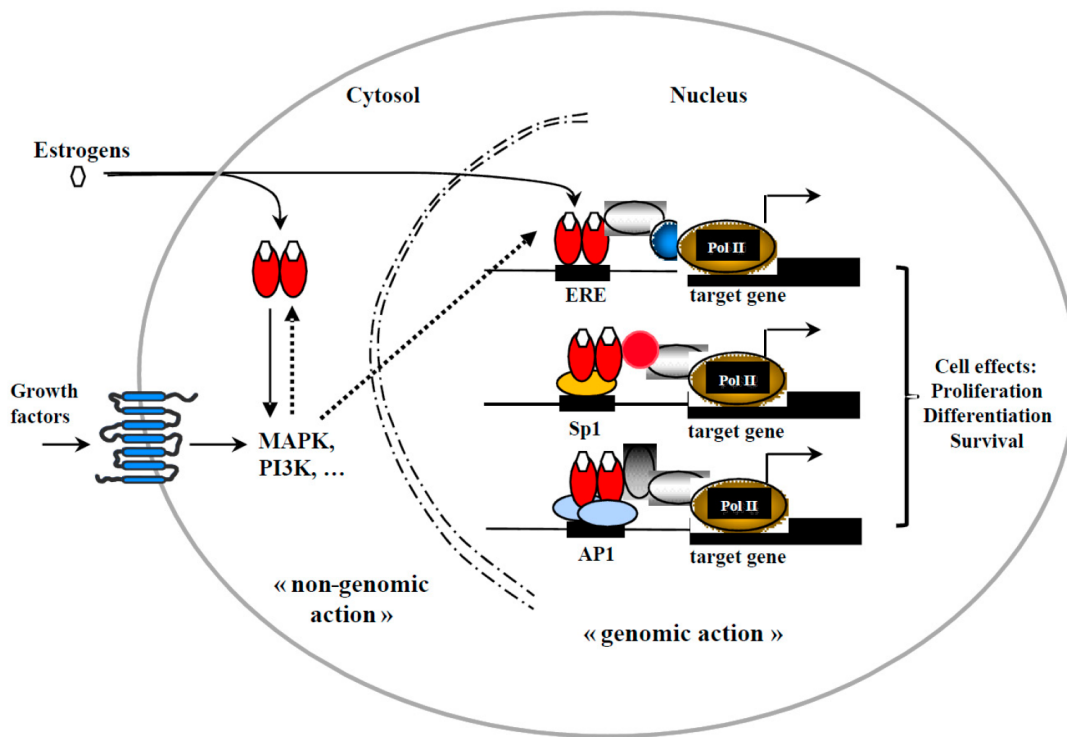


Figure 1.2. Estrogen receptors signaling pathway. Estrogens can bind to ER in the cytoplasm or the nucleus. In the nucleus, the activated ER forms a dimer that binds to the estrogen-responsive-elements sites or indirectly at Sp1 and AP1 sites. The activated ER modulates the transcription of the target genes. On the other hand, ERs can also exert a rapid non-genomic action through the activation of intracellular kinases related or not to the growth factor signaling. Reproduced from (Lecomte et al., 2017).

ERs have different cell growth effects, for example, whereas ER α agonists exert pro-proliferative effects, ER β agonists are typically antiproliferative (Sugiyama et al., 2010). Therefore, the varying intracellular ER α /ER β ratio observed in various cancer types may alter ER signaling and consequently lead to distinct clinical outcomes (Thomas and Gustafsson, 2011). Interestingly, growth inhibitory effects of RES may be explained in part by its ability to interact with ERs, in particular ER β (Robb and Stuart, 2011). In the following sections, RES targets will be described in more detail.

1.3.1 Mitochondria

Mitochondria are highly dynamic, double-membraned organelles, that participate in a wide array of functions within eukaryotic cells, such as energy production, fatty acid synthesis, amino acid production, heme synthesis and iron-sulfur cluster biogenesis. To ensure proper mitochondrial function – which is essential for health and survival – mitochondria have developed elaborate mechanisms of quality control. This process is regulated by the generation of new mitochondria (biogenesis) and the removal of damaged and unwanted mitochondria (i.e. mitophagy). Together, these processes constitute mitochondrial turnover.

1.3.1.1 Mitochondrial biogenesis

Mitochondrial biogenesis is a complicated process of complete organelle replication that requires the coordinated expression of both nuclear and mitochondrial genes (reviewed in (Hock

and Kralli, 2009)). Peroxisome proliferator-activated receptor- γ -coactivator-1 (PGC-1) is a transcriptional coactivator involved in mitochondrial biogenesis. There are three isoforms of PGC-1: PGC-1 α , PGC-1 β , and PGC-1 α related activator (PRC) (reviewed in (Scarpulla, 2011)). PGC-1 α is known as the master regulator of mitochondrial biogenesis that coactivates the nuclear respiratory factor 1 and/or 2 (NRF-1 and NRF-2), and the estrogen-related receptor α (ERR α), which stimulate the transcription of several nuclear-encoded genes whose protein products localize to mitochondria (Yang et al., 2014). In addition to nuclear-specific regulation, mitochondria-related mechanisms, such as mtDNA transcription have an essential role in mitochondrial biogenesis. In mammals, mitochondrial transcription requires the mitochondrial RNA polymerase and the transcription factor A mitochondrial (TFAM) (Kanki et al., 2004).

PGC-1 α expression is regulated by the transcription factors cAMP response element-binding protein (CREB) and forkhead box class-O (FoxO1) (reviewed in (Hock and Kralli, 2009)), while its activity is regulated by phosphorylation or deacetylation by the NAD⁺-dependent protein deacetylase sirtuin 1 (SIRT1) (Aquilano et al., 2010; Fernandez-Marcos and Auwerx, 2011). Indeed, SIRT 1 upregulation results in an increased PGC-1 α activity (Cantó et al., 2009). On the other hand, when mitochondria are too abundant, or when they become aged or damaged, a process of mitochondrial clearance is set in motion.

1.3.1.2 Mitophagy

The elimination of whole mitochondria is accomplished by a selective form of autophagy, coined mitophagy (Lemasters, 2005). Mitophagy is considered an important step in mitochondria

quality control, and it is stimulated when mitochondria are defective or have impaired function (e.g. mitochondrial membrane potential depolarization) (reviewed in (Ashrafi and Schwarz, 2013)). The most studied pathway of mitophagy regulation is mediated by the PTEN-induced putative protein kinase 1 (PINK1) and the E3 ubiquitin ligase Parkin (Eiyama and Okamoto, 2015; Narendra et al., 2008). Briefly, under normal conditions, PINK1 is translocated to the mitochondrial matrix, and rapidly cleaved by the mitochondrial processing peptidase (MPP) and by the presenilin-associated rhomboid-like (PARL) protease. The resulting PINK1 fragments are released in the cytoplasm and act as mitophagy inhibitors by binding to Parkin and blocking its translocation and stabilization to the outer mitochondrial membrane (OMM). However, in mitochondria with dissipated membrane potential, PINK1 escapes cleavage which recruits Parkin to the OMM (Narendra et al., 2008). After ubiquitination of OMM proteins, mitochondria may be engulfed by an active autophagosome, thereby leading to mitochondria degradation.

Mitochondria are well known targets of RES (reviewed in (De Oliveira et al., 2016)). One mechanism by which RES exerts its beneficial health effects is through increased mitochondrial biogenesis (Csiszar et al., 2009; Lagouge et al., 2006). For example, RES through a SIRT1-dependent process can induce the expression and activity of several mitochondrial biogenesis factors, such as PGC-1 α , NRF-1 and TFAM (Davinelli et al., 2013; Lagouge et al., 2006; Menzies et al., 2013).

1.3.1.3 Mitochondrial morphology

Mitochondria are dynamic organelles that are in a constant dynamic equilibrium between fusion and fission states (McBride et al., 2006; Pernas and Scorrano, 2016). Generally, mitochondria fluctuate between a highly fused, interconnected network and a fragmented state characterized by the presence of individual puncta or rod-like structures. Structural remodeling is achieved in part by three large GTPases of the dynamin superfamily: Mitofusin (Mfn) 1, Mfn 2 and optic atrophy 1 (Opa1). Mfn 1 and 2 mediate OMM fusion (Franco et al., 2016) while Opa1 regulates inner mitochondrial membrane (IMM) fusion (Ban et al., 2017). This is a two-step process, where the outer and inner membrane fuse in separate steps. Complementary to fusion is mitochondria fission. This process is also mediated by a large GTPase named dynamin-related protein-1 (DRP1), that is recruited to the mitochondrial outer membrane by several receptor proteins (e.g. Mff, Fis1, MiD49, and MiD50) (Youle and van der Bliek, 2012).

Mitochondrial network architecture appears to be closely associated with cell metabolism. Indeed, mitochondrial morphology varies tremendously across tissues of varying metabolic needs (Yamaguchi et al., 2012). For example, increased OXPHOS activity and ATP production are associated with a hyperfused mitochondria (Mitra et al., 2009). On the other hand, impaired OXPHOS triggered due to excessive nutrient availability and severe stress is associated with a fragmented mitochondria (Liesa and Shirihai, 2013) – a phenotype observed in many cancer cell lines.

Mitochondrial morphological changes also occur during the cell cycle (reviewed in (Horbay and Bilyy, 2016)) **Figure 1.3**. The G1/S transition is characterized by a highly interconnected mitochondria network, with increased levels of Mfn1 and 2. This hyperfused state

is associated with a highly oxidative metabolism (Mitra et al., 2009). On the other hand, S-phase is characterized by a more fragmented mitochondrial network with higher levels of Drp1 and a more glycolytic cellular metabolism. During G₂-phase and G₂/M transition, mitochondria go through further mitochondrial morphological changes. While the former phase is characterized by highly fused mitochondria, the latter phase is characterized by a fragmented mitochondria, which remains in that state until mitosis completion (Taguchi et al., 2007).

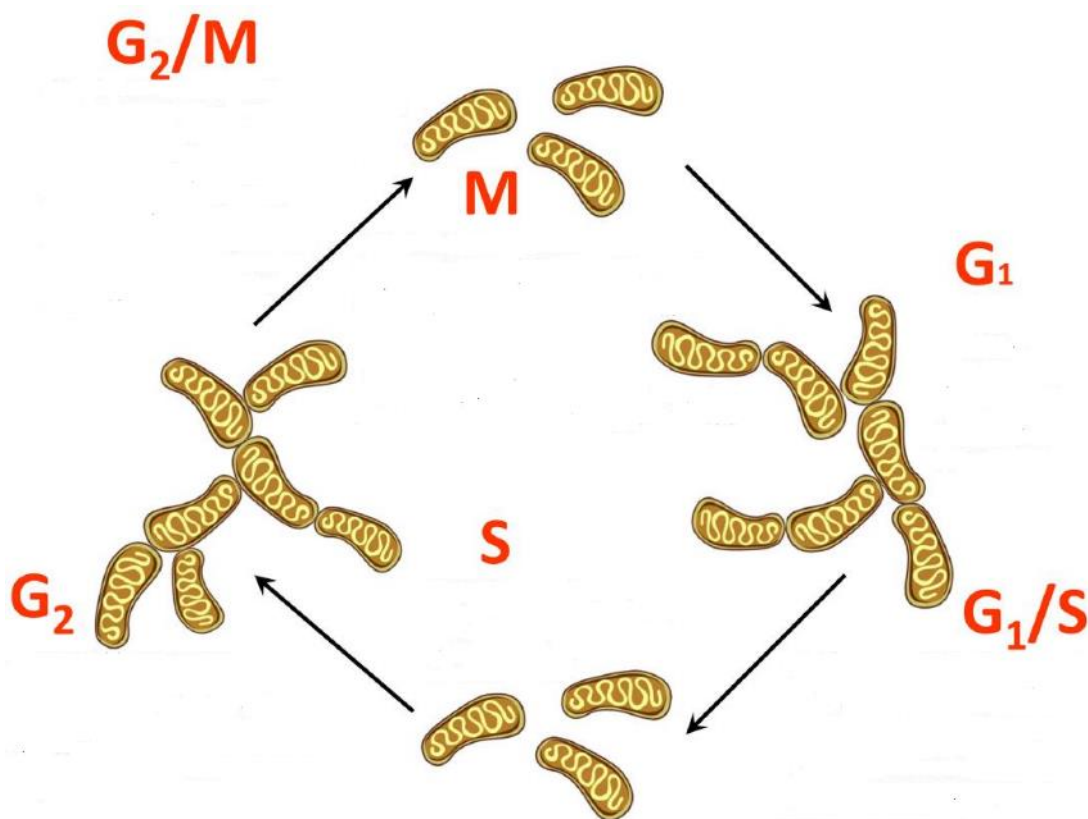


Figure 1.3 - Mitochondria dynamics and cell cycle regulation. A proper balance between mitochondria fusion and fission is essential for cell cycle progression. This guarantees that the cell energetic requirements are met. For example, during active phases (*e.g.* G₁/S transition) of the cell cycle mitochondria networks are hyperfused. On the other hand, while entering mitosis mitochondria adopt a more fragmented state. G₁ – Gap 1; S – Synthesis; G₂ – Gap 2; M - mitosis Adapted from (Horbay and Bilyy, 2016)).

Alterations of mitochondrial networks also play important roles in apoptosis (Suen et al., 2008), mitophagy (Gegg et al., 2010), stress resistance (Youle and van der Bliek, 2012) and mtDNA stability (Chen et al., 2010). Loss of balance between mitochondria biogenesis and mitophagy can lead to apoptosis and cell death. Therefore, it is not surprising that genetic disruption of genes involved in fusion and fission have a striking effect on mammalian health (reviewed in (Babbar and Sheikh, 2013)). Indeed, mitochondrial dysfunction has been associated with several pathophysiological conditions, such as metabolic disorders (reviewed in (Blake and Trounce, 2014; Peinado et al., 2014)), neurodegeneration (reviewed in (Federico et al., 2012)), tumor development (reviewed in (Hertweck and Dasgupta, 2017)) and cardiovascular diseases (reviewed in (Bayeva et al., 2013)). For example, mutations in Mfn2 are known to cause Charcot-Marie-Tooth disease type 2A, a peripheral neuropathy affecting long motor and sensory neurons (Züchner et al., 2004). Of note, RES has been shown to modulate mitochondrial morphology. More specifically, RES increases mitochondrial network fusion through a process that requires an increase in the expression of Mfn 1, Mfn2 and Opa1 (Meira Martins et al., 2014; Robb et al., 2017).

1.3.1.3.1 Mitochondrial Network Analysis

The importance of mitochondrial morphology for proper cell function has motivated the development of tools for the analysis of the different mitochondrial network features. Until recently, most mitochondrial network analysis was reliant on qualitative or semi-quantitative observations. Therefore, in order to remove the subjectivity of this analysis our lab developed a new tool called Mitochondrial Network Analysis (MiNA) (Valente et al., 2017). The goal of MiNA is to provide an accurate measurement of mitochondrial network characteristics.

MiNA recognizes two distinct mitochondrial structures, individuals, and networks. Individuals are mitochondrial structures with no junctions and consist of punctae (a single pixel in the skeletonized image) or rods (unbranched structures with two or more pixels in the skeletonized image). Networks are mitochondrial structures containing at least a single node and three branches (Valente et al., 2017). For these two types of mitochondrial structures, MiNA can compute several parameters: number of ‘individual’ structures with no branches (puncta and rods), number of networks, mean number of branches per network and mitochondrial footprint. The latter parameter represents the total area in the image consumed by signal (minus the background) and gives a proxy of mitochondrial biogenesis. A higher number of individuals is associated with a more fragmented mitochondrion, while an increase in the number of networks and branches per network is correlated with a more fused state (**Figure 1.4**).

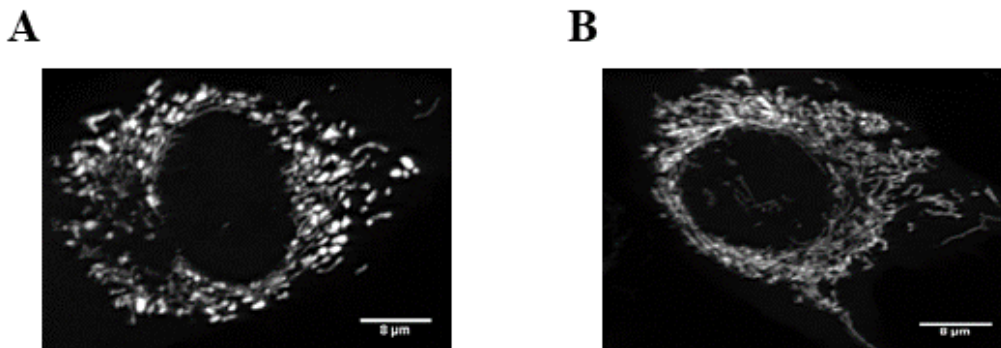


Figure 1.4 – Mitochondria morphology. The image on the left (**A**) shows an example of a highly fragmented mitochondria, demonstrated by the presence of a higher number of individuals. On the other hand, the image on the right (**B**) shows mitochondria in a highly fused state, which is demonstrated by an increased number of networks and branches per network.

1.3.1.4 Mitochondrial reactive oxygen species

For over 20 years, ROS have been regarded as important mediators in several physiological and pathological processes (Sundaresan et al., 1995). However, only recently (with the help of newly developed ROS detection methods) some of the mechanisms by which ROS signaling is transmitted started to be understood (reviewed in (Reczek and Chandel, 2015)).

ROS refer to a variety of molecules that are formed upon partial reduction of O_2 (reviewed in (Sies, 2017)). Briefly, one-electron reduction of molecular O_2 forms $O_2^{\cdot-}$, the precursor of many ROS. $O_2^{\cdot-}$ can rapidly dismutate, either spontaneously or enzymatically to H_2O_2 , a low reactive and highly diffusible molecule that has been shown to cross the mitochondrial membrane through specific members of the aquaporin family (Bienert and Chaumont, 2014; Bienert et al., 2007). ROS can undergo chemical reactions to generate secondary oxidative species. For example, $O_2^{\cdot-}$ can react with nitric oxide ($\cdot NO$) to generate peroxynitrite ($ONOO^-$) (Radi, 2013). Furthermore, $O_2^{\cdot-}$ and H_2O_2 can generate the highly reactive $\cdot OH$, in the presence of trace metals through Fenton/Haber-Weiss reactions (Kehrer, 2000; Winterbourn, 1995).

Mitochondria are an important source of ROS, such as $O_2^{\cdot-}$ and H_2O_2 (generated from $O_2^{\cdot-}$ dismutation) in eukaryotic cells (reviewed in (Murphy, 2009)). During respiration, mitochondria produce ROS, with up to eleven known sites capable of generating $O_2^{\cdot-}$ (Goncalves et al., 2015). However, most evidence suggests that the main sources of ROS in mitochondria are formed predominantly at complex I (NADPH dehydrogenase; matrix) and complex III (ubiquinone-cytochrome c reductase; matrix and inner mitochondrial space) (Murphy, 2009; Quinlan et al., 2013). Experiments with isolated mitochondria show that superoxide formation from complex I occurs mainly through two mechanisms; O_2 reaction with reduced flavin mononucleotide (FMN)

(Kusssmaul and Hirst, 2006) or reverse electron transfer (RET), which occurs when CoQ is reduced (Korshunov et al., 1997). Complex III generates $O_2^{\cdot-}$ by the reaction of O_2 with ubisemiquinone bound to the complex (Turrens et al., 1985). A growing body of literature has discussed the role of mitochondrial ROS production on several cellular signalling pathways (Dan Dunn et al., 2015; Sena and Chandel, 2012), including hypoxia (Klimova and Chandel, 2008), differentiation (Tormos et al., 2011) and apoptosis (Circu and Aw, 2010; Giorgio et al., 2005).

1.3.1.5 Mitochondrial antioxidant defense systems

A balance between ROS production and removal is crucial for normal cellular function. While at low concentrations, ROS are essential participants in mitochondrial dynamics, cell proliferation and differentiation, apoptosis and senescence (Ray et al., 2012; Schieber and Chandel, 2014; Weidinger and Kozlov, 2015), excess ROS production can disrupt normal cell function and promote damage to cellular lipids, nucleic acids, and proteins (Evans et al., 2004; Stadtman and Levine, 2000). In order to keep ROS within a range compatible with normal cellular function, organisms have developed several antioxidant systems. Examples of these antioxidant systems are SODs, glutathione (GSH), thioredoxin (Trx) and catalase.

Most of the $O_2^{\cdot-}$ generated at the mitochondria can rapidly dismutate, either spontaneously or enzymatically, to H_2O_2 , with the help of SODs. SODs are the major antioxidant defense system against $O_2^{\cdot-}$, which in mammals is comprised of three isoforms. Cu/ZnSOD (SOD1), localized in the intermembrane space and cytosol; MnSOD (SOD2) localized in the mitochondrial matrix; Cu/ZnSOD (SOD3) localized in the extracellular milieu, all of which require a catalytic metal (Cu

or Mn) for their activation. MnSOD is the first-defense against $O_2^{\cdot-}$ formation in the mitochondrial electron transport chain (ETC) and its importance is highlighted by the neonatal lethality of the SOD2^{-/-} mouse (Lebovitz et al., 1996; Li et al., 1995).

Original observations from our lab showed that RES induces expression of MnSOD (Robb et al., 2008). Although the exact molecular mechanism by which RES modulates MnSOD expression is still unknown, we do think RES effects are mediated by the ER β , since MnSOD expression is prevented in a ER β knockout cell line and when using a specific ER β antagonist (Robb and Stuart, 2011, 2014). Furthermore, mitochondrial respiration is not required for ER β mediated induction of MnSOD, since RES strongly upregulated MnSOD levels in respiratory deficient rho⁰ PC3 cells (Robb and Stuart, 2014).

Reduction of H₂O₂ into H₂O is regulated by both the catalase and peroxidase systems, such as glutathione/glutathione peroxidase (GSH/GPx) and thioredoxin/thioredoxin reductase/peroxiredoxin (Trx/TrxR/Prx) (Weydert and Cullen, 2010). In mitochondria, GSH and Trx systems are the main H₂O₂ degrading pathways (Handy and Loscalzo, 2012). However, catalase which is usually localized in peroxisomes, has also been found in liver and cardiac mitochondria (Rindler et al., 2016; Slade et al., 2017).

The tripeptide GSH is the most abundant non-protein thiol found in cells and is known to fulfill a number of important roles in mitochondria (Marí et al., 2009). GSH can act alone or as a cofactor of several enzyme catalysts, such as glutaredoxins (GRx) and glutathione peroxidases (GPx). GPx are an important group of isoenzymes capable of metabolizing H₂O₂, using reduced glutathione (GSH) as a cofactor. From GPx family, GPx1 and GPx4 isoforms are localized in mitochondria (Brigelius-Flohé and Maiorino, 2013; Calabrese et al., 2017). In the presence of

reduced GSH, GPx catalyzes the reduction of mitochondrial H₂O₂ to H₂O. This results in glutathione oxidation (to GSSG), which can then be reduced back to GSH by GR in the presence of NADPH (Venditti et al., 2013).

The mitochondrial Trx/TrxR/Prx consist of a unique Trx2, thioredoxin reductase-2 (TrxR2) and Prx3 (Cox et al., 2009). The Trx system utilizes the catalytic activity of Prx, a thiol-specific peroxidase, which reduces H₂O₂. This promotes Trx2 oxidation, which can be then reduced via NADPH by its unique corresponding TrxR2 (Wood et al., 2003)

RES effects on GPx expression and GSH metabolism have also been well characterized. For example, RES treatments increased GPx1 activity in a process that required PGC-1 α activation (Zhou et al., 2014). RES has also been shown to up-regulate the expression of γ -glutamylcysteine synthetase (a rate-limiting enzyme in the synthesis of GSH), and this up-regulation is dependent on the presence of nuclear factor (erythroid-derived 2) related factor 2 (Nrf2) (Ungvari et al., 2010). Nrf2 is a transcription factor that exerts mitochondrial protection by modulating the expression of several antioxidant enzymes, such as GSH and Trx (Dinkova-Kostova and Abramov, 2015). In mice lacking Nrf2, RES protective effects against oxidative stress are not observed (Ungvari et al., 2010).

1.3.2 Warburg effect

Healthy non-dividing cells in the presence of O₂ tend to fully oxidize pyruvate into carbon dioxide in mitochondria through the tricarboxylic acid (TCA) cycle and OXPHOS. On the other hand, under anaerobic conditions, these cells tend to reduce pyruvate into lactate. In contrast to this, normal proliferating cells and tumor cells tend to increase their glycolytic rate even in the presence of O₂ (reviewed in (Vander Heiden et al., 2009)). This phenomenon was termed aerobic glycolysis or the Warburg effect, due to the pioneering work developed by the German scientist Otto Warburg (Warburg, 1956).

When compared to oxidative phosphorylation, aerobic glycolysis is a less efficient energetic process (2 ATP molecules instead of 36 ATP molecules). However, during aerobic glycolysis other cellular processes, such as macromolecular biosynthesis (e.g. nucleotides, lipids and proteins) and redox homeostasis (reviewed in (Cantor and Sabatini, 2012; Lunt and Vander Heiden, 2011)) are upregulated, which allow cancer cells to maintain their increased rate of proliferation. The metabolic program of normal proliferating and cancer cells is met by an increased uptake of glucose and glutamine. These two substrates are then utilized in several biosynthetic pathways. For example, enhanced glucose uptake can lead to higher levels of fructose-6-phosphate and glucose-6-phosphate being shunted into the pentose phosphate pathway (PPP) (Patra and Hay, 2014). Feeding this pathway can ultimately lead to nucleotide biosynthesis and NADPH formation, the latter of which is involved in cellular defense against oxidative stress (Hamanaka and Chandel, 2011). These metabolic changes decrease cell reliance on OXPHOS as the main source of ATP. On the other hand, TCA cycle activity is not completely abolished. Instead, proliferative cells activate anaplerotic mechanisms that feed the TCA cycle, which is required for fatty acid (FA) and amino acid biosynthesis (reviewed in (Boroughs and DeBerardinis,

2015)). For example, citrate and α -ketoglutarate can be used for lipid biosynthesis and nonessential amino acid generation, respectively. This is mainly achieved by increasing the pace of glutamine utilization (Altman et al., 2016; Zhang et al., 2017). So, although originally thought to be dysfunctional, mitochondria are not only functional, but are also critical to adjust proliferative cells' metabolic activity (Ward and Thompson, 2012) (**Figure 1.5**).

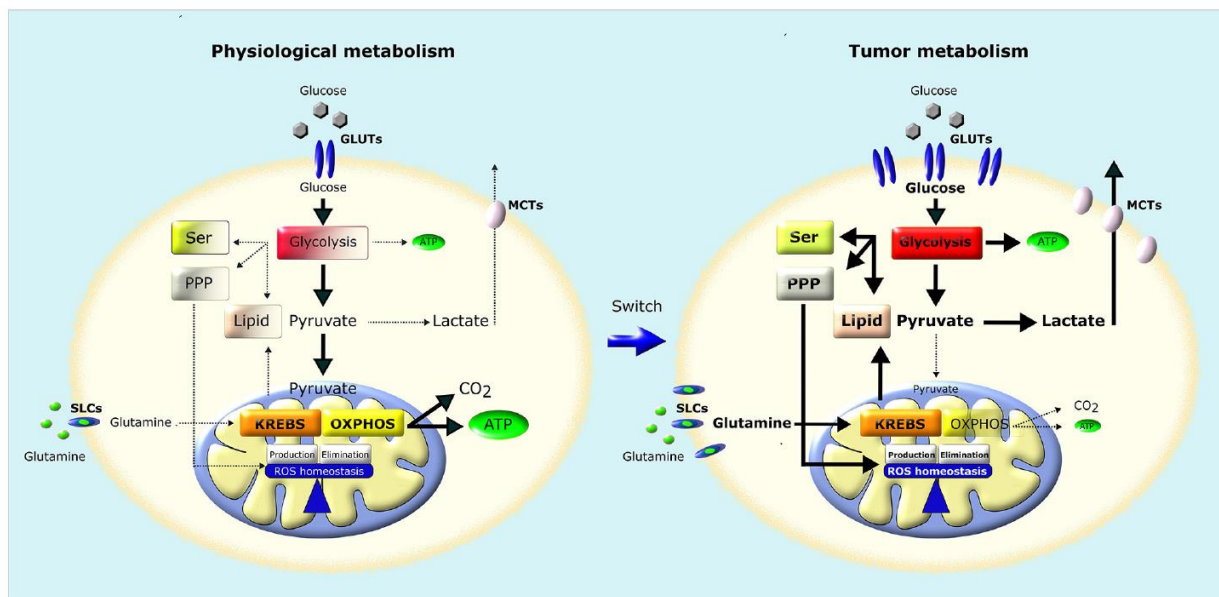


Figure 1.5 - Metabolic reprogramming of cancer cells. Normal cells (left) rely heavily on OXPHOS as main source of ATP. On the other, cancer cells (right) convert most of glucose into lactate regardless of O_2 availability (aerobic glycolysis). During this process, cells increase their glucose and glutamine consumption, which allow them to generate the building blocks required for the anabolic needs required to maintain a high rate of proliferation. **PPP** – Pentose Phosphate Pathway, **SER** – Serine biosynthesis pathway, **GLUTs** - Glucose transporters, **MCTs** – Lactate transporters, **SLCs** – Solute carriers. Reproduced from (Cannino et al., 2018).

Altered cellular metabolism is an important hallmark of cancer and suppressing the glycolytic phenotype of cancer cells could be of great therapeutic value. RES has been shown to

have *in vitro* and *in vivo* anti-cancer properties (Carter et al., 2014; Gomez et al., 2013; Jang et al., 1997), which have been explained mainly by its activities in cell cycle control and apoptosis induction. However, RES's antitumoral activities may also be related to its ability to promote a metabolic reprogramming towards a more oxidative phenotype that is less conducive to proliferative growth (Blanquer-Rosselló et al., 2017; Saunier et al., 2017).

1.3.3 Hypoxia inducible factor

A central regulator involved in metabolic reprogramming is the transcription factor, hypoxia inducible factor 1 α (HIF-1 α) (reviewed in (Semenza, 2011)), which regulates the transcription of glycolytic metabolic enzymes. HIF-1 is a heterodimeric protein that is composed of an O₂-regulated alpha subunit (three isoforms present in humans, HIF-1 α , HIF-2 α , HIF-3 α) and a constitutively expressed HIF β subunit (also known as Aryl Hydrocarbon Nuclear Translocator, ARNT) (Semenza, 2012). HIF- α levels are regulated by O₂ via proteasome-dependent degradation. In the presence of O₂, HIF-1 α is hydroxylated on two proline residues (402 and 564) by a family of prolyl hydroxylase domain (PHD) proteins (e.g. PHD2). Indeed, if this hydroxylation is prevented by switching the proline into alanine, a mutant HIF-1 α that is constitutively expressed is formed. PHD activity is dependent on the presence of Fe(II), α -ketoglutarate and O₂.

O₂ is a key substrate for hydroxylation and with a K_m (O₂) close to 200 μ M (which is slightly above the oxygen concentration in aqueous solutions saturated by room air), PHD activity is highly sensitive to O₂ levels (Ehrismann et al., 2007; Hirsilä et al., 2003).

After hydroxylation by PHDs, HIF- α is bound by the von Hippel-Lindau tumour suppressor (VHL) which recruits an ubiquitin ligase that targets HIF- α for degradation by the proteasome (reviewed in (Kaelin and Ratcliffe, 2008)) (**Figure 1.6**).

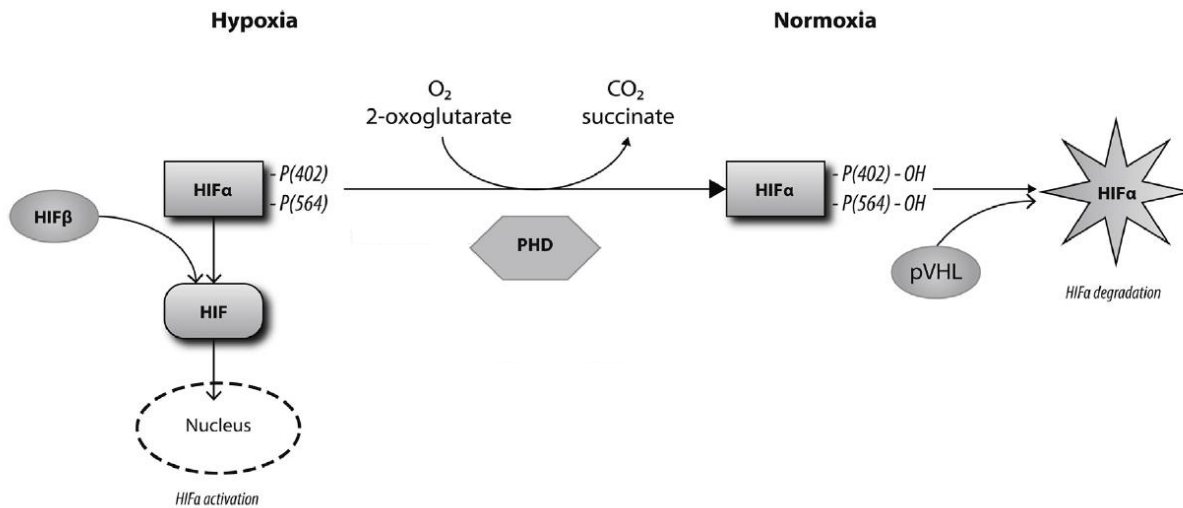


Figure 1.6 - HIF-1 α regulation by PHD. Under normoxia, PHD hydroxylates HIF1 α at two proline residues, P402 and P564. After hydroxylation, HIF-1 α is recognized by the pVHL protein, which induces its ubiquitination and triggers its subsequent proteolytic degradation by the E3 ubiquitin ligase complex. On the other hand, when O₂ levels are low (e.g. hypoxic conditions), PHD activity is inhibited and HIF-1 α accumulates. When stable, HIF-1 α translocates to the nucleus, where it interacts with HIF-1 β and induces the expression of different target genes. Reproduced from (Nguyen and Durán, 2016).

In addition to regulation by PHD, HIF-1 α stabilization can be negatively regulated by an O₂-dependent hydroxylation of a key asparagine residue by the factor-inhibiting HIF (FIH). This promotes a steric inhibition of the interaction between HIF1 α and the transcriptional coactivator p300 (Semenza, 2007).

After stabilization, HIF1- α translocates to the nucleus and dimerizes with HIF-1 β . Following dimerization, HIF-1 binds to specific DNA sequences (hypoxia response elements, HREs) in target gene promoters and/or enhancers, driving the expression of genes that regulate cellular processes related to hypoxia adaptation, such as cell metabolism.

1.3.3.1 Cell metabolic regulation by HIF-1

HIF-1 is able to regulate cells metabolic adaptation by increasing synthesis of machinery needed for glucose fermentation (e.g. lactate dehydrogenase (LDH)) (Kim et al., 2006), while suppressing OXPHOS. This transcriptional program pushes pyruvate away from the TCA cycle toward conversion into lactate. During lactate formation, NAD⁺ is produced, maintaining a proper NAD⁺/NADH balance required for a sustained glycolytic activity (Greer et al., 2012). Interestingly, regulatory loops between mitochondria and the transcriptional response triggered by HIF have been observed (LaGory and Giaccia, 2016). For example, PGC-1 α , a central regulator of mitochondrial biogenesis, stabilizes HIF-1 α by stimulating mitochondrial O₂ consumption and increasing intracellular hypoxia (O'Hagan et al., 2009). Furthermore, mutations in subunits of succinate dehydrogenase and fumarate hydratase lead to accumulation of succinate and fumarate respectively. These metabolites competitively inhibit α -ketoglutarate-dependent dioxygenases (e.g. PHD) (Nowicki and Gottlieb, 2015) and promote HIF-1 α accumulation (Pollard et al., 2005). This demonstrated for the first time that mitochondria could play an important role in tumor onset regulation.

Interestingly, HIF-1 α expression (Jung et al., 2013) and therefore the expression of several glycolytic enzymes (Iqbal and Bamezai, 2012) have been shown to be negatively regulated by RES.

1.3.3.2 PHD downstream targets

In mammalian cells, three different PHD isoforms are encoded by three different genes, EGLN1 for PHD2, EGLN2 for PHD1 and EGLN3 for PHD3. PHDs have unique but also partially overlapping expression patterns. PHD2 is the most abundantly expressed isoform across tissues. On the other hand, PHD1 and PHD3 tissue distribution is more restricted (Cioffi et al., 2003; Jokilehto and Jaakkola, 2010). PHD1 is highly expressed in the testis, brain, kidney, and liver. PHD3 is mostly expressed in the heart.

PHD enzymes are key regulators of HIF-1 activity; however other PHD-targets have been described. Indeed, PHD enzymes display HIF-independent and hydroxylase-independent functions, which control several cellular pathways. One such example is cellular metabolism. For example, PHD controls glycolysis through the regulation of pyruvate kinase M2 (PKM2) (Chen et al., 2011) and pyruvate dehydrogenase (PDH) (Kikuchi et al., 2014) activities. Other cellular processes regulated by PHD in an HIF-independent manner are intracellular nutrient sensing (i.e. amino acid availability) (Durán et al., 2013), cell growth (Garvalov et al., 2014), immune response (Hamm et al., 2013) and apoptosis (Xie et al., 2012). In conclusion, besides O₂ sensing, PHDs have also an important role in cell metabolic monitoring.

1.3.4. NADPH oxidases

Initially thought to be only present in phagocytic cells, nicotinamide adenine dinucleotide phosphate (NADPH) oxidases (NOXs) are membrane-bound enzymes that are widely expressed and evolutionarily conserved. NOXs family is comprised of 7 NOX isoforms, NOX1-5 and dual oxidase 1-2 (reviewed in (Bedard and Krause, 2007)). NOXs transfer electrons across biological membranes to reduce O_2 to either $O_2^{\cdot-}$ (which is rapidly converted into H_2O_2) or H_2O_2 (e.g. NOX4) and are the only enzymes whose sole known purpose is to generate ROS. ROS generation by NOX is initiated by NADPH as the 2-electron donor, and its subsequent transfer through FAD and heme cofactors to O_2 (Bedard and Krause, 2007).

NOX family members can be distinguished by their tissue distribution, structure, and regulation. For example, NOX1 is highly expressed in colon epithelial cells (Suh et al., 1999). On the other hand, NOX3 and NOX5 are expressed in kidney (Geiszt et al., 2000) and testis (Bánfi et al., 2001), respectively. Lastly, NOX4 is widely expressed in mammalian tissues (Panday et al., 2015). In addition to plasma membrane-bound isoforms, NOX enzymes localize to subcellular organelles. For example, NOX4 has been localized in the endoplasmic reticulum (Van Buul et al., 2005), mitochondria (Block et al., 2009; Graham et al., 2010) and in the nucleus (Hilenski et al., 2004; Kuroda et al., 2005). In contrast to the other NOXs, NOX4 primarily generates H_2O_2 . This selective H_2O_2 formation may be explained by the fact that NOX4 contains a highly conserved histidine residue located in an extended E-loop, that may serve as a source of protons or as a trapping mechanism which accelerates the spontaneous dismutation of superoxide at this site (Takac et al., 2011). NOX activity is dependent on regulatory subunits, except for NOX4, which is constitutively active and is independent of cytosolic activator proteins.

NOXs are key enzymes in redox signaling (Bedard and Krause, 2007; Brown and Griendling, 2009). Indeed, they are known to be involved in several signaling events, including cell growth, cell survival and cell death (Brown and Griendling, 2009). In a pathophysiological context, NOXs have been associated with resistance to apoptosis, tumor cell proliferation and metastasis, as well as enhanced angiogenesis (Block and Gorin, 2012; Kamata, 2009; Meitzler et al., 2014).

Of note, several studies have shown that RES modulates NOX expression and activity (Chen et al., 2013; He et al., 2015, 2016; Schilder et al., 2009; Zhang et al., 2012). From all NOX isoforms, NOX1 and NOX4 seem to be the ones whose expression and/or activity is the most affected by RES. This observation may be partially explained by their different expression across tissues, with NOX4 being the most abundantly expressed isoform (Brown and Griendling, 2009).

1.4 Redox signaling

Intracellular signaling can be mediated through a variety of mechanisms, such as enzymatic post-translational modifications of substrate proteins (e.g. acetylation and phosphorylation), interactions of proteins with small molecules or ions (e.g. Ca^{2+}) and reversible post-translational modification of protein thiols (i.e. redox signaling). From the broad spectrum of ROS, H_2O_2 is considered most likely to play a key role in oxidative signaling.

1.4.1 Hydrogen peroxide

A few examples of intracellular H_2O_2 sources are the mitochondria (through $\text{O}_2^{\cdot-}$ dismutation), NOX4, xanthine and monoamine oxidases (Kelley et al., 2010; Nisimoto et al., 2014). Despite being a strong two-electron oxidant, H_2O_2 reacts slowly with most biological molecules. Therefore, direct reactions of H_2O_2 are restricted to cysteine residues in proteins and transition metal centers (reviewed in (Winterbourn, 2013)).

The unique characteristics of H_2O_2 , such as low reactivity, long half-life and large diffusion distances, make it an important signaling molecule (D'Autréaux and Toledano, 2007). H_2O_2 signaling can occur mainly through two different mechanisms. One that implies a direct oxidation of cysteine residues in redox-regulated target proteins (e.g. phosphatases and kinases) (Finkel, 2011; García-Santamarina et al., 2014) and another one that depends on a redox relay mechanism (e.g. peroxiredoxin oxidation) (Stöcker et al., 2018). However, both these models are not mutually exclusive. Depending on the context and situation H_2O_2 signaling may occur through both ways.

While at high concentrations H_2O_2 can cause oxidative damage of biomolecules resulting in cell cycle arrest and eventual apoptosis (Giorgio et al., 2007), at low concentrations H_2O_2 is an important signaling molecule. H_2O_2 most well known targets are cysteine residues and transition metal centers.

1.4.1.1 Cysteine

The most important mechanism by which H_2O_2 molecule act as a mediator of the cellular signaling is the reversible oxidation of specific cysteine thiol groups (reviewed in (Jones, 2008)). Even though cysteine is one of the least abundant amino acids present in eukaryotic cells, it is frequently observed in functionally important sites of proteins (Marino and Gladyshev, 2010). In the presence of low H_2O_2 levels, the cysteine thiol can be easily oxidized to a sulfenic acid (SOH), which through further oxidations can form sulfinic (SO_2H) or sulfonic (SO_3H) acid (reviewed in (Grek et al., 2013)). The latter two modifications are irreversible and cannot be repaired within cells. Ultimately, these modifications lead to changes in the activity and conformation of a target protein (reviewed in (Jones and Sies, 2015)).

A well characterized way in which H_2O_2 influences a plethora of signaling cascades is through the inhibition of protein tyrosine phosphatases (PTPs) (Rhee et al., 2000). Other important targets of oxidative cysteine modification range from mitochondrial fusion and fission proteins (Shutt et al., 2012) to transcription factors (e.g. Nrf2) (García-Santamarina et al., 2014).

1.4.1.2 Transitional metal centers

Transition metals such as Fe^{2+} and Cu^{2+} can cleave the O-O bond of H_2O_2 to generate hydroxyl radicals or activated metal complexes (Imlay, 2008). This reaction is called the Fenton reaction (although strictly speaking, Fenton chemistry refers only to iron). The ROS originated from this reaction are usually more reactive and less specific than H_2O_2 itself and are prone to initiate free radical reactions (Imlay, 2003). Although, their role in cell signaling has not been completely discarded (Winterbourn, 2013). For example, mROS produced from complex III activates HIF (Klimova and Chandel, 2008), and the presence of small molecules that selectively scavenge superoxide from complex III diminish HIF stabilization (Orr et al., 2015). Although, the exact mechanism is still unclear, one possible explanation is the oxidation of the Fe^{2+} required for PHD enzymes function, thereby reducing HIF- α degradation (Kaelin, 2005).

1.4.2 Hydrogen peroxide detection

Given the highly important role of redox-signaling in cellular function, measuring H_2O_2 formation should be a common practice in redox biology. However, currently available detection methods still display some limitations in terms of sensitivity, resolution and specificity in the detection of low H_2O_2 concentrations.

Three main classes of H_2O_2 -sensitive probes have been developed:

- 1) Horseradish peroxidase (HRP)- dependent probes
- 2) Boronates
- 3) Protein-based redox probes

From the probe classes mentioned above, the HRP-dependent probes are one of the most commonly used assays to detect H_2O_2 . These probes are reliable, simple and highly sensitive. Because of that, this assay has been largely applied in cell culture. In this class, the most used method of detection is the Amplex Red (Votyakova and Reynolds, 2004).

Amplex Red (10-acetyl-3,7-dihydroxyphenoxazine) is a colorless non-fluorescent compound (Zhou et al., 1997), which can be readily oxidized to resorufin in a H_2O_2 /HRP catalyzed reaction. Resorufin is a pink fluorescent compound that can be easily detected by fluorescence spectrophotometry. The sensitivity threshold for Amplex Red in H_2O_2 detection is 50nM (Zhou et al., 1997) and quantitative data can be obtained through comparison against a H_2O_2 standard curve.

Despite being a very robust assay, H₂O₂ detection is restricted to the extracellular space. Furthermore, because the probe is irreversibly oxidized, fluorescent probes do not typically permit measuring dynamic changes of redox signals in cells. To surpass this limitation a new set of fluorescent probes have been recently developed (Žamojć et al., 2016).

A promising class of H₂O₂-sensitive probes are the genetically encoded fluorescent redox sensors (reviewed in (Lukyanov and Belousov, 2014)). These probes utilize a combination of redox-sensitive cysteines with conformational changes of fluorescent proteins, which allows for easy detection of the cellular redox state. The two main types of genetically encoded sensors for H₂O₂ currently available are Hyper (from Hydrogen peroxide) and roGFP2-Orp1. From these two probes, Hyper is the most popular due to its sensitivity and easy manipulation. The main advantage of these probes is the visualization of compartmentalized redox signaling with real-time dynamics and subcellular resolution.

The first Hyper construct was developed in 2006 (Belousov et al., 2006). Currently four hyper constructs have been developed (Hyper 1-3 and Hyper-Red) with the newest versions possessing a higher sensitivity for H₂O₂ (Belousov et al., 2006; Bilan et al., 2013; Ermakova et al., 2014; Markvicheva et al., 2011). Hyper probes take advantage of the redox sensitivity of the prokaryote transcription factor OxyR. This bacterial transcription factor senses H₂O₂ and activates the expression of several antioxidant genes in response on increasing levels of H₂O₂, thus protecting the cells against oxidative stress (Choi et al., 2001). Basically, these probes consist of the H₂O₂-sensitive regulatory domain of the *E. coli* transcription factor OxyR with the circularly permuted yellow fluorescent protein (cpYFP). The C-terminal domain of the OxyR functions as a sensor for H₂O₂ by selectivity and reversibly reacting with H₂O₂. Oxidation of OxyR by H₂O₂ in Cys-199

and Cys-208 is coupled with conformational changes, which causes a fluorescence shift (**Figure 1.6**).

One major advantage of Hyper sensors is that they are ratiometric sensors, which enables the detection of small changes in signal concentrations and eliminates artifacts due to variations in loading/retention of the probe. Hyper has two excitation peaks at 420 and 500nm and a single emission peak at 516nm. Hyper oxidation by H_2O_2 alters the fluorescence excitation spectrum (i.e. it shifts the fluorescence intensities at 420 and 500nm) (**Figure 1.7**) (Belousov et al., 2006). On the other hand, Hyper-Red is an intensimetric probe, with one excitation peak at 575nm and one emission peak at 605nm (Ermakova et al., 2014). Hyper-Red is a red variant of Hyper obtained by replacing cpYFP with mApple.

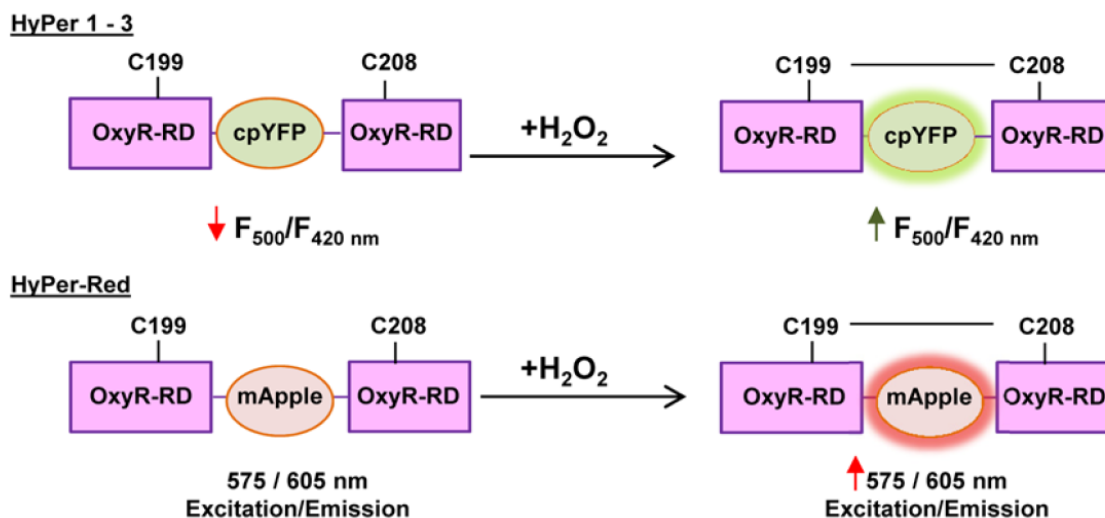


Figure 1.7 - Genetically encoded fluorescent biosensor Hyper for H_2O_2 measuring. Scheme of Hyper structure. cpYFP (Hyper 1-3) or mApple (hyper-Red) are fused with the redox sensitive OxyR. This sensor contains cysteines which upon oxidation by H_2O_2 triggers conformational changes in OxyR which alters the excitation features of these fluorescent proteins. Hyper 1-3 possess two excitations peaks with maxima at 420nm and 500nm and only one emission peak. Upon oxidation excitation peaks change ratiometrically. On the other hand, Hyper-Red measurements rely solely on fluorescent signal intensity, with one excitation peak at 575nm and one emission at 650nm. Reproduced from (Rezende et al., 2018).

In vitro, Hyper can detect as low as 25nM H₂O₂ and most importantly it can successfully discriminate between H₂O₂ and other ROS, such as O₂^{•-}, ONOO⁻ and •NO (Belousov et al., 2006). Additional benefits of these probes are their reversibility, real time measurements and subcellular specificity. The latter can be achieved by encoding protein-targeting sequences in the gene (Malinouski et al., 2011).

A caveat of these probes is their high sensitivity to pH changes within the physiological range (e.g. acidic conditions promote an increase in the intensity of the excitation peak at 420nm and a decrease at 500nm) (Belousov et al., 2006; Schwarzländer et al., 2011). This is of major importance since in many physiological and pathological processes pH changes are observed. In order to overcome that limitation a pH control named SypHer was developed (Cys-199 was replaced by Ser 199; Hyper-C199S) (Poburko et al., 2011). SypHer does not respond to H₂O₂ while maintaining Hyper's pH sensitivity. Due to its pH sensitivity, SypHer has become a useful tool to measure intracellular pH (Shirmanova et al., 2015).

1.5 Cell culture

1.5.1 Background

Cell culture is a powerful technique used since the 1960s by researchers worldwide with the goal of elucidating several cellular processes. Indeed, *in vitro* cell culture is the method of choice when studying cellular mechanisms that are not possible to be studied in an *in vivo* setting. Furthermore, cell culture has a wide application in the medical and industrial sector. Some of these applications include the production of recombinant proteins (e.g. monoclonal antibodies), as well as vaccine manufacture.

The main goal of using cell culture is to provide an isolated environment that emulates the physicochemical conditions of the tissue of origin. To achieve that, several important conditions of a cell's microenvironment, such as pH, buffering, osmolarity, temperature, amino acids, vitamins, viscosity, hormones, growth factors, antibiotics, serum, glucose and O₂ must be taken into consideration. However, cell culture still possesses some drawbacks. In the next few paragraphs a brief overview on how this useful technique was developed will be provided with the goal of enhancing the understanding *in vitro* cell culture pros and cons.

Cultivation experiments began in the late 19th-century with the culture of organs and animal tissue. Unfortunately, the cells did not survive in culture for too long (reviewed in (Yao and Asayama, 2017)). Because of that until the 1930's cell culture was considered a failure since it was difficult to manage and had almost no application. The first great leap in the cell culture technique did not come till the early 1940's with the development of immortal mouse fibroblasts (Earle et al., 1943). Healthy somatic cells stop growing after a certain number of divisions, a phenomenon later called the Hayflick limit (Hayflick and Moorhead, 1961), and as a result, researchers had to

use cells from fresh animal samples for each experiment. Therefore, in order to surpass this limitation (Earle et al., 1943) used carcinogens to successfully create an immortal cell line. In 1951, George O. Gey and his coworkers created an immortal cell line from a tissue of a patient with uterine cervical cancer, best known as HeLa cells (reviewed in (Lucey et al., 2009)). Their robustness, as well as their easiness to propagate, made HeLa cells an ideal *in vitro* research tool.

While cell line establishment was being perfected, important developments in cell media were also being made. In the 1950's, Harry Eagle developed the minimum essential medium (MEM) which is composed of the minimal essential components (glucose, six inorganic salts, 13 amino acids, eight water-soluble vitamins, and dialyzed serum) required for a proper cell growth (Eagle, 1955). Later, these media were modified by increasing the concentration of certain nutrients, such as glucose and glutamine, with the goal of avoiding nutrient exhaustion when leaving the culture unattended for longer periods of time. One such example, is the Dulbecco's modified Eagle's medium (DMEM), a standard cell culture media widely used in current's research labs.

In the last few decades, cell culture has seen enormous developments. However, very little attention has been paid to whether *in vitro* conditions do represent the *in vivo* physiological environment. Indeed, both media formulation (e.g. glucose content) and O₂ levels in cell culture are far from what is observed in normal physiological conditions. The main reason behind this lack of awareness is associated with the great convenience of working with cell cultures growing in ambient atmosphere O₂ and commercial media (i.e. without the necessity of media formulation optimization), as well as the absence of suitable methods and instruments for precise regulation of pericellular O₂ levels and media composition.

1.5.2 Influence of O₂ levels in cell culture

O₂ is an important constituent of the gas phase of the culture media, and while essential for appropriate cell culture, its concentration needs to be monitored. For example, while most cells in healthy human tissues experience O₂ levels ranging in between 0.5 - 10% (physioxia) (reviewed in (Carreau et al., 2011); **Table 1**) cell culture is usually carried in an hyperoxic (~18% O₂) environment (**Figure 1.8**) (reviewed in (Keeley and Mann, 2019)).

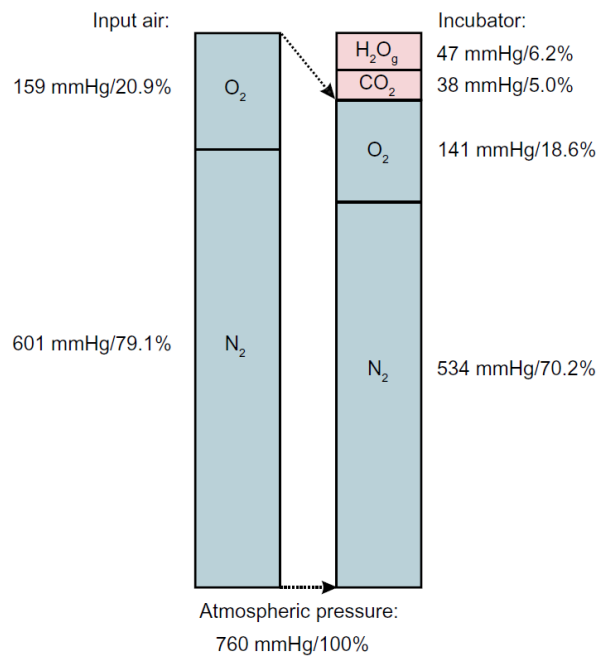


Figure 1.8 - Gas phase composition in a typical cell culture incubator. The left bar depicts the relative gas concentrations in dry air. The bar on the right is representative of the relative gas concentrations in a typical incubator where there is addition of CO₂ gas and water vapor at 100% humidity. Reproduced from (Wenger et al., 2015).

Table 1. Oxygen partial pressure (pO₂) values observed in various human tissues. pO₂ values, defined as the balance between oxygen delivery and its consumption, range from as low as 1% O₂ (e.g. mitochondria) to ~15% O₂ (e.g. alveoli). Of note, most tissues experience pO₂ values well below the ones experienced *in vitro*. pO₂ values are expressed in mmHg and in percentage of O₂. Reproduced from (Carreau et al., 2011).

	pO ₂	
	mmHg	%
Air	160	21.1
Inspired air (in the tracheus)	150	19.7
Air in the alveoli	110	14.5
Arterial blood	100	13.2
Venous blood	40	5.3
Cell	9.9–19	1.3–2.5
Mitochondria	<9.9	<1.3
Brain	33.8 ± 2.6	4.4 ± 0.3
Lung	42.8	5.6
Skin (sub-papillary plexus)	35.2 ± 8	4.6 ± 1.1
Skin (dermal papillae)	24 ± 6.4	3.2 ± 0.8
Skin (superficial region)	8 ± 3.2	1.1 ± 0.4
Intestinal tissue	57.6 ± 2.3	7.6 ± 0.3
Liver	40.6 ± 5.4	5.4 ± 0.7
Kidney	72 ± 20	9.5 ± 2.6
Muscle	29.2 ± 1.8	3.8 ± 0.2
Bone marrow	48.9 ± 4.5	6.4 ± 0.6

Ambient O₂ levels in cell culture influence several cellular processes, such as cell metabolism, differentiation, development and senescence (Parrinello et al., 2003; Timpano et al., 2019). One potential consequence of elevated O₂ in cell culture media is the increased cellular production of reactive oxygen and nitrogen species (Halliwell, 2003). Indeed, direct measurements with Amplex Red/horseradish peroxidase (see **section 1.4.2** for further detail) in cultured cells showed that, H₂O₂ efflux rate ($\mu\text{moles}\cdot\text{h}^{-1}\cdot 10^6 \text{ cells}^{-1}$) was higher for all cell lines growing at 18% O₂

(Maddalena et al., 2017), when compared to a more physiological relevant O₂ levels (5% O₂). This oxidative stress observed *in vitro* can affect important cellular functions (Holmström and Finkel, 2014).

O₂ levels in cell culture conditions were initially kept high to ensure that mitochondrial respiration was not limited by O₂ availability. Indeed, when highly confluent cells or cells growing in respiration-promoting media (for more information on *in vitro* manipulation of cellular energy metabolism see **section 1.6**) are grown at 5-6% headspace O₂, mitochondria respiration might be limited. However, typical cell culture O₂ levels are considerable higher (close to 10 times) than what is required for maximal mitochondrial respiration rates (Gnaiger, 2001; Hoffman and Brookes, 2009; Marcinek et al., 2003). This may have unintended consequences in several ROS producing enzymes that are widely expressed in several cell lines.

ROS are produced by a wide range of organelles and enzymes. A few important ones are the mitochondria, NOXs, xanthine oxidase/oxidoreductase, uncoupled nitric oxidase synthase, trans-plasma membrane redox system, cyclooxygenase, cytochrome P450 enzymes, monoamine oxidase and lipoxygenase. Interestingly, all of them possess different O₂ sensitivities. Therefore, it is expected that their activity/expression will differ widely in the range between physioxia and 18% O₂.

Mitochondria are often regarded as the major cellular ROS producers; however, this has yet to be demonstrated (Brown and Borutaite, 2012). Furthermore, complex I FMN site and complex III Q₀ site, which are considered the main sites of ROS production in culture cells, are both saturated at low O₂ levels (Hoffman and Brookes, 2009; Hoffman et al., 2007). Based on this observation, under standard cell culture conditions the rate of mitochondrial ROS production is likely not O₂-

limited, and therefore no significant difference is expected to be observed between physioxia and hyperoxia conditions.

O₂ levels in cell culture have been shown to affect NOXs protein expression (Diebold et al., 2010; Gregg et al., 2014; Stuart et al., 2018) and activity. NOX4 isoform has a K_m of ~18% O₂, and therefore its activity is highly sensitive to O₂ variations in the range between physioxia and 18% O₂. For example, between 3% and 12% O₂ NOX4 activity increases by 300% (Nisimoto et al., 2014). Furthermore, in our lab when NOX1 and NOX4 isoforms were selectively inhibited with GKTT138731, in cultured PC3 and C2C12 cells, a decrease in H₂O₂ efflux rate ($\mu\text{moles}\cdot\text{h}^{-1}\cdot 10^6\text{ cells}^{-1}$) at 18% O₂ was observed. However, no inhibitory effect was observed at 5% O₂ (Maddalena et al., 2017). Similarly, H₂O₂ efflux rate at 18% O₂ in NOXs knock-out mouse models (e.g. NOX1/2/4 triple knockout mouse dermal fibroblasts) is drastically reduced when compared to wild-type fibroblasts (Stuart et al., 2018). In addition to enzymatic-activity, O₂ levels in cell culture seem to influence NOXs expression. Indeed, several ROS-producing enzymes, including the NOXs enzymes are transcriptionally regulated by the transcriptional factor HIF-1 (Diebold et al., 2010; Goyal et al., 2004). On the other hand, both NOX1 and NOX4 protein levels were reduced at 18% O₂ versus 5% O₂ (Stuart et al., 2018).

Lastly, often inadequate terminology is used to describe O₂ levels in cell culture. For example, cells cultured in incubators without O₂ regulation are considered to be in a “normoxic” environment, while cells cultured in incubators at physiological O₂ levels are commonly referred as “hypoxic” (McKeown, 2014a). Consideration of this fact is of extreme importance when attempting to extrapolate results from *in vitro* findings to *in vivo* models of health and disease.

Failure to do so can lead to a low rate of reproducibility between *in vivo* and *in vitro* research findings (Al-Ani et al., 2018).

1.5.3 Influence of glucose levels in cell culture

Having sufficient nutrient levels in the medium is essential for appropriate cell growth. Indeed, depending on cell metabolic activity and proliferative rate, some cell types require higher levels of nutrients than others do. However, traditional synthetic cell culture does not take that into account, and most importantly they do not mimic human plasma (reviewed in (McKee and Komarova, 2017)). For example, *in vitro* cell cultures are conducted at high glucose concentrations (25 mM), which is around five-times what normal healthy cells experience. This poses a huge challenge when studying cell metabolism.

Cell lines have long been used to study metabolism, and while it is well known that cell metabolism is flexible (reviewed in (Lehuédé et al., 2016; Torrence and Manning, 2018)) and greatly influenced by environmental metabolites (reviewed in (DeBerardinis and Chandel, 2016)), little investigation has been done on how cell culture media composition impacts metabolism. For example, high glucose levels in cell culture media can lead to lactate accumulation and pH changes (reviewed in (Yao and Asayama, 2017)). Furthermore, high glucose has been associated with altered redox homeostasis, a process involving mitochondria and NADPH oxidase (Teshima et al., 2014). Indeed, an hyperglycemic state is associated with an increase in NADPH oxidases expression and/or activity (Manea et al., 2015).

1.5.4 Caveats of resveratrol's *in vitro* studies

Cell culture approaches have been widely used to study RES's effect in human health. However, most of these studies lack any physiological relevance. For example, RES concentrations used *in vitro* are often relatively high ($\geq 25\mu\text{M}$), when compared to the concentrations that are achieved *in vivo* (in the low micromolar range in the plasma) (Sergides et al., 2016), and therefore may lack some physiological relevance. Indeed, disparities between RES's *in vitro* and *in vivo* effects have been observed (Tomé-Carneiro et al., 2013); probably due to the low bioavailability of RES *in vivo* (Cottart et al., 2010; Walle et al., 2004). Both in humans and in rodents, RES is rapidly metabolized in the intestine after oral consumption. On top of that, the use of high doses of RES can trigger several cytotoxic effects such as oxidative damage and cell death (Madreiter-Sokolowski et al., 2016, 2017). In this thesis low concentrations of RES ($1\mu\text{M} - 10\mu\text{M}$) that are compatible with the plasma levels of free and metabolized RES reported in rodents and humans after oral consumption were used (Baur and Sinclair, 2006).

Furthermore, some of the cell culture parameters, such as O_2 and glucose levels do not mimic the *in vivo* conditions. As mentioned previously, O_2 levels influence the rates of ROS production, with a direct correlation between O_2 levels and ROS production (Maddalena et al., 2017). Therefore, RES's health benefits, which are modulated by ROS, need to be assessed at more physiological levels.

1.6 *In vitro* manipulation of cellular energy metabolism

Cultured cells are usually grown in conditions that stimulate high rates of proliferation. Under these conditions, cells are highly reliant on aerobic glycolysis, to meet the metabolic requirements. Therefore, by providing an alternative carbohydrate source in culture media it is possible to manipulate the cellular energy metabolism. A common way to increase reliance on oxidative phosphorylation is to replace glucose with galactose in cell culture (Aguer et al., 2011; Marroquin et al., 2007). Galactose can be converted to glucose (through a process named Leloir pathway), however, this multi-step conversion is relatively slow (Holden et al., 2003). This limits the rate of ATP formation from aerobic glycolysis, and consequently cell proliferation. As a result, growth of mammalian cells in galactose media increases the contribution of oxidative phosphorylation to glucose oxidation (Rossignol et al., 2004a). To achieve this, cells are forced to utilize other metabolic substrates provided in the cell culture medium for ATP generation (DeBerardinis et al., 2007). An important amino acid present at high concentrations in culture media is glutamine, and a higher reliance on glutamine to meet cell metabolic requirements leads to an increased cellular O₂ consumption and lowered glycolytic activity (Rossignol et al., 2004a). In the same way, cells growing in a more physiological glucose (5mM glucose) rely more on oxidative phosphorylation to meet their metabolic requirements, when compared to the standard cell culture hyperglycemic media.

1.7 Study aims and general hypothesis

One of the most robust and studied effects of RES is its anti-proliferative properties (Stuart and Robb, 2013). However, the molecular mechanisms behind these properties are still not well defined.

The first part of my study involved the **investigation of key contributors to RES's anti-proliferative properties. (Figure 1.9).** To achieve the study goals several *in vitro* approaches aimed at manipulating cells' metabolism were used (**Figure 2.2**). Metabolic rewiring towards aerobic glycolysis is an important hallmark of cancer cells and HIF-1 activation is an important step in this process.

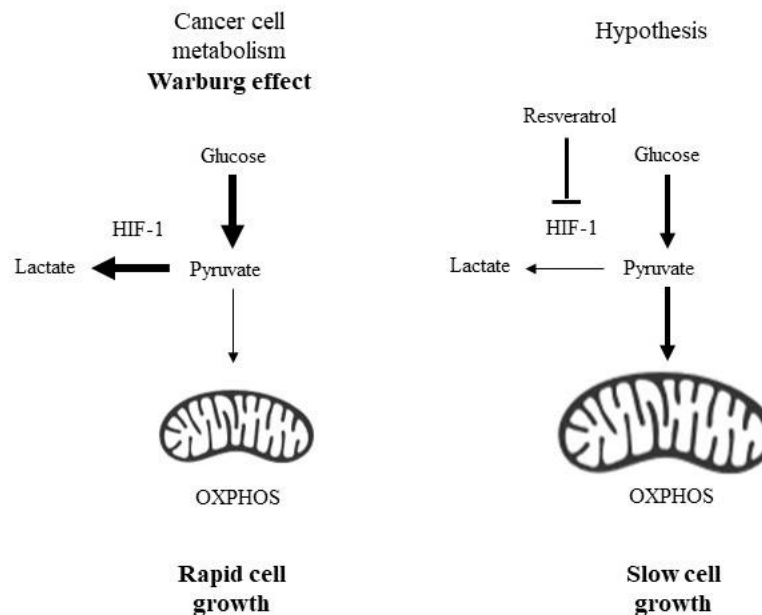


Figure 1.9 Chapter 2 hypothesis. The image on the left shows a simplified version of the preferred metabolic pathway of cancer cells (i.e. glucose fermentation). The image on the right shows a possible mechanism by which RES promotes its *in vitro* anti-proliferative effects. Here, I hypothesize that RES would inhibit *in vitro* cancer cell growth of a prostate cancer cell line (PC3) via reversal of the Warburg effect (i.e. increase reliance on OXPHOS as main source of ATP). This might be achieved by decreasing the expression of HIF-1 (a key transcription factor involved in the glycolytic pathway). Bold arrows indicate the preferred metabolic pathway. A bigger mitochondrion represents a higher reliance on OXPHOS as source of ATP.

Given the importance of O₂ levels and cells' metabolism (i.e. induction of a metabolic reprogramming) on RES's anti-proliferative *in vitro* effects, the second part of my study was aimed at **investigating the implications that non-physiological *in vitro* conditions have on RES *in vitro* effects (Figure 1.10)**. More specifically, I'll be looking at how supraphysiological glucose (25mM) and O₂ levels (~18% O₂), affect some of RES key targets, such as cell growth, mitochondria morphology and ROS production, when compared to more relevant physiological conditions (glucose – 5mM; O₂ – 5% O₂).

This part of the study involved the culture of C2C12 mouse myoblasts and PC3 human prostate cancer cells (two commonly studied cell lines in which RES *in vitro* effects have been well characterized) under different conditions of O₂ and glucose levels and the characterization of cell growth, hydrogen peroxide production and mitochondrial dynamics.

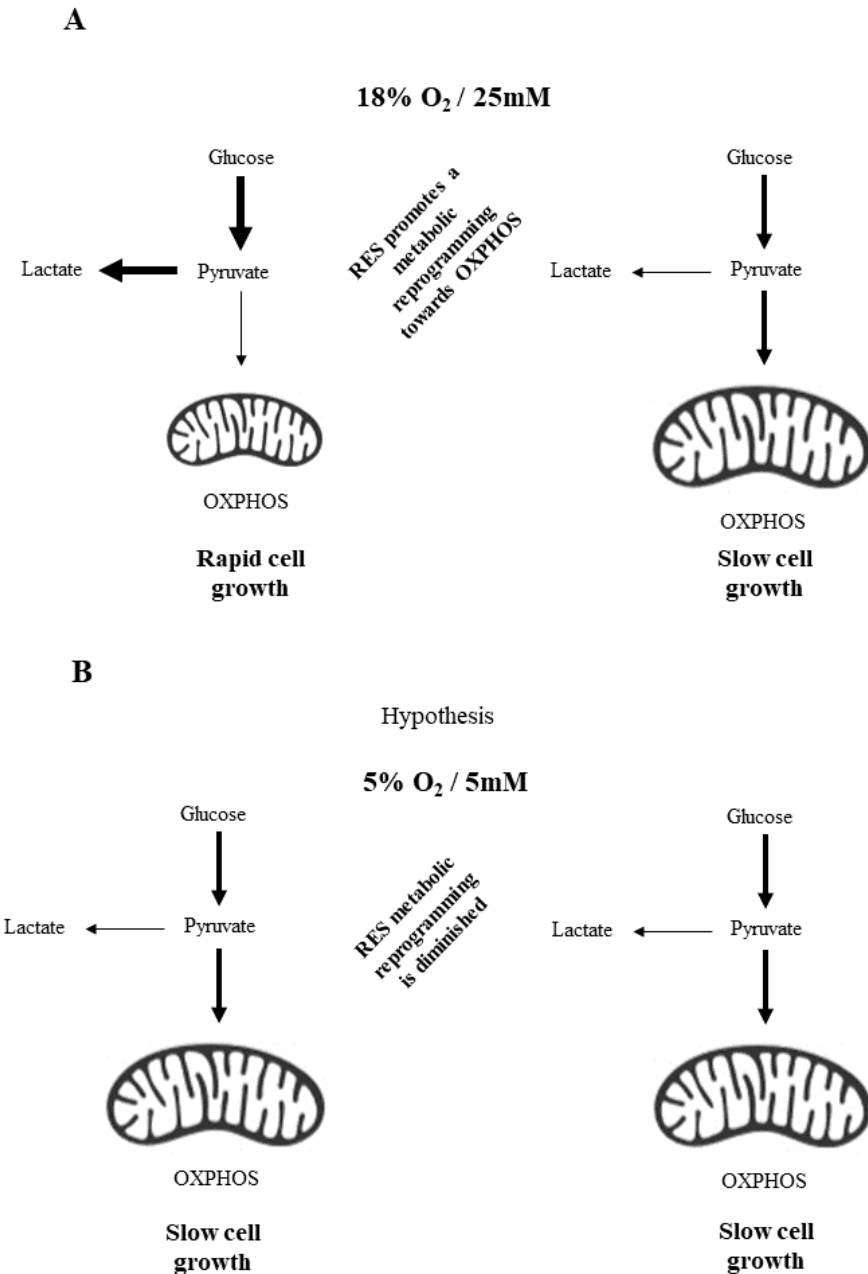


Figure 1.10 Chapter 3 hypothesis. Under standard cell culture (18% O₂/5mM glucose) conditions RES promotes a metabolic reprogramming, which slows cell growth (**A**). On the other, under physiological conditions (here represented as 5% O₂/5mM glucose) (**B**), I hypothesized that cells would be already relying on OXPHOS as a main source of ATP, and therefore RES effects on cell growth would be diminished. Of note, key mediators of RES *in vitro* effects, such as ROS and mitochondria morphology are influenced by O₂ and glucose levels. Therefore, I also hypothesized that RES *in vitro* effects on both mitochondria morphology and ROS production would be affected by these parameters. Bold arrows indicate the preferred metabolic pathway. A bigger mitochondrion represents a higher reliance on OXPHOS as source of ATP.

Chapter 2. Resveratrol stimulates a shift toward oxidative metabolism that underlies the growth its growth inhibition effects on PC3 prostate cancer cells

Hypothesis

A metabolic reprogramming toward oxidative metabolism is required for RES-mediated growth inhibition in PC3 cells. Given the role of HIF-1 as a metabolic regulator, this metabolic reprogramming involves HIF-1 regulation, and therefore RES might be a particularly effective inhibitor of PC3 cell growth under hypoxic condition (e.g. *in vivo* tumors).

Objectives

The objectives of this project are to: **1)** Determine whether a metabolic shift toward oxidative phosphorylation is a requirement for RES-mediated growth inhibition effects; **2)** Evaluate the importance of HIF-1 regulation in RES's growth inhibition effects

Publication of results

Fonseca, J., Moradi, F., Maddalena, L., Ferreira-Tollstadius, B., Selim, S., & Stuart, J. (2019). Resveratrol integrates metabolic and growth effects in PC3 prostate cancer cells-involvement of prolyl hydroxylase and hypoxia inducible factor-1. *Oncology Letters*, *17*, 697–705. <https://doi.org/10.3892/ol.2018.9526>

Contributions

JS and JF conceived and supervised experiments. JF, FM, LAM, BFT, and SMS performed experiments. JF performed all data analysis. JS and JF wrote the manuscript.

2.1 Introduction

Cancer cells use exceptionally high rates of glucose catabolism to produce ATP, NADPH, and anabolic building blocks needed for the production of daughter cells, a metabolic phenotype termed ‘the Warburg effect’ (Diaz-Ruiz et al., 2011; Vander Heiden et al., 2009; Pavlova and Thompson, 2016). Although the Warburg effect was originally attributed to mitochondrial defects compromising oxidative phosphorylation, it is now appreciated to occur in cells with competent oxidative phosphorylation (Koppenol et al., 2011). Strategies targeting the Warburg effect by inhibiting glucose fermentation and shifting cellular metabolism toward oxidative phosphorylation can slow the growth of cancer cells (Fantin et al., 2006; Le et al., 2010). Since hypoxia inducible factor-1 plays a key role in establishing the Warburg phenotype, this protein in particular is an important target for inhibiting cancer growth (Greer et al., 2012; Masoud and Li, 2015).

The plant polyphenol RES inhibits cell cycle progression (Han et al., 2015) and thus proliferative growth in many cancer cell lines (Stuart and Robb, 2013). Coincident with these growth inhibitory effects, RES promotes mitochondria network fusion (Robb et al., 2017), mitochondrial biogenesis, and oxidative phosphorylation (De Oliveira et al., 2016) in a variety of cancer cell lines. Thus, RES appears to reverse the Warburg effect in many cancer cells. RES has also been reported to reduce HIF-1 expression in vitro (Zhang et al., 2005) and in vivo (Zhang et al., 2014), suggesting that this could underlie the metabolic phenotype.

Here I used PC3 prostate cancer cells, in which RES inhibits growth and reduces HIF-1 α levels to investigate the interactions between RES’s effects on the metabolic phenotype and growth. I show that the inhibition of PC3 cell growth by treatment with 10 μ M RES is coincident with increased mitochondrial network fusion, biogenesis, and respiration. I then prevented RES-

induced metabolic switching from the glycolytic to oxidative metabolism by growing cells in galactose medium, which does not support glucose fermentation (Rossignol et al., 2004b) or stabilizing HIF-1 α using pharmacological or genetic approaches. Under these conditions, the effects of RES on growth and metabolism were either attenuated or abolished. These observations suggest that the metabolic and growth effects of RES on PC3 cells are inter-dependent. The ability of RES to reduce HIF-1 α levels suggests that it could be particularly effective in hypoxic conditions, as are common in growing tumours. Indeed, RES inhibited PC3 cell growth more strongly and at lower concentrations under hypoxic conditions. These observations have important implications for understanding how RES may inhibit cancer growth under conditions prevailing in vivo.

2.2 Material and Methods

2.2.1 Materials

Dulbecco's Modified Eagle Medium high glucose (4500 mg/L) containing L-glutamine, sodium pyruvate and sodium bicarbonate (Cat. #D6429), supplement-free Dulbecco's Modified Eagle Medium powdered media (Cat. #D5030), fetal bovine serum (Cat. #F1051), non-essential amino acids, penicillin/streptomycin solution, 0.25% trypsin/EDTA solution, bovine serum albumin (BSA), Glucose Oxidase from *Aspergillus niger* (Cat. #G2133), Horseradish Peroxidase (2KU; Cat. #P6140), Bradford reagent (Cat. #B6916), IOX2 (Cat. #SML0652), MG132 (Cat. #C2211) and deferoxamine mesylate salt (DFO; Cat. #D9533) were obtained from Sigma-Aldrich (St. Louis, USA). *trans*-RES (Product #70675) was purchased from Cayman Chemical (Ann Arbor, MI, USA). Dimethylsulfoxide (DMSO), DL-dithiothreitol (DTT), Bradford reagent, D-

galactose, L-glutamine, HEPES ((4-(2-hydroxyethyl)-1-piperazineethanesulfonic acid) and Trypan blue were obtained from BioShop (Burlington, ON). Tissue culture dishes (100x20 mm & 60x15 mm) and cell scrapers were obtained from Sarstedt, Inc (Newton, SC, USA). MitoTracker Red CMXRos and Lipofectamine 2000 transfection reagent was purchased from Life Technologies Incorporated (Burlington, ON, Canada). Polyvinylidene difluoride (PVDF) membranes were purchased from BioRad (Hercules, CA, USA). Mouse anti-human HIF-1 α (Product #610958; Lot #5174837 and Product #610959; Lot #4073775) was obtained from BD Biosciences (Franklin Lakes, NJ, USA). Rabbit polyclonal Lamin B1 antibody (Product #ab16048; Lot #GR-263244-1) was obtained from Abcam (Cambridge, UK). Ham's F12 Nutrient Mix powdered media (Cat. #21700-075) and Alexa Fluor® 647-conjugated secondary (IgG) antibody against mouse (Cat. #A-31571; Lot #1069838) were purchased from ThermoFisher (Scientific Waltham, MA, USA). Goat anti-mouse (Cat. sc2005; Lot #C0316) and goat anti-rabbit (Cat. sc2030; Lot #C2204) horseradish peroxidase conjugated (IgG-HRP) secondary antibody were obtained from Santa Cruz Biotechnology (Dallas TX, USA). EMD Millipore™ Immobilon™ Western Chemiluminescent HRP substrates were obtained from Millipore (Burlington, MA, USA). HA-HIF1 α -pcDNA3 (plasmid #18949), and HA-HIF1 α P402A/P564A-pcDNA3 (plasmid #18955) were purchased from Addgene (Cambridge, MA, USA). Human HIF-1 α recombinant protein (Cat. #GWB-184E1F) was purchased from GenWay Biotech, Inc. (San Diego, CA, USA).

2.2.2 Cell lines and culture conditions

PC3, LNCaP, C2C12, and SHSY5Y cell lines were acquired from ATCC and cultured in high glucose DMEM unless otherwise indicated. For experiments performed in galactose medium, cells grown in glucose were harvested and then seeded in glucose-free DMEM supplemented with 10mM galactose, 6mM L-glutamine, 10mM HEPES, 1mM sodium pyruvate for at least 3 days before starting experiments. Cells were cultured at 37°C in humidified 5% CO₂ atmosphere, 18% O₂ atmosphere, unless otherwise indicated. Cell density and population doubling time were determined by hemocytometer counting using Trypan Blue exclusion to identify live cells. Treatments were added directly to the culture media for 48h. Media and treatments were refreshed every day.

2.2.3 Hypoxia conditions

For atmospheric hypoxia experiments, cells were grown within a humidified hypoxia modulator incubator chamber (MIC-101; Billups-Rothenberg) maintained at ≤ 0.4 O₂%, 5% CO₂ with the aid of a Roxy-1 Universal O₂ Controller (Sable Systems, USA). Culture media was refreshed daily with pre-conditioned hypoxic media kept in the same chamber. Alternatively, in some experiments (where indicated) ‘pseudo-hypoxia’ was induced through chemical means via treatment with the PHD inhibitor IOX2 (25 μ M). Cells were incubated overnight with IOX2 prior to commencing experiments of interest.

2.2.4 Preparation of whole cell lysates

Cells were harvested and washed in PBS then lysed in ice cold lysis buffer (10mM Tris pH 8.0, 150mM NaCl, 2mM EDTA, 2mM DTT, 40% glycerol (v/v), 0.5% (v/v) NP40) with either periodic vortexing or sonication (Ultrasonic Inc., Sonicator W-375; setting 3) for 30 minutes on ice. Subsequently, lysates were centrifuged at 10,000 x g at 4°C for 10 minutes (Thermo Scientific, IEC, Micromax/Micromax RF) and the pellet discarded. The protein concentration of the resulting supernatant was determined by the Bradford method. BSA was used as the protein standard. Cell lysates were stored at -80°C.

2.2.5 Preparation of nuclear lysates

Cells were lysed on the plate with cold homogenization buffer (10mM HEPES pH 7.9, 1.5mM MgCl₂, 10mM KCl, 2mM DTT, 2mM MG132, 200µM DFO), with subsequent centrifugation at 450 g for 5 min. After centrifugation, the cell pellet was resuspended in 200µL homogenization buffer and disrupted with the aid of a pre-chilled glass pestle and tube. The homogenate was then centrifuged for 10 minutes at 10,000 x g at 4°C and the pellet was gently re-suspended in 150µL of extraction buffer (20mM HEPES pH 7.9, 1.5mM MgCl₂, 1.4M KCl, 0.2mM EDTA, 25% glycerol, 2mM dithiothreitol, 2mM MG132, 200µM DFO), followed by a 30 minute incubation on ice in an orbital shaker (Madell Corporation, USA). After incubation, cell lysates were centrifuged at 15,000 x g (4°C) for 30 minutes (Thermo Scientific, IEC Micromax/Micromax RF). The supernatant was then transferred to a fresh centrifuge tube and stored at -80°C.

2.2.6 Lactate Dehydrogenase activity

Lactate dehydrogenase (LDH) activity was measured in a solution containing 20mM HEPES buffer (pH 7.3), 0.2mM NADH, 10mM pyruvate and 5 μ g of sample protein. The conversion of NADH to NAD⁺ after pyruvate addition was followed spectrophotometrically (340nm) using a Varian Cary 100 UV-visible spectrophotometer (Agilent Technologies, Santa Clara, CA, USA). Assays were performed at 30°C.

2.2.7 Western blots

Equal amounts of protein (25 μ g) from nuclear cells lysates were electrophoretically separated in a 6% glycine based SDS-PAGE gel. Separated proteins were then transferred onto a polyvinylidene difluoride (PVDF) membranes using a semi-dry transfer setting on a BioRad Trans-Blot Turbo transfer apparatus.

Fluorescent detection:

Membranes were blocked for an hour at room temperature and incubated overnight at 4°C independently with primary antibodies to HIF-1 α (1:100; *w/v*) or the nuclear loading control Lamin B1 (1:500; *w/v*). Incubations with either an Alexa Fluor 647-conjugated anti-mouse antibody (1:500; *w/v*) or an infrared fluorophore-conjugated anti-rabbit antibody (1:1000; *w/v*) were performed at room temperature (2h). Membranes were visualized using a VersaDoc MP 4000 Imaging System (BioRad).

Chemiluminescent detection:

Blotted membranes were blocked for an hour at room temperature with a 3% (w/v) BSA/TBS-t solution. Next, membranes probed with primary antibody directed against HIF (1:500), Lamin B1 (1:1000) diluted in 3% (w/v) BSA/TBS-t solution. After this, HIF-1 and Lamin B1 membranes were immunoprobed at room temperature (1h) with goat anti-mouse (1:1000) and goat anti-rabbit (1:2000) horseradish peroxidase conjugated secondary antibody, respectively. The antigen-antibody complexes were detected with EMD Millipore™ Immobilon™ Western Chemiluminescent HRP substrate using a C-Digit® Blot Scanner (LI-COR, NE,USA). Densities of protein bands were quantified using Image Studio™ (LI-COR).

2.2.8 Glucose oxidase activity

Cellular glucose uptake was assessed by observing the generation of Amplex Red reagent red-fluorescent oxidation product, resorufin, in a Varian Cary Eclipse fluorescence spectrophotometer equipped with a microplate reader (Agilent Technologies, Santa Clara, CA, USA). Briefly, 5×10^5 cells were seeded in high glucose DMEM and then treated with either RES or DMSO for 48h at 0.4% O₂ (hypoxia). After 48h the cells were incubated under the same conditions for 5h in a 5mM glucose media. A sample of the media was then mixed with a solution containing HEPES buffer (20mM, pH 7.3), Glucose oxidase from *Aspergillus niger* (0.1U/mL), Horseradish peroxidase (0.2U/mL) and Amplex Red (50μM). The formation rate of resorufin was continuously measured for a period of 3 minutes by using excitation and emission wavelengths of 535nm and 595nm, respectively. Maximal reaction rates [Arbitrary Fluorescence Units (AFU) per

minute] were calculated during the reaction linear range by using the Cary Eclipse Kinetics software (Walnut Creek, USA). For each experiment a standard curve was used to quantify glucose concentration in media. At the end of each experiment, cells were counted in order to assess cell density and glucose uptake was converted into $\text{nmol glucose} \cdot 10^6 \text{ cells}^{-1} \cdot \text{min}^{-1}$.

2.2.9 Plasmid DNA transfections

HA-HIF1alpha P402A/P564A-pcDNA3 (Addgene plasmid #18955) and HA-HIF1alpha-pcDNA3 (Addgene plasmid #18949) were gifts from William Kaelin. pC1-Hyper-3 (Addgene plasmid #42131) was a gift from Vsevolov Belousov. Plasmid DNA was initially isolated and purified from bacterial cultures via a plasmid DNA Miniprep Kit (Norgen Biotek, Canada). Plasmid DNA purity (260 nm/280 nm absorbance ratio) and concentration were assessed by using a NanoPhotometer (Montreal Biotech Inc., Canada) Transfections were performed with Lipofectamine 2000 reagent in accordance with manufacturer's instructions. PC3 cells stably expressing HA-HIF1alpha P402A/P564A-pcDNA3 or HA-HIF1alpha-pcDNA3 were selected and maintained with G418.

2.2.10 Fluorescence microscopy and image analysis

Fluorescence images using structured illumination of live PC3 cells were obtained using a Zeiss Axio Observer.Z1 inverted light/epifluorescence microscope equipped with ApoTome.2 optical sectioning and a Hamamatsu ORCA-Flash4.0 V2 digital camera. Cells were cultured on

MatTek 35 mm poly-D-lysine-coated glass bottom culture dishes with phenol red-free culture media and were viewed with a Plan-Apochromat 63x/1.40 oil objective. The microscope stage was maintained at 37°C and 5% CO₂ (O₂ levels were not regulated). MitoTracker Red CMXRos signal was imaged using excitation and emission wavelengths of 587 nm and 610 nm, respectively. Mitochondrial network morphology in MitoTracker Red-labelled PC3 cells were quantitatively analyzed using the ImageJ tool “MiNA” (Valente et al., 2017).

2.2.11 Cell cycle analysis

Approximately 5×10^5 cells were harvested via trypsinization and centrifugation (5 minutes at 240 x g). The resulting pellets were washed once with PBS and then fixed via drop-wise addition of ice-cold ethanol (75% v/v) with routine vortexing. After an overnight incubation at -20°C, the suspension was centrifuged (5 minutes at 240 x g) and washed twice with ice-cold PBS. The fixed cells were then incubated with 0.5 mL Propidium Iodide (PI) / RNase Staining Buffer (BD Pharmingen, USA) in darkness at room temperature for 15 minutes. The DNA content was immediately measured using a BD Accuri C6 flow cytometer (BD Biosciences, USA). The PI signal was detected using a 562-588nm band pass filter. For each sample, 100,000 events were recorded using a medium data acquisition rate, as per the manufacturer guidelines. The percentages of cells in G₀-G₁, S, and G₂-M phases were determined using the CFlow Plus software (BD Biosciences, USA).

2.2.12 Cellular respiration measurements

O₂ consumption rates of intact cultured cells were measured using a Clark-type oxygen electrode (Rank Brothers Dual Digital Model 20 Respirometer; Bottisham, UK) within a chamber maintained at 37°C. Cells were harvested via trypsinization and centrifugation before being re-suspended in 1 mL of complete culture media. Maximal was measured in the presence of the uncoupler FCCP. The chamber was capped and the rate of O₂ consumption was recorded via an attached polygraph unit. All respiration rates were converted to nanomoles O₂ consumed·minute⁻¹·10⁶ cells⁻¹.

2.2.13 Statistics

Where appropriate T-tests were performed using Microsoft Excel (Redmond, USA). T-tests (unpaired, two-tailed) were used for data sets containing two experimental groups. P-values < 0.05 were considered significant for all statistical tests. For data sets including more than two experimental groups, ANOVA followed by Bonferroni comparisons of means were performed using GraphPad Prism 5 software (San Diego, USA).

2.3 Experimental design

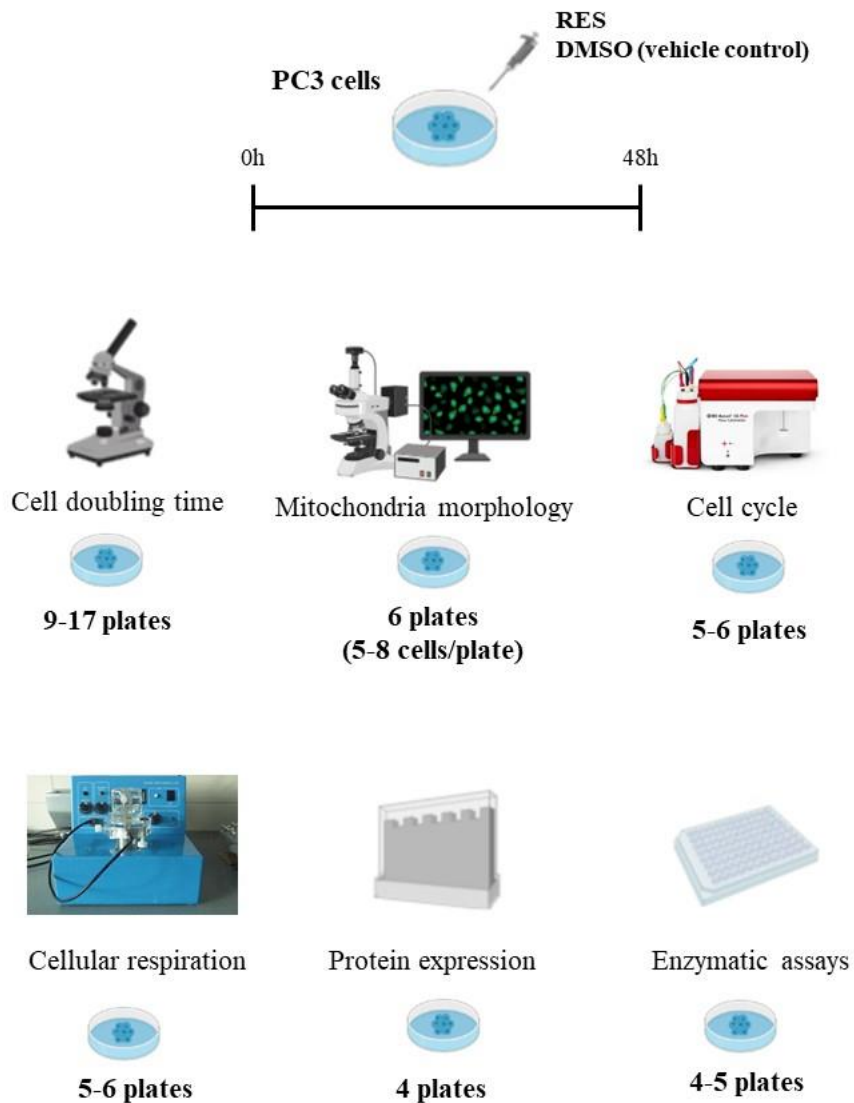


Figure 2.1 Experimental design. PC3 cells were seeded overnight and treated for 48h with RES or the vehicle control DMSO. Biological replicates for each experiment are also represented in the figure.

2.4 *In vitro* models

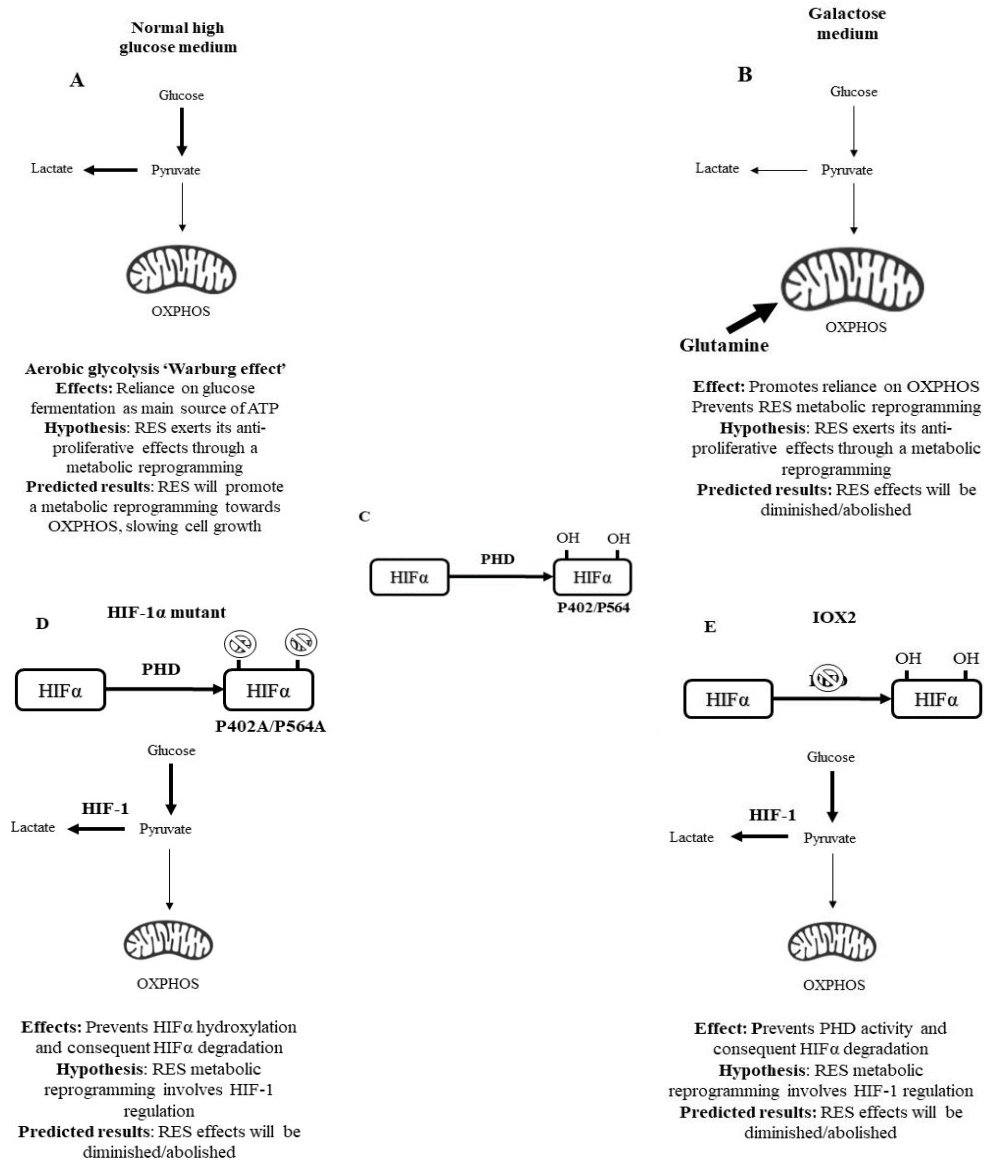


Figure 2.2 Chapter 2 *In vitro* models, hypothesis and predicted results. (A) At standard cell culture conditions, cancer cells' main source of ATP is through glucose fermentation. Under these conditions, I predict that RES *in vitro* antiproliferative effects are promoted by a metabolic reprogramming towards OXPHOS. However, when this metabolic reprogramming is prevented by either growing cells in galactose (B) or increasing HIF-1 levels (this can be achieved by using a HIF-1 α mutant cell line (D) or by treating cells with the specific PHD2 inhibitor, IOX2 (E)) I hypothesized that RES *in vitro* anti-proliferative effects would be diminished/abolished. (C) Post-translational mechanism of HIF-1 regulation. Under normoxic, conditions PHD hydroxylates HIF-1, which is then sent for degradation.

2.5 Results

In PC3 cells growing in high glucose media, 48h treatment with 10 μ M RES stimulated cellular respiration rates (basal respiration – DMSO vs RES, **p=0.0067**; Maximal respiration – DMSO vs RES, **p=0.0129**; **Fig. 2.3A**), mitochondrial biogenesis (measured here as ‘mitochondrial footprint’, i.e. area of cell image occupied by mitochondria, **p<0.0001**; **Fig. 2.3B**) and increased the mean mitochondrial network size (number of branches per network, **p=0.0091**; **Fig. 2.3B**). On the other hand, number of rods/puncta (**p=0.0687**) and number of networks (**p=0.1246**) were not altered by RES treatments. At the same time, RES-treated cells showed a reduced growth rate, **p<0.0001** (**Fig. 2.3C**) and an increase in G0/G1 phase arrest, **p=0.003**. The opposite was observed for the G2/M phase, **p= 0.0046** (**Fig. 2.3D**). Of note, this effect may be partially explained by RES ability to modulate intracellular H₂O₂ levels (**Appendix S1.1**), a key regulator of cell growth and proliferation (Sarsour et al., 2014)

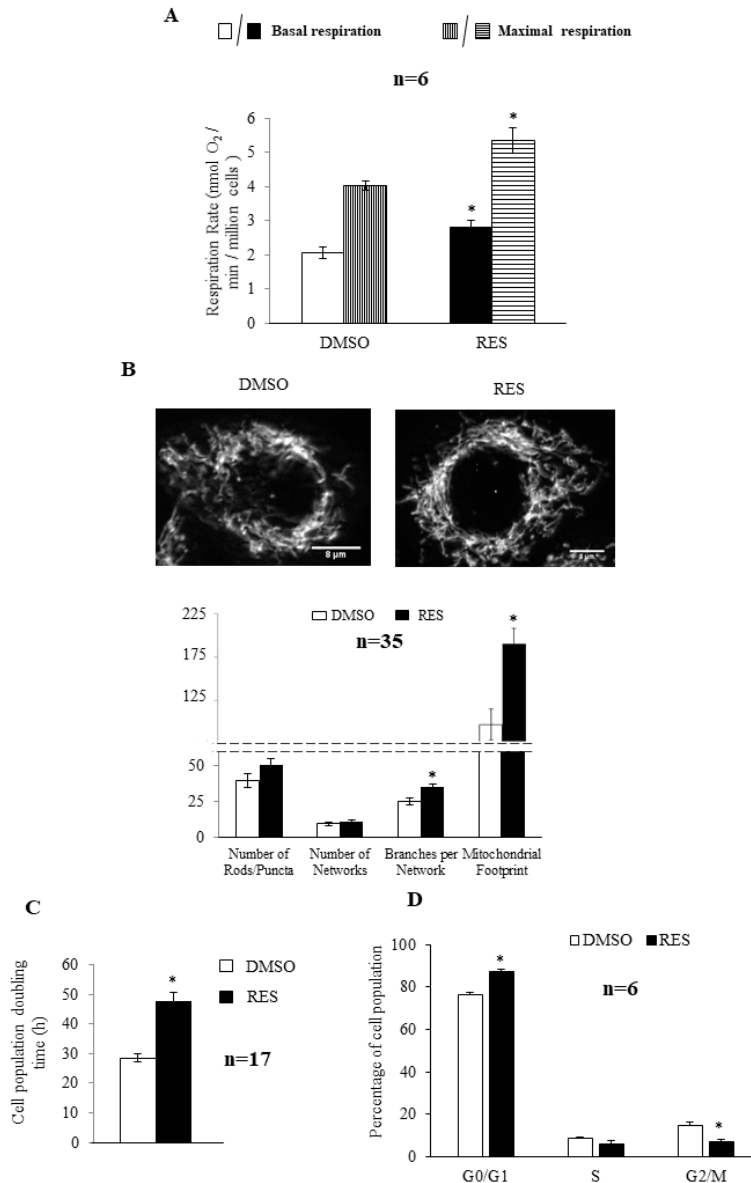


Figure 2.3. RES stimulates PC3 cell respiration and mitochondrial fusion while slowing cell growth. (A) RES increased basal (open bar; solid bar) and FCCP (carbonylcyanide-p-trifluoromethoxyphenylhydrazine) uncoupled (vertical striped bar; horizontal stripe bar) cellular respiration rates. (B) In the same experiment, RES stimulated increased mitochondrial fusion (mean number of branches per network) and mitochondrial footprint (area of cell image occupied by mitochondria); number of puncta/rods, networks and branches per network are counts, mitochondrial footprint is area in μm^2 . Total magnification – 630x. (C) Population doubling time increased and the (D) distribution of cells in different cell cycle phases was altered such that cells accumulated in G0/G1. In all experiments, PC3 cells were treated for 48h with 10 μM RES (filled bars) or an equal volume of DMSO (open bars). Data shown are means \pm SEM. ‘*’ = difference between RES-treated and DMSO vehicle control cells. P values were calculated by t-test (unpaired, two-tailed).

To investigate the potential role of the metabolic shift toward oxidative phosphorylation in RES's growth effects, the experiment was repeated using PC3 cells cultured in the same medium but with galactose replacing glucose as carbon fuel. Cells growing in galactose medium cannot meet ATP demand by glucose fermentation and become reliant on oxidative phosphorylation (Rossignol et al., 2004b). Growth in galactose medium increased respiration rates relative to high glucose medium ($F_{1,20}=13.27$, $p=0.0016$) (Fig. 2.4A) but abolished the RES effect on these rates ($p=0.1296$). Similarly, while the mitochondrial footprint ($p<0.0001$) (Fig. 2.4B) was greater in galactose medium compared to glucose medium, the effect of RES on this parameter was absent ($p=0.9436$). Other mitochondrial network features were also not affected by RES treatment in cells growing in galactose (number of rods/puncta, $p=0.4898$; number of networks, $p=0.6867$, branches per network, $p=0.8548$) (Fig. 2.4B). Coincidentally with the absence of metabolic effects, RES did not inhibit PC3 cell growth, $p=0.7396$ (a main effect of media was observed $F_{1,54}=28,92$ $p<0.0001$) (Fig. 2.4C) or cell cycle distribution (G0/G1 – $p=0.8581$; S – $p=0.9981$; G2/M – $p=0.8586$) (Fig. 2.4D) in galactose medium. Thus, in the absence of a switch between glycolytic and oxidative metabolism RES had no metabolic or growth effects.

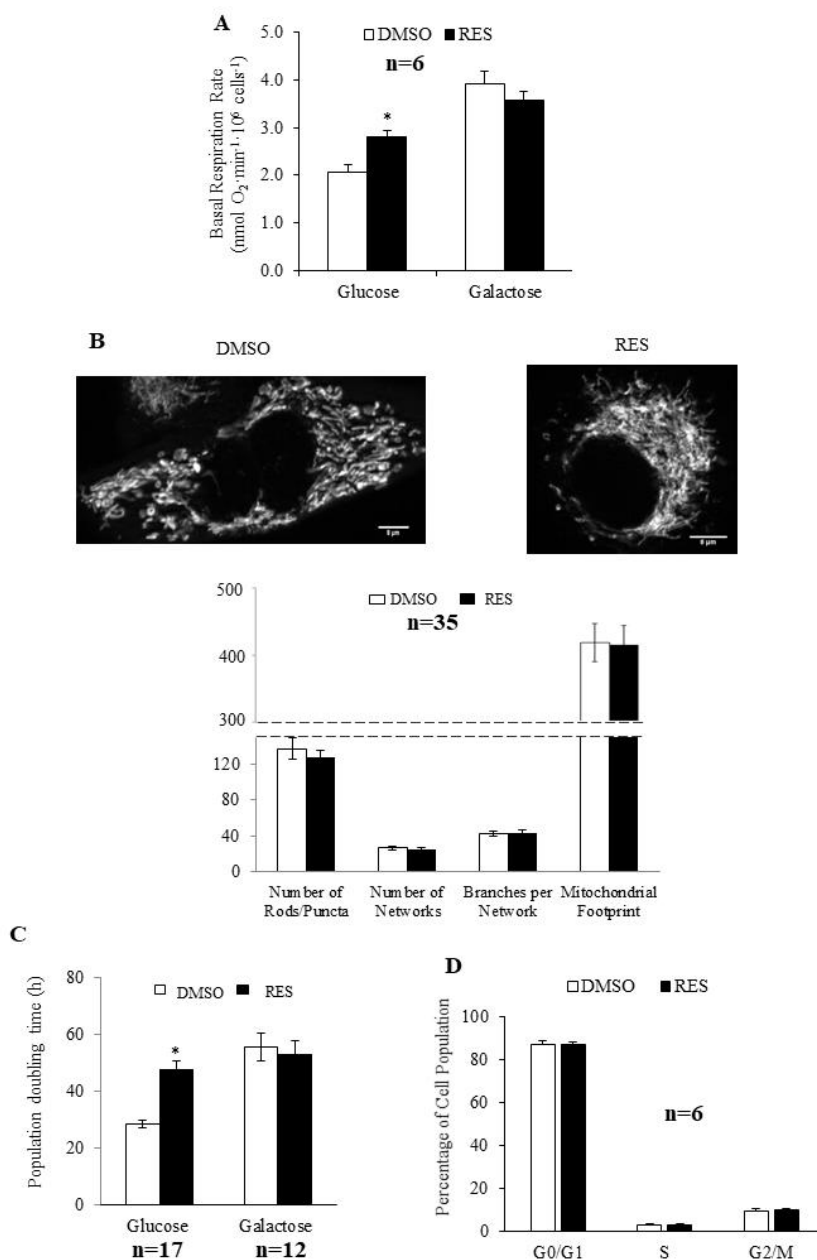


Figure 2.4. Growth in galactose medium abolishes effects of RES. No effect of RES on (A) respiration or (B) mitochondrial network characteristics (number of puncta/rods, networks and branches per network are counts, mitochondrial footprint is area in μm^2 ; Total magnification – 630x) when PC3 cells were grown in galactose medium. Similarly, RES had no effect on (C) cell growth or (D) cell cycle distribution. Experiments were done as in Figure 1, but cells were cultured in galactose medium (without glucose) except where indicated. In all experiments, cells were treated for 48h with 10 μM RES (filled bars) or an equal volume of DMSO (open bars). ‘*’ = difference between RES-treated and DMSO-treated cells. P values were calculated by ANOVA (A, C) followed by post-hoc analysis and t-test (unpaired, two-tailed) (B, D).

Given the role of HIF-1 as a metabolic regulator, and previous reports of RES effects on HIF-1 activity (Huang et al., 2014a, 2014b), I hypothesized that the metabolic switch observed with RES involves HIF-1 regulation. HIF-1 heterodimer activity is regulated by HIF-1 α levels, which are in turn regulated by the hydroxylation by prolyl hydroxylases (PHDs) of key prolines 402 and 564. I used two strategies to prevent this proline hydroxylation and thus stabilize HIF-1 α in PC3 cells growing in high glucose medium: PC3 cells were either stably transfected with a mutant HIF-1 α lacking prolines 402 and 564 (Yan et al., 2007) or were treated throughout the experiment with IOX2. IOX2 is a selective PHD inhibitor that stabilizes HIF-1 α in normoxia (Sen et al., 2013).

HIF-1 α was detectable in cells stably expressing the mutant protein (P402A/P564A), **p=0.004 (Fig. 2.5A)**. In these cells, the effects of RES on respiration (basal respiration – **p=0.1406**; maximal respiration – **p=0.3486**) (**Fig. 2.5B**) and mitochondrial network characteristics (number of rods/puncta – **p=0.6649**; number of networks – **p=0.9877**; branches per network – **p=0.7445**; mitochondrial footprint – **p=0.5442**) (**Fig. 2.5C**) were absent. The effects of RES on cell growth (**p=0.002**, PC3-HIFwt vs PC3-HIFmut) (**Fig. 2.5D**) and cell cycle distribution (G0/G1 – **p=0.4036**) (**Fig. 2.5E**) were reduced in PC3 cells expressing mutant HIF-1 α , though they were not absent entirely. An interaction between cell line and treatment (**F_{2,64}=5.2, p=0.0087**) and a main effect of cell line (**F_{2,64}=24.67, p<0.0001**) were observed.

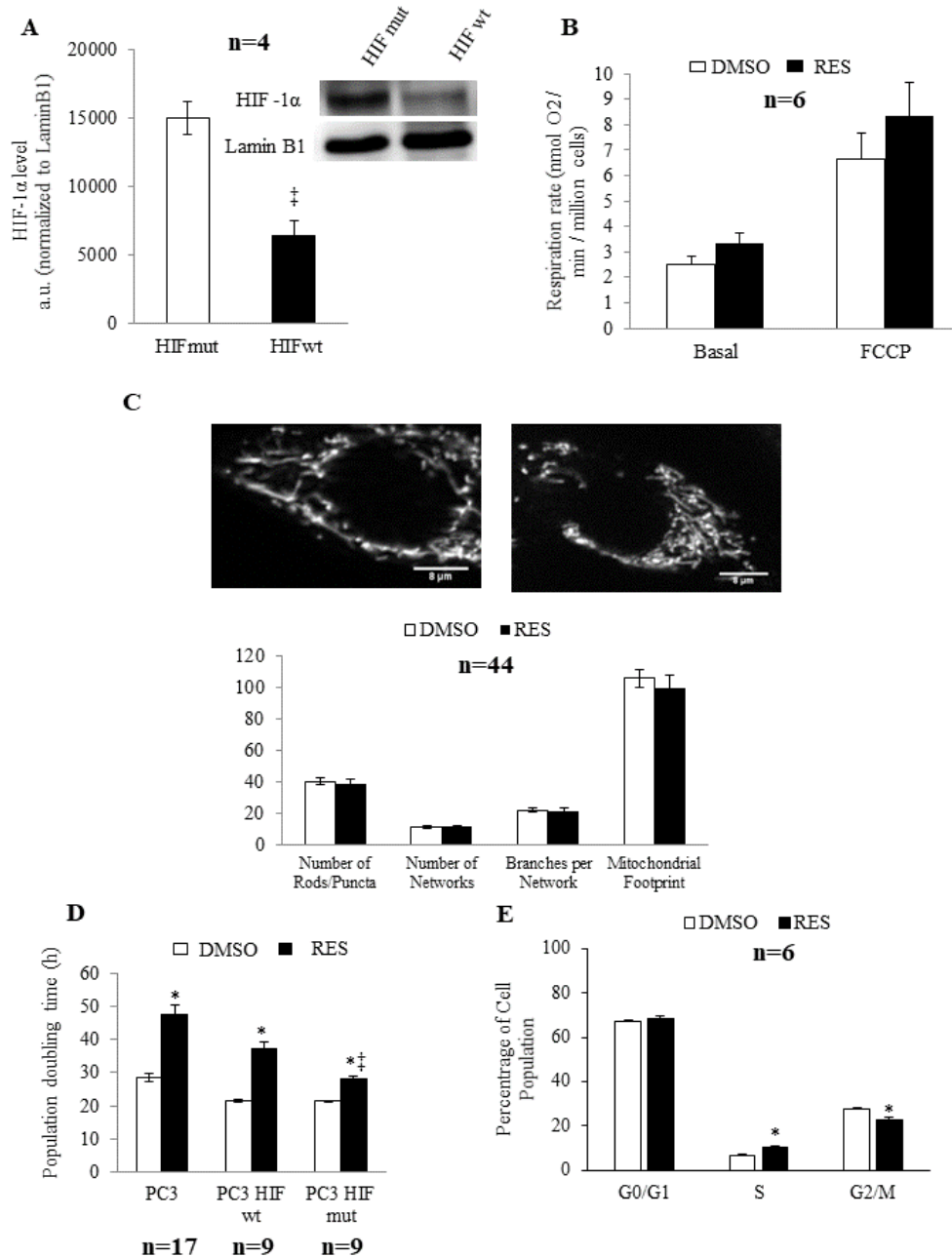


Figure 2.5. Effects of RES were diminished in PC3 cells expressing a stable HIF-1 α mutant.

(a) HIF-1 α in cells expressing wt or mutant HIF-1 α in normoxic conditions. (b) Cellular respiration rates and (c) mitochondrial network characteristics (number of puncta/rods, networks and branches per network are counts, mitochondrial footprint is area in μm^2 ; Total magnification – 630x) in cells expressing mutant HIF-1 α and treated with either 10 μM RES or vehicle control (DMSO) for 48h. (d) Population doubling time and (e) cell cycle distribution for cells expressing mutant HIF-1 α . In (b-e) open bars are DMSO vehicle control and filled bars are 10 μM RES. Data shown are means \pm SEM. ‘*’ = difference between RES-treated and DMSO-treated cells. ‘ \dagger ’ = difference between wtHIF-1 α and mutHIF-1 α . P values were calculated by t-test (unpaired, two-tailed) (A, B, C, E) and ANOVA followed by post-hoc analysis (D).

Rather than accumulating in G0/G1 phase cells expressing the RES treated HIF-1 α mutants showed a slight accumulation in S-phase (**p=0.0020**). Similar results were observed using IOX2, with the exception that this treatment more fully abolished RES's effects on respiration (basal respiration – **p=0.8605**; maximal respiration – **p=0.2641**) (**Fig. 2.6A**) and mitochondrial network characteristics (number of rods/puncta – **p=0.6378**; number of networks – **p=0.2225**; branches per network – **p=0.6755**; mitochondrial footprint – **p=0.3568**) (**Fig. 2.6B**). The effects of RES on cell growth (**Fig. 2.6C**) were reduced in PC3 cells treated with IOX2 **p=0.0693** ($F_{1,20} = 59.27$, **p<0.0001**, interaction between treatment and IOX2). Similar results were observed in the presence of the hypoxic 'mimetic' CoCl₂ (**Appendix S1.2**). RES effects on cell cycle distribution appear to be absent (G0/G1 – **p=0.787**; S – **p=0.3936**; G2/M – **p=0.6340**) (**Fig. 2.6D**).

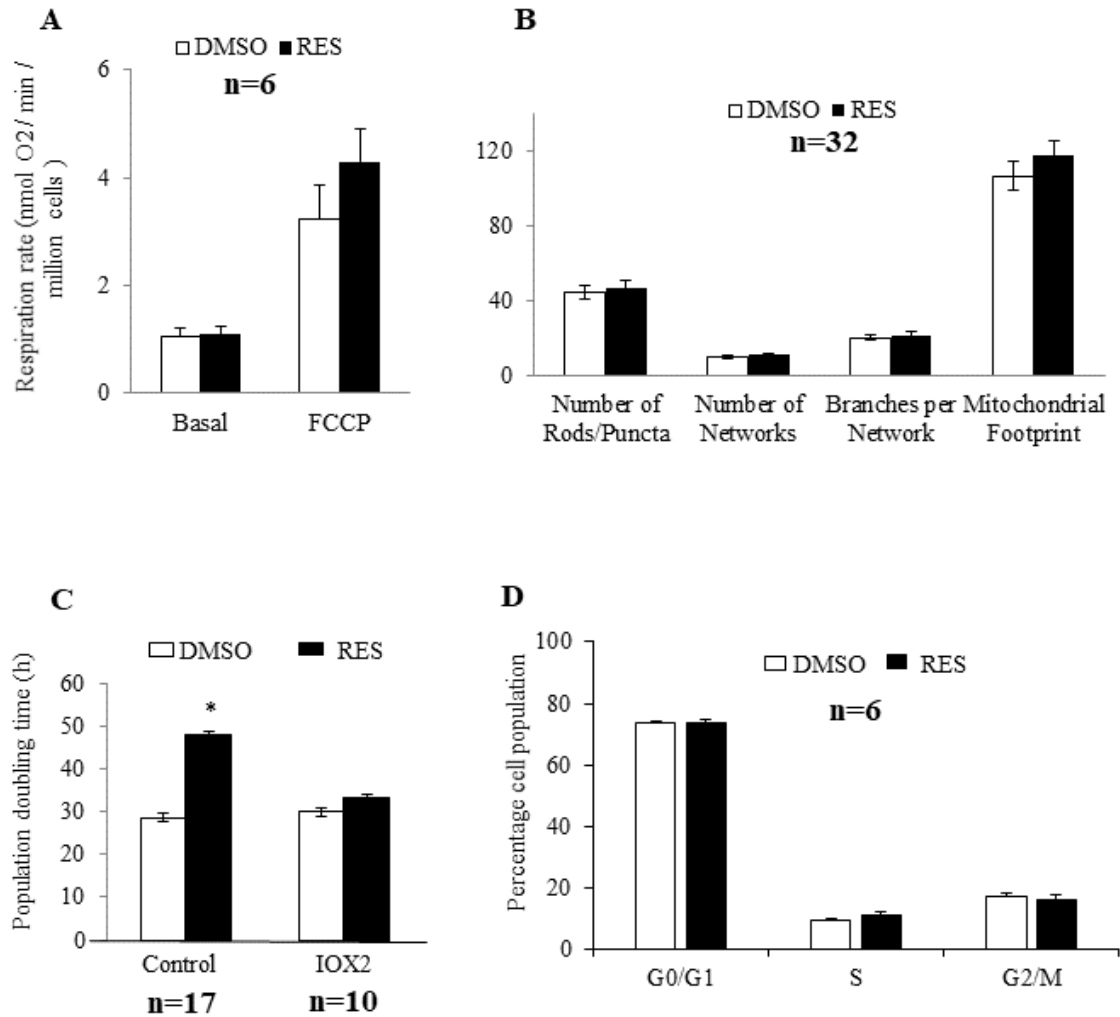


Figure 2.6. Inhibition of prolyl hydroxylase activity with IOX2 abolished RES effects on (A) cellular respiration, (B) mitochondrial network features, (C) cell growth, (D) cell cycle distribution. In all experiments, PC3 cells were treated for 48h with 10 μ M RES (filled bars) or an equal volume of DMSO (open bars). In both DMSO and RES groups, cells were simultaneously treated with IOX2 as in Material and Methods, except where indicated in (C). Number of puncta/rods, networks and branches per network are counts, mitochondrial footprint is area in μm^2 . Total magnification – 630x. Data shown are means \pm SEM. ‘*’ = difference between RES-treated and DMSO-treated cells. P values were calculated by t-test (unpaired, two-tailed) (A, B, D) and ANOVA followed by post-hoc analysis (C).

To determine whether the ability of IOX2 to modulate RES's growth effects were specific to PC3 cells ($p=0.0693$), this experiment was repeated with another prostate cancer cell line (LNCaP), and two non-prostate cancer cell lines: C2C12 mouse myoblasts and SHSY5Y human neuroblastoma. Interestingly, although IOX2 similarly abolished RES's effect on growth in LNCaP cells ($p=0.0615$), it was either partially effective or ineffective in the two non-prostate cancer cell lines (SH-SY5Y - $p=0.0388$; C2C12 - $p<0.0001$) (Fig. 2.7). An interaction between treatment and IOX2 was observed for PC3 ($F_{1,20}=59.27$ $p<0.0001$), LNCAP ($F_{1,20}=29.12$ $p<0.0001$), SH-SY5Y ($F_{1,20}=9.17$ $p=0.0066$), but not for C2C12 ($F_{1,20}=2.32$ $p=0.14$). A statistical difference between RES and IOX2 + RES treated cells was observed for PC3 ($p<0.0001$), LNCAP ($p=0.0002$), SH-SY5Y ($p=0.0388$), but not for C2C12 ($p=0.2466$).

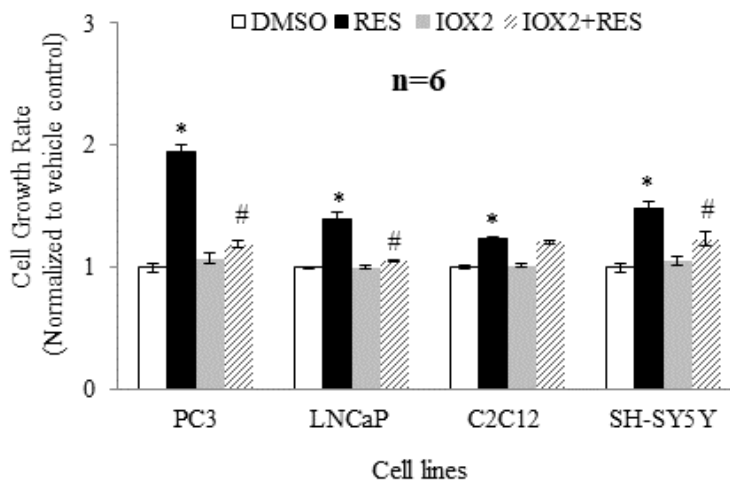


Figure 2.7. IOX2 inhibition of prolyl hydroxylase activity abolishes RES's effects on growth in PC3 and LNCaP, but not C2C12 or SHSY5Y cells. Cells were treated with the PHD inhibitor IOX2 (25 μ M) or vehicle control (DMSO) overnight prior to commencing experiments. RES treatments were started on the following day and continued for 48h. All treatments (IOX2 and RES) were refreshed every 24h. Data shown are means \pm SEM. '*' = difference between RES-treated and DMSO-treated cells. '#' = difference between RES-treated and IOX2+ RES treated cells. P values were calculated by ANOVA followed by post-hoc analysis.

Given the implication of HIF-1 in mediating RES's effects on PC3 cells, I hypothesized that RES might be a particularly effective inhibitor of PC3 cell growth under hypoxic conditions, as would be prevalent in vivo (Muz et al., 2015). Indeed, RES treatment prevented the stabilization of HIF-1 α under hypoxia (**p<0.0001; Fig. 2.8A**), prevented the increase in LDH activity (**p=0.0048; Fig. 2.8B**), associated with hypoxia (**F_{1,28}=9.61 p=0.0065**) and reduced the rate of glucose import (**p=0.0491; Fig. 2.8C**). Furthermore, under hypoxic conditions RES also decreased glucose-6-phosphate dehydrogenase enzyme activity, an enzyme that catalyzes the first reaction and rate-limiting step in the pentose phosphate pathway (**Appendix S1.3**).

Finally, RES strongly inhibited PC3 cell growth under hypoxic conditions (**p<0.0001; Fig. 2.8D**). An interaction between oxygen and treatment was observed (**F_{1,38}=10.56 p=0.0031; Fig. 2.8D**). Importantly, PC3 cell growth under hypoxic conditions was inhibited at lower concentrations of RES (hypoxia 1 μ M – **p=0.0247**; normoxia 1 μ M – **p=0.7379; Fig. 2.8E**). An interaction between oxygen levels and RES concentration was observed (**F_{3,76}=5.20 p=0.0035**). However, this seems to be cell line specific (**Appendix S1.4**).

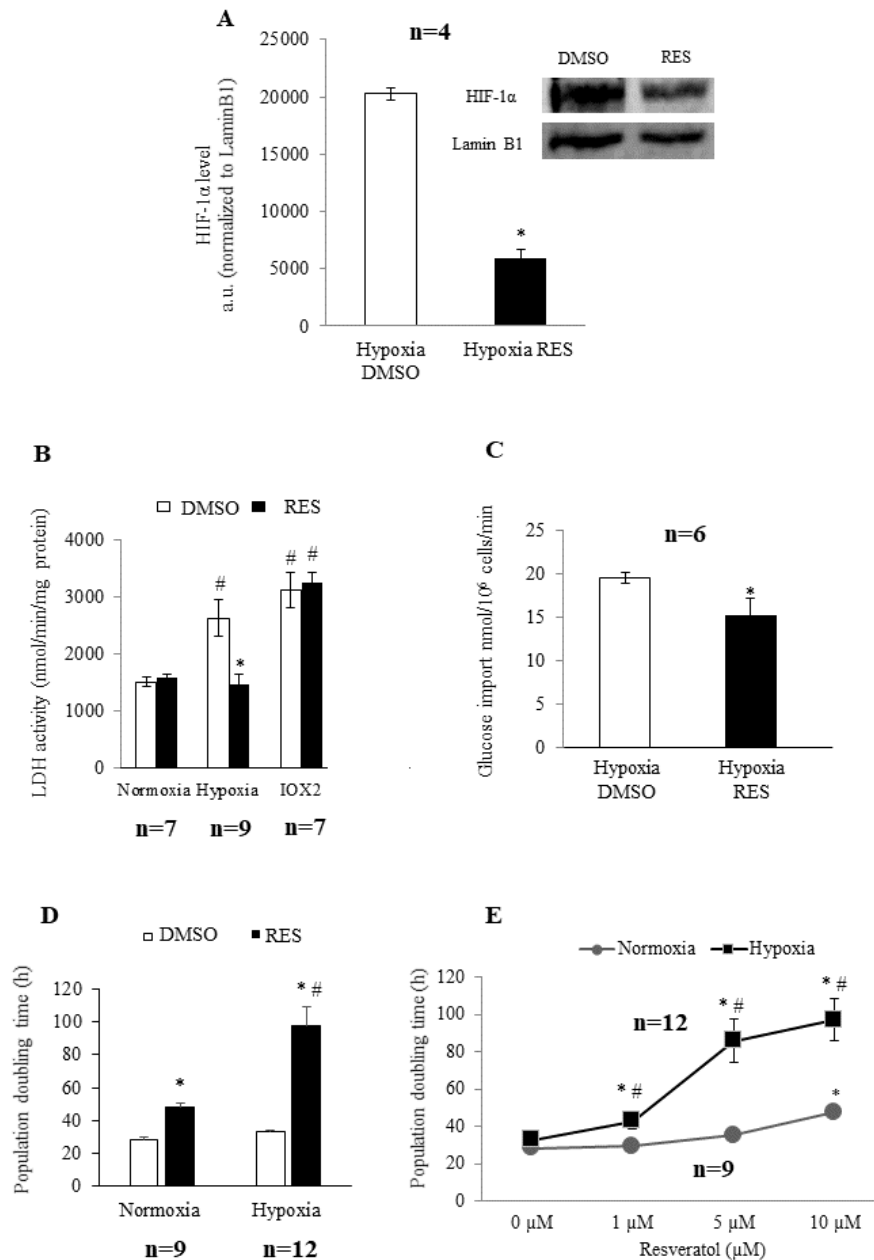


Figure 2.8. RES strongly inhibits PC3 cell growth under hypoxic conditions. RES prevents HIF-1 α stabilization under hypoxia. (a) representative western blot and normalized HIF-1 α levels in DMSO and RES treated cells. RES reduces (b) lactate dehydrogenase activity and (c) glucose import in hypoxia. (d) RES more strongly inhibits cell growth in hypoxia versus normoxia. (e) Low concentrations of RES are effective at inhibiting cell growth under hypoxic, but not normoxic conditions. In all experiments, PC3 cells were treated for 48h with 10 μ M RES (filled bars) or an equal volume of DMSO (open bars). Data shown are means \pm SEM. ‘*’ = difference between RES-treated and DMSO-treated cells. ‘#’ = difference between hypoxia and normoxia. P values were calculated by t-test (unpaired, two-tailed) (A, C) and ANOVA followed by post-hoc analysis (B, D, E).

Finally, RES strong inhibitory effects observed under hypoxic conditions are diminished when a specific mitochondrial ROS (mtROS) scavenger (MitoQ) is used (**Appendix S1.5**).

2.6 Discussion

Cancer cells are generally typified by a high flux of glucose through glycolysis and the pentose phosphate pathway and this metabolic predisposition has emerged as a pharmacological target (Amoedo et al., 2017; Hirschey et al., 2015). Strategies aimed at inhibiting these pathways and/or shifting glucose catabolism toward complete mitochondrial oxidation have been effective in slowing cancer cell and tumour growth (Fantin et al., 2006; Greer et al., 2012; Kankotia and Stacpoole, 2014).

In our experiments, RES treatment stimulated a shift toward oxidative metabolism in PC3 cells concomitantly with the inhibition of growth, and when this metabolic shift was absent growth effects were also absent. The RES effects on PC3 cell mitochondrial and growth characteristics were completely abolished when the cells were grown in galactose medium containing no glucose. Growth of mammalian cells in galactose medium increases the contribution of oxidative phosphorylation to glucose oxidation (Rossignol et al., 2004b), apparently related to the relatively slow multi-step Leloir pathway converting galactose to glucose-1-phosphate (Holden et al., 2003) that limits rates of ATP synthesis from glycolysis. PC3 cells grown in galactose had higher rates of respiration and more mitochondria (mitochondrial footprint, **Fig. 2.4**), suggesting the metabolic shift toward oxidative metabolism observed in glucose-grown PC3 cells treated with RES was

already present. The inability of RES to affect cell growth under these conditions suggests that the metabolic shift from glucose fermentation to oxidation is an essential component of RES's growth inhibition effect. Interestingly, we have observed similar results previously (Robb and Stuart, 2014); rho⁰ PC3 cells that are unable to respire also show no growth inhibition by RES. Similarly, mouse embryonic fibroblast cells lacking the mitofusin-2 have compromised respiration and growth that is insensitive to RES (Robb et al., 2017). Taken together, these observations suggest that RES's growth inhibitory effect in PC3 cells (and perhaps also other cell types) is related to its ability to shift metabolism toward oxidative phosphorylation.

HIF-1 is a key mediator of the Warburg effect in cancer cells (Courtney et al., 2015; Hirschev et al., 2015), and thus a target of strategies to promote oxidative metabolism and slow growth. Our results strongly suggest that HIF-1 is involved in the metabolic switch stimulated by RES treatment, since changes in HIF-1 α stabilization were required for RES's effects on cellular respiration, mitochondrial network characteristics, and cell growth to manifest. The most complete abolishment of RES's effects was observed when PHD was inhibited by IOX2. PHD post-translationally modifies multiple proteins to exert broad effects on cellular metabolism (Boulahbel et al., 2009; Jokilehto and Jaakkola, 2010; Nguyen and Durán, 2016). Though I focused here on HIF-1 α , other PHD targets including HIF-2 α may also be involved. This could explain why HIF-1 α stabilization only partly abrogated RES's effects.

Given the evidence above for a role of PHD and HIF-1, it follows that RES might be a particularly strong inhibitor of growth in hypoxic PC3 cells where the importance of the HIF-1 pathway is enhanced. I found this to be the case, as PC3 cell population doubling time (PDT) was increased by more than two-fold in hypoxia, compared to an approximately 50% increase in PDT under atmospheric O₂ levels. Perhaps even more importantly, much lower concentrations of RES

could elicit increases in PDT in hypoxia (1 μ M in hypoxia versus 10 μ M in atmospheric O₂). This observation has practical significance. One of the contradictions apparent in the literature on RES and cancer is that, while 10-100 μ M RES is typically required to slow cell growth in vitro, the RES concentrations reached in mammalian blood plasma and tissues in vivo are much lower (Stuart and Robb, 2013). And yet, RES treatment by various means has nonetheless been shown to slow tumour growth in many instances, including prostate cancer (Li et al., 2013). The observation that RES interferes with HIF-1 activity may explain this apparent disjunction, given HIF-1's role in the growth of some cancers. In this respect, it is interesting that LNCaP cells responded similarly to the PHD inhibitor IOX2 in terms of the RES effect on growth, while this was largely absent in C2C12 or SHSY5Y cells. It will be interesting to investigate the connections between RES, HIF-1, mitochondrial respiration, and growth in other cancer cell types in which HIF-1 is known to play a particularly critical role (Chen et al., 2014).

Chapter 3. Oxygen and glucose levels in cell culture media determine resveratrol's effects on growth, hydrogen peroxide production, and mitochondria dynamics

Hypothesis

In vitro cell culture is performed under supraphysiological O₂ and glucose conditions, which influences reactive oxygen species production (i.e. increases H₂O₂ production) and concomitantly mitochondrial network characteristics (i.e. increases mitochondrial fission). Therefore, given the role that RES has on ROS and mitochondria network characteristics, I hypothesized that RES *in vitro* effects on cell growth, hydrogen peroxide and mitochondrial morphology would be influenced by *in vitro* non-physiological conditions. More specifically, I hypothesized that RES *in vitro* effects on cells growing under more relevant physiological conditions (5% O₂ and 5mM glucose) would be diminished or even abolished.

Objectives

The objectives of this project are to: 1) Determine how RES effects on cell growth, hydrogen peroxide and mitochondrial dynamics are influenced by non-physiological O₂ and glucose levels.

Publication of results

Fonseca, J., Moradi, F., Valente, A. J. F., & Stuart, J. A. (2018). Oxygen and Glucose Levels in Cell Culture Media Determine Resveratrol's Effects on Growth, Hydrogen Peroxide Production, and Mitochondrial Dynamics. *Antioxidants (Basel, Switzerland)*, 7(11), 157. <https://doi.org/10.3390/antiox7110157>

Contributions

Conceptualization, JAS; Formal analysis, JF, FM, AJFV; Investigation, JF, FM, AJFV; Methodology, JF, FM, AJFV and JAS; Writing-original draft, JF; Writing-review & editing, JAS.

3.1 Introduction

Reactive oxygen species (ROS), such as hydrogen peroxide (H_2O_2), are a normal product of cellular activity with important roles in cellular functions like mitosis, differentiation, and mitochondrial dynamics. On the other hand, abnormally high cellular ROS levels promote structural and functional changes in key macromolecules including proteins and DNA. However, in certain pathological conditions, such as cancer and neurodegeneration, ROS homeostasis may be impaired (Kalyanaraman et al., 2018). Small molecules that can modulate cellular ROS metabolism therefore have therapeutic potential and have attracted significant interest.

RES a natural polyphenolic compound, can affect cellular ROS metabolism, either directly as an antioxidant or pro-oxidant (de la Lastra and Villegas, 2007; Leonard et al., 2003), or indirectly by regulating expression of ROS-producing enzymes/organelles or antioxidant enzymes (Truong et al., 2018). In the former instance, it appears that the concentration of RES used in cell culture experiments determines whether it behaves as a pro- or antioxidant (Plauth et al., 2016). In the latter case, RES treatment of cells in culture can affect ROS metabolism by increasing mitochondrial abundance (Csiszar et al., 2009; Davinelli et al., 2013) and regulating the expression and/or activity of NADPH oxidases (NOXs) (He et al., 2015) and nitric oxide synthases (NOSs) (Xia et al., 2014).

RES effects on animal cells are virtually always studied under standard cell culture conditions in which incubator O_2 levels are not regulated, and headspace O_2 is approximately 18%. This O_2 level is substantially hyperoxic compared to in vivo (Habler and Messmer, 1997), where the O_2 levels experienced by most tissues cells are in the range of 1–6% (Carreau et al., 2011). All cells that we have tested previously produce more H_2O_2 at 18% O_2 compared to 5% O_2 , and NOX

isoforms 1 and/or 4 appear to be major contributors to this difference (Maddalena et al., 2017). Given that RES interacts at multiple levels with cellular ROS metabolism it may be problematic to study RES effects under conditions of supra-physiological O₂—there is a danger of measuring effects of RES that would not occur under physiologically relevant O₂ levels.

In addition to being hyperoxic, standard cell culture conditions are also typically hyperglycemic. Standard Dulbecco's Modified Eagles Medium (DMEM) includes 25 mM glucose, which is approximately 5-times higher than normal plasma (glucose) in a healthy human. A robust effect of RES is its ability to promote a metabolic shift away from glucose fermentation and towards oxidative phosphorylation (De Oliveira et al., 2016). I have previously shown that many of RES's effects on mitochondria observed in high glucose DMEM, including effects on mitochondrial dynamics, are absent in DMEM with galactose, which promotes oxidative phosphorylation (Fonseca et al., 2019). In addition, since mitochondrial fusion is modulated by redox modifications of key proteins (Shutt et al., 2012), maintaining appropriate O₂ and glucose levels may be important.

Given the issues outlined above, it is important to consider the extent to which cell culture conditions might influence the outcome of experiments designed to determine effects of RES on a wide variety of cellular activities. To address this issue, here I have studied effects of low micromolar RES on two commonly studied cell lines (C2C12 mouse myoblasts and PC3 human prostate cancer) in which we have previously demonstrated RES effects ((Fonseca et al., 2019; Robb et al., 2017)). Here I use four conditions: physiological O₂ and glucose levels; physiological O₂ and high glucose; supraphysiological O₂ and physiological glucose; and supraphysiological O₂

and high glucose. I show that RES's effects on cell growth, cell cycle, H₂O₂ production and mitochondria network morphology are all dependent on media O₂ and glucose levels.

3.2 Experimental Procedures

3.2.1 Materials

Dulbecco's Modified Eagle Medium (DMEM) high glucose (4500 mg/L; 25 mM) or low glucose (900 mg/L; 5 mM) containing L-glutamine, sodium pyruvate and sodium bicarbonate (Cat. #D6429), supplement-free Dulbecco's Modified Eagle Medium powdered media (Cat. #D5030), fetal bovine serum (Cat. #F1051), non-essential amino acids, penicillin/streptomycin solution, 0.25% trypsin/EDTA solution, bovine serum albumin (BSA), horseradish peroxidase (2KU; Cat. #P6140) and H₂O₂ were obtained from Sigma-Aldrich (St. Louis, MO, USA). *trans*-RES (item 70675) and Amplex Red reagent (10-acetyl-3,7-dehydroxyphenoxazine; item 10010469) were purchased from Cayman Chemical (Ann Arbor, MI, USA). Dimethylsulfoxide (DMSO), Tissue culture dishes (100 × 20 mm & 60 × 15 mm) were obtained from Sarstedt, Inc (Newton, SC, USA). MitoTracker Red CMXRos and Lipofectamine 2000 transfection reagent was purchased from Life. C2C12 and PC3 cells were purchased from American Type Culture Collection (Manassas, VA, USA). Propidium Iodide (PI)/RNase Staining Buffer was purchased from BD bioscience (Cat#550825, SanDiego, CA, USA). All other reagents were obtained from Sigma-Aldrich (St. Louis, MO, USA).

3.2.2 Cell Lines and Culture Conditions

C2C12 and PC3 cells were cultured according to the distributor's protocol in high or low glucose DMEM supplemented with 10% fetal bovine serum (FBS), 2× MEM nonessential amino acid solution, and penicillin (50 I.U./mL)/streptomycin (50 µg/mL) solution. All cells were cultured within a humidified 5% CO₂ atmosphere at 37 °C in one of two Forma 3110 water-jacketed incubators with O₂ control (ThermoFisher, Waltham, MA, USA) set to either 18% O₂ (supraphysiological) or 5% O₂ (physiological) levels. In all cases, media was stored in cell culture dishes in the appropriate incubator for at least 24 h prior to its use to ensure equilibration with ambient conditions. For fluorescence microscopy experiments conducted at 5% O₂, oxygen levels in the on-stage incubator were regulated with in-flow of humidified 5% O₂/5% CO₂/90% N₂ gas mix.

After thawing, cells were cultured at different oxygen (5% O₂ or 18% O₂) and glucose (25 mM and 5 mM) conditions for at least three days before starting the experiments. Cell density and population doubling time were determined by hemocytometer counting using Trypan Blue exclusion to identify live cells. RES and vehicle control (DMSO) were added directly to the culture media, and both media and treatments were exchanged every day. All media, solutions and buffers used during cell culture were pre-warmed to 37 °C in an Isotemp 110 water bath (Fisher Scientific, Mississauga, ON, Canada) for at least an hour prior to use.

3.2.3 Cell Cycle Analysis

Cell cycle distribution was analyzed as in (Fonseca et al., 2019). Briefly, cells ($\sim 5 \times 10^5$) were removed from plates by trypsinization, washed once with PBS, and then cell pellets fixed with ice-cold ethanol (75% v/v) and incubated overnight at -20°C . The following day the suspension was transferred to room temperature, centrifuged (5 min at $240\times g$), washed twice with ice-cold PBS, and then incubated with 0.5 mL Propidium Iodide (PI)/RNase Staining Buffer (BD Pharmingen, San Jose, CA, USA) in darkness for 15 min. DNA content (PI signal) of the cell suspensions was immediately analyzed using a BD Accuri C6 flow cytometer (BD Biosciences, USA). The percentages of cells in G0-G1, S, and G2-M phases were determined using the CFlow Plus software (BD Biosciences, San Jose, CA, USA).

3.2.4 Hydrogen Peroxide Efflux Determination

Cellular H_2O_2 efflux was measured as in (Maddalena et al., 2017), using an Amplex Red reagent (10-acetyl-3,7-dihydroxyphenoxazine)-based assay, in which the fluorescent oxidation product resorufin serves as a proxy for H_2O_2 levels ((Zhou et al., 1997)). Briefly, cells were seeded in either 25 mM or 5 mM glucose and placed in either 18% O_2 or 5% O_2 incubator overnight, before starting the treatments. Treatments were conducted for 48 h and refreshed every day. Immediately prior to experiments, cells were washed and then incubated in Krebs-Ringer buffer (KRB; 135 mM NaCl, 5 mM KCl, 1 mM MgSO_4 , 0.4 mM K_2HPO_4 , 20 mM HEPES, 5.5mM glucose supplemented with 10% fetal bovine serum) containing freshly added Amplex Red reagent (50 μM) and horseradish peroxidase (0.1 units/mL).

A standard curve for H₂O₂ (0 μM to 3 μM) was included with each experiment. Cells were incubated for 2 h in 0.5 mL of KRB buffer, after which the buffer was collected and resorufin fluorescence measured using excitation and emission wavelengths of 535 nm and 595 nm, respectively (Cary Eclipse fluorescence spectrophotometer, Agilent Technologies, Santa Clara, CA USA). Simultaneously, cells were trypsinized and counted with a hemocytometer. H₂O₂ efflux rates (μmol·h⁻¹) were standardized to cell number.

3.2.5 Stable C2C12 and PC3 Emerald Fluorescent Protein-Labelled Mitochondria

The plasmid mEmeral-Mito-7 was a gift from Michael Davidson (Florida State University). The plasmid contains a kanamycin-resistance gene for bacterial selection and geneticin (G418)-resistance gene for mammalian cell selection. Plasmid DNA was initially isolated and purified from bacterial cultures via a plasmid DNA Miniprep Kit (Norgen Biotek, Thorold, ON, Canada). Plasmid DNA purity (260 nm/280 nm absorbance ratio) and concentration were assessed by using a NanoPhotometer instrument (Montreal Biotech Inc., Ville Saint Laurent, PQ, Canada).

To create stable cell lines, PC3 and C2C12 cells were plated in a 24-well plate with a desired cell density that allow cells to reach ~80% confluency after 24 h. Briefly, cells were transfected with Lipofectamine 2000 reagent and different combinations of plasmid DNA:Lipofectamine reagent were used. After 24 h, stable transfected cells were selected with G418 for 10 days (G418 concentration was determined in a prior screening experiment). After 10 days of selection, the concentration of G418 in culture media was dropped to a maintenance concentration. To confirm

mitochondrial localization of the mEFP, colocalization of mEFP signal with the mitochondria-targeted fluorescent dye MitoTracker RedCMXRos was detected using confocal microscopy.

3.2.6 Fluorescence Microscopy

Fluorescence micrographs of live cells were obtained using a Carl Zeiss Axio Observer. Z1 inverted light/epifluorescence microscope equipped with ApoTome.2 optical sectioning and a Hamamatsu ORCA-Flash 4.0 V2 digital camera. C2C12 and PC3 cells were cultured on Matek 35mm poly-D-lysine-coated glass bottom culture dishes for 48h under the glucose and O₂ conditions indicated. Media was refreshed every 24 h. Cells were switched to phenol red free media at least an hour prior to imaging. Cells were viewed with a Plan-Apochromat 63x/1.40 Oil DIC M27 microscope objective. The microscope stage and objectives were maintained at 37 °C, with temperature control achieved through TempModule S-controlled stage heater and objective heater (PeCon, Erbach, Germany). A humidified 5% CO₂ environment with either 18% or 5% O₂ was also maintained throughout the experiments. Green fluorescence was detected using a fluorescence channel possessing excitation and emission wavelength filter sets of 450–490 nm and 500–550 nm, respectively. Both the intensity of fluorescence illumination and camera exposure time were held constant throughout all experiments. Z-stacks consisted of 20 slices, each 0.25 μm apart. Maximum intensity projections were generated for each stack using the Fiji distribution of ImageJ.

3.2.7 Quantitative Analysis of Mitochondrial Morphology

Mitochondrial morphology was assessed with the Mitochondrial Network Analysis tool (MiNA; (Valente et al., 2017)). To improve contrast between all mitochondrial structures and background, several pre-processing steps, such as contrast limited adaptive histogram equalization (CLAHE), median filtering and ‘unsharp mask’ were used. It was previously assessed that this combination of pre-processing steps provided the most accurate results. In the processed imaged, fluorescent mitochondrial signal was subjected to thresholding in order to eliminate background signal, which could generate an artifact. The binary image was then converted to a skeleton image in which mitochondrial signal was converted to lines of one pixel in width. From the skeletonized mitochondrial signal, skeleton structures were classified as either individuals (skeletons without branching) or networks (skeletons containing at least one branching point). Mitochondrial footprint, the total area in the image consumed by signal was also assessed. At least 30 cells per condition were selected randomly from at least three separate experiments.

3.2.8 Statistics

Statistical analyses were performed using JASP version 9 software and consisted of analyses of variance (ANOVA). Between-subject factors were oxygen (5%, 18%), treatment (DMSO, RES), and glucose level (Low, High). Alpha was set at $p < 0.05$. After determining the overall statistically significant difference in group means (i.e. ANOVA interaction), post-hoc analyses consisting of independent-sample t-tests were performed. All data are presented as means \pm standard error of the mean (SEM).

3.3 Experimental design

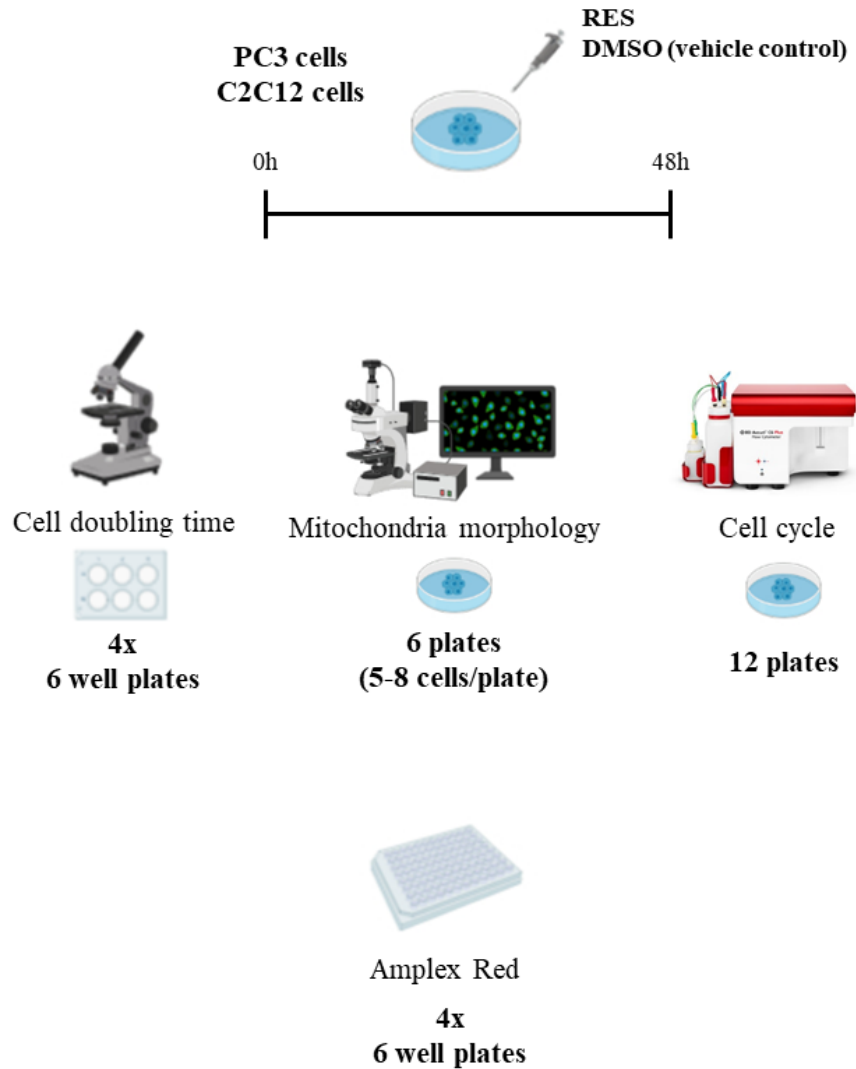


Figure 3.1 Experimental design. PC3 and C2C12 cells were seeded overnight and treated for 48h with RES or the vehicle control DMSO. Biological replicates for each experiment are also represented in the figure.

3.4 *In vitro* models

C2C12 mouse myoblasts and PC3 human prostate cancer cells were culture under the following conditions:

- Physiological O₂ (5% O₂) and glucose (5mM)
- Physiological O₂ (5% O₂) and hyperglycemia (25mM)
- Hyperoxia (18% O₂) and physiological glucose (5mM)
- Supraphysiological O₂ (18% O₂) and glucose (25mM)

3.5 Results

One of the most robust effects of RES is the inhibition of cell proliferation. I investigated whether RES's antiproliferative effects are influenced by O₂ and glucose levels. For these experiments, C2C12 and PC3 cells were cultured at either 5% O₂ or 18% O₂ in either low (5 mM) or high (25 mM) glucose DMEM. C2C12 cell growth rates were strongly affected by media O₂ and glucose levels ($F_{1,92} = 14.54$, $p = 0.0003$), with lower O₂ and lower glucose both favoring more rapid growth (**Figure 3.2A**). The effect of RES on C2C12 growth was dependent upon media conditions during the experiment ($F_{1,184} = 11.70$, $p = 0.0008$): in cells growing in high glucose medium at 18% O₂, 48 h treatment with 10 μ M RES inhibited growth and increased cell population doubling time by almost 25% ($p < 0.0001$). However, at 5% O₂ and high glucose RES increased C2C12 population doubling time by only about 10% ($p < 0.0001$; **Figure 3.2A**). Media glucose levels also modulated RES's effects on proliferative cell growth. The ability of RES to slow growth was reduced in low glucose. In contrast with C2C12 cells, neither O₂ nor glucose levels affected

PC3 cell growth rates under control conditions ($F_{1,92} = 1.16$, $p = 0.3570$; **Figure 3.2B**). However, RES more strongly inhibited growth in high glucose medium compared to low glucose ($F_{1,184} = 37.60$, $p < 0.0001$) (RES 18% O_2 – $p = 0.0003$; RES 5% O_2 = $p < 0.0001$; **Figure 3.2B**). To better understand the nature of RES's O_2 - and glucose-dependent effects on C2C12 cell growth, I measured its effects on cell cycle distribution under the same four conditions. Under control conditions, low glucose media increased the proportion of cells in G2/M phase ($F_{1,20} = 160.54$, $p < 0.0001$) (**Figure 3.2C**), regardless of the O_2 level ($F_{1,20} = 2.15$, $p = 0.1584$). RES effects on cell cycle distribution were subtly affected by O_2 or glucose levels (G0/G1 – main effect of glucose $F_{1,41} = 9.06$, $p = 0.0045$; G2/M – main effect of glucose $F_{1,41} = 14.62$, $p = 0.0004$); under all conditions RES treatment caused an increase, or a trend toward increase, in the proportion of cells in S-phase (interaction oxygen*glucose*treatment, $F_{1,41} = 8.95$, $p = 0.0047$; **Figure 3.2C**). Taken together, these results indicate that O_2 and glucose levels interact with RES's effects on C2C12 cell growth.

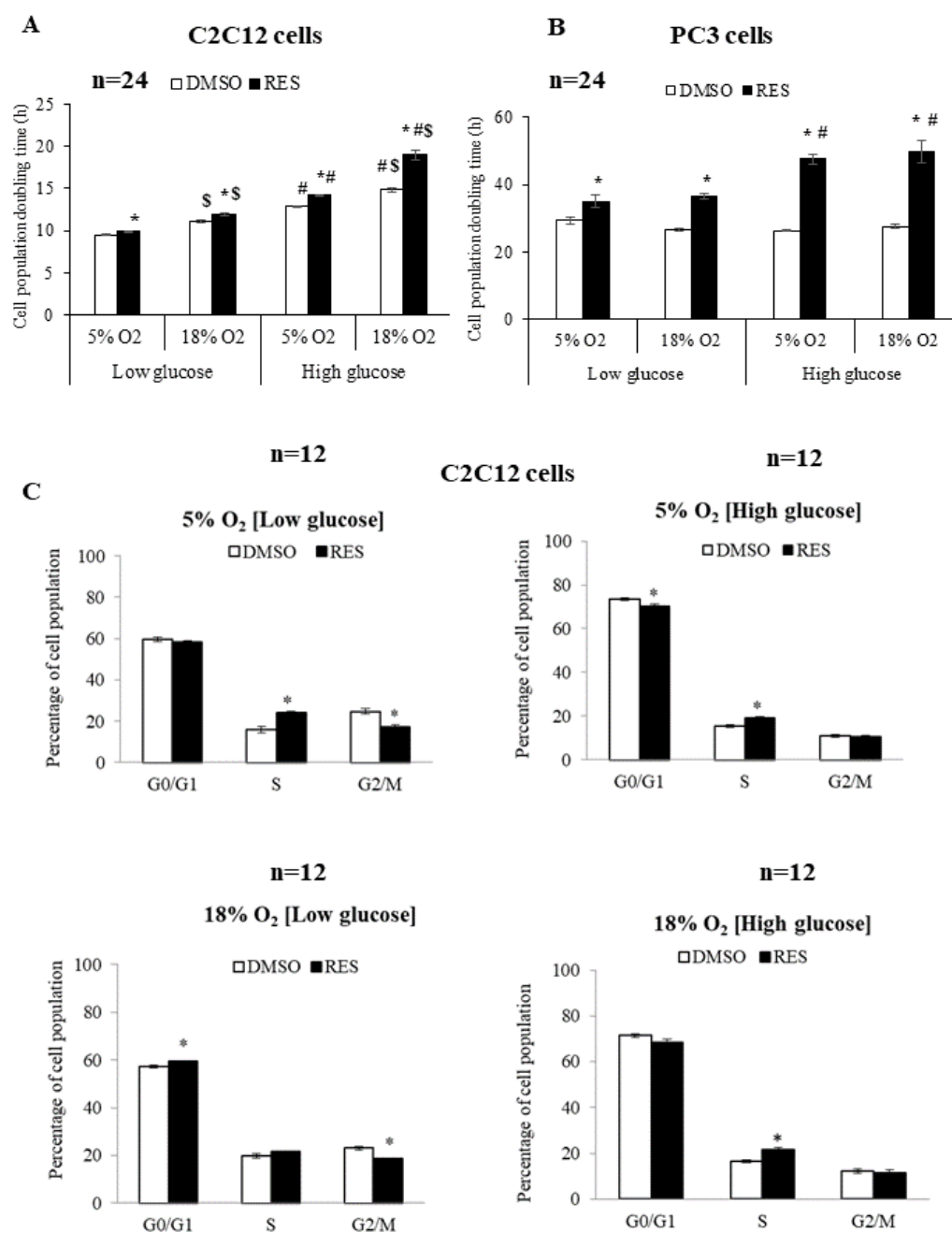


Figure 3.2. Media O₂ and glucose levels determine RES's effects on cell growth. Cell doubling time was measured following 48 h treatment with either RES (10 μ M; filled bars) or vehicle control (DMSO; open bars). C2C12 (A) and PC3 (B) cells were cultured at either 5% O₂ or 18% O₂ in either low (5 mM) or high (25 mM) glucose Dulbecco's Modified Eagles Medium (DMEM). (C) Distribution of C2C12 cells in different cell cycle stages was determined by flow cytometry. Data shown are means \pm SEM. '*' represents differences between RES-treated and DMSO-treated cells. '#' represents differences between low and high glucose levels. '\$' represents differences between low and high O₂ levels. P values were calculated by ANOVA followed by post-hoc analysis.

RES affects cellular ROS metabolism via its chemical antioxidant/pro-oxidant activities (Truong et al., 2018), its ability to stimulate mitochondrial respiration and biogenesis, (Blanquer-Rosselló et al., 2017), as well as the expression of ROS-producing enzymes such as NOX (He et al., 2015; Schilder et al., 2009). I investigated whether O₂ and glucose interact with these RES effects by measuring cellular H₂O₂ production under all four O₂ and glucose combinations. For C2C12 cells I found a main effect of each of the three variables glucose (**F_{1,100}=33.14, p<0.0001**), O₂ (**F_{1,100}=10.67, p=0.0015**), and treatment (RES; **F_{1,100}=34.49, p<0.0001**) on H₂O₂ production (**Figure 3.3A**). The highest rates of H₂O₂ production under control conditions were seen in high glucose/high O₂, while low glucose/high O₂ resulted in the lowest rates of production. Interactions between O₂*glucose (**F_{1,100}=63.41, p<0.0001**) and O₂*treatment (**F_{1,100}=16, p=0.0001**) were also observed (**Figure 3.3A**). Overall, RES increased H₂O₂ production at 18% O₂ irrespective of glucose level. Importantly, at physiological O₂ and glucose levels, RES had no effect on H₂O₂ production in C2C12 cells (**p=0.0849; Figure 3.3A**).

In PC3 cells, H₂O₂ production was greater in high O₂ for both glucose levels. Again, however, while RES had complex effects on H₂O₂ production in PC3 cells growing in supraphysiological O₂ and/or glucose (**F_{1,88}=25.88, p<0.0001**), there was no effect of RES under more physiologically appropriate conditions of low glucose/low O₂ (**p=0.9218; Figure 3.3B**).

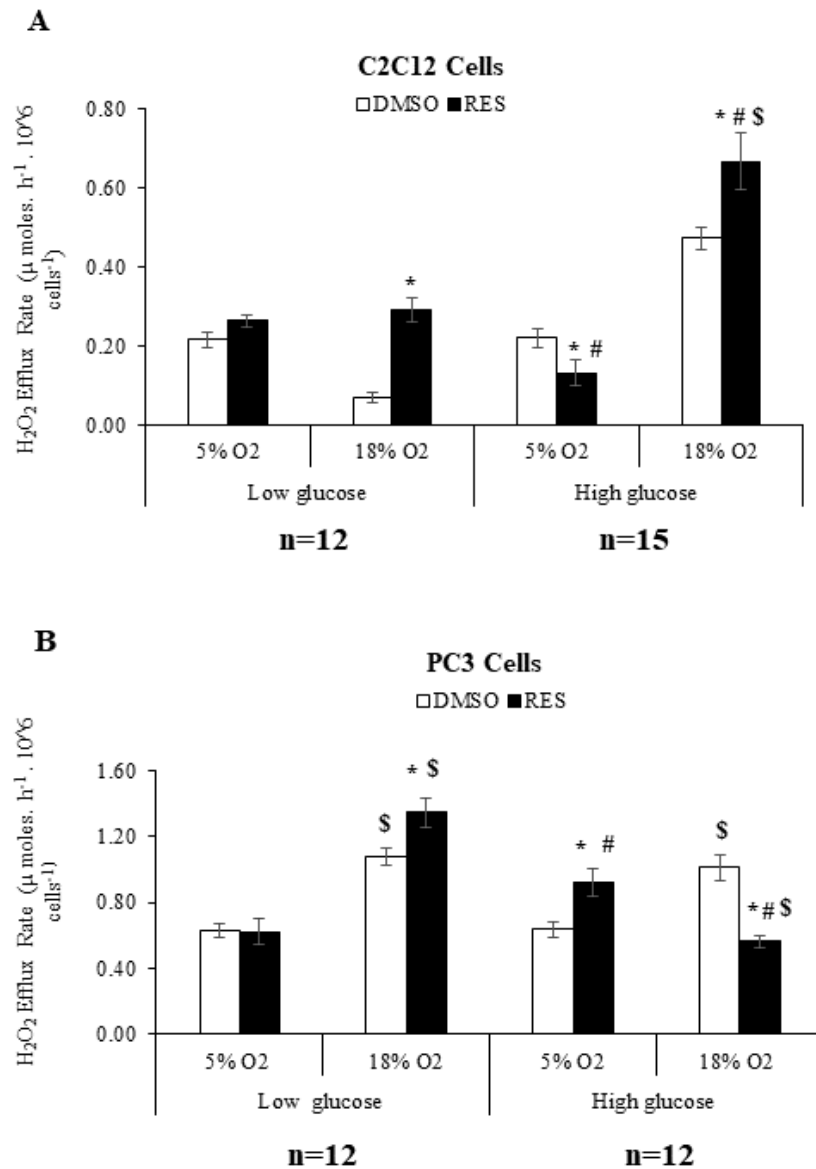


Figure 3.3. Media O₂ and glucose levels determine RES's effects on cellular hydrogen peroxide production. C2C12 (A) and PC3 (B) cells were cultured at either 5% O₂ or 18% O₂ in either low (5 mM) or high (25 mM) glucose DMEM. RES effects on H₂O₂ production were modulated by O₂ and glucose levels in both C2C12 (A) and PC3 (B) cells. In all experiments, cells were treated for 48 h with 10 μM RES (filled bars) or an equal volume of vehicle control (DMSO; open bars). Data shown are means ± SEM. '*' represents differences between RES-treated and DMSO-treated cells. '#' represents differences between low and high glucose levels. '\$' represents differences between low and high O₂ levels. P values were calculated by ANOVA followed by post-hoc analysis.

Mitochondria and mitochondrial network characteristics are dependent on cytosolic redox state (Shutt et al., 2012) and media glucose levels (Elkalaf et al., 2013; Rossignol et al., 2004a). Therefore, interactions between RES, O₂, and glucose would be expected to affect experimental outcomes. Indeed, I found that RES effects on mitochondrial network morphology in both C2C12 and PC3 cells were dependent on media glucose and O₂ levels (**Figures 3.4 and 3.5**). Mitochondrial network characteristics were analyzed using the Mitochondrial Network Analysis tool (MiNA) that we recently developed and have described in detail elsewhere (Valente et al., 2017). Briefly, MiNA can be used to identify and quantify features like ‘mitochondrial footprint’ (area of a 2D cell image occupied by mitochondria), the number of branched mitochondrial networks versus individual structures like rods or punctae, the number of individual branches per network, and the length of network branches or individual rod-shaped structures.

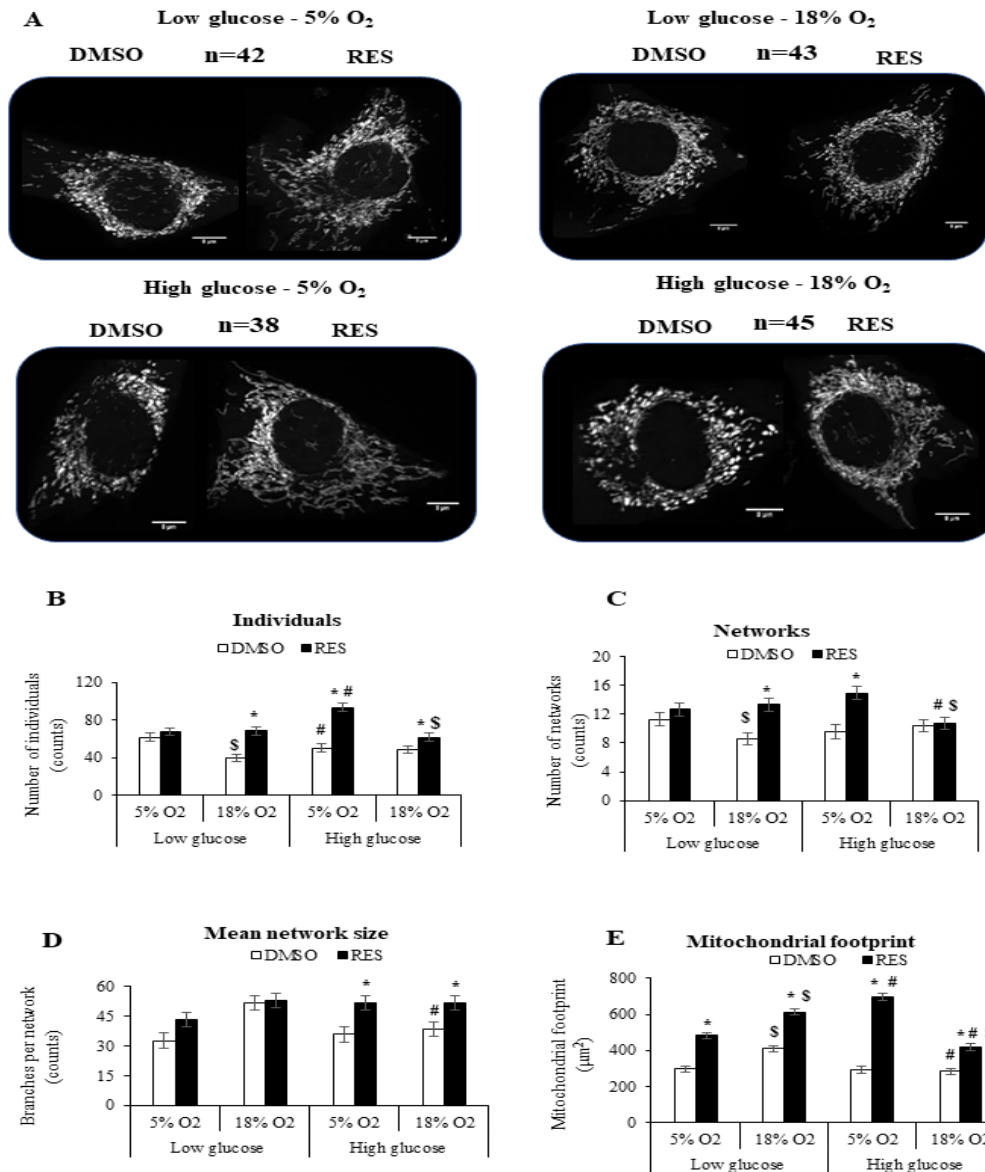


Figure 3.4. RES effects on mitochondrial network parameters are subtly affected by media glucose and O₂ levels in C2C12 cells. (A) Representative images of mitochondrial networks in C2C12 cells. There was a main effect of RES on the number of individuals (B), networks (C), mean network size (branches per network) (D) and mitochondrial footprint (E). Overall, treatment with RES increased all these mitochondrial network parameters. An interaction between O₂*glucose*treatment was also observed between individuals (B), number of networks (C) and mitochondrial footprint (E). A glucose and O₂ interaction was observed for mean network size (branches per network) (D). Total magnification in all experiments was 630×. Cells were treated for 48 h with 10 μM RES (filled bars) or an equal volume of vehicle control (DMSO; open bars). Data shown are means ± SEM. Randomly selected individual cells were analyzed using MiNA. ‘*’ represents differences between RES-treated and DMSO-treated cells. ‘#’ represents differences between low and high glucose levels. ‘\$’ represents differences between low and high O₂ levels. P values were calculated by ANOVA followed by post-hoc analysis.

I found that O₂ and glucose levels in culture affected mitochondrial network characteristics under control conditions. For C2C12 there was an interaction between oxygen and glucose for individuals ($F_{1,164} = 10.13$, $p=0.0017$), networks ($F_{1,164} = 5.49$, $p=0.0203$), mean network size ($F_{1,164} = 6.63$, $p=0.0109$) and mitochondrial footprint ($F_{1,164} = 22.22$, $p<0.0001$). For PC3 an interaction between oxygen and glucose for mean network size ($F_{1,138} = 7.26$, $p=0.0080$), but not for individuals ($F_{1,138} = 1.01$, $p=0.3162$), networks ($F_{1,138} = 6.52$, $p=2.4353$) and mitochondrial footprint ($F_{1,138} = 0.0039$, $p=0.9505$). In low glucose and 18% O₂, C2C12 cell mitochondria tended to be highly fused into relatively large networks and increased mitochondrial footprint. RES's effects on mitochondrial network characteristics were influenced by initial conditions of glucose and oxygen (individuals - $F_{1,328} = 18.97$, $p<0.0001$; networks - $F_{1,328} = 11.27$, $p=0.0009$; mitochondrial footprint - $F_{1,328} = 31.46$, $p<0.0001$). RES had no effect in C2C12 cells on the number of individual structures (rods and puncta) ($p=0.2875$), or the number of networks ($p=0.2547$), when cells were growing in 5% O₂ and low glucose, effects on these parameters were observed under other culture conditions (**Figure 3.4B–D**). In contrast, RES increased the mitochondrial footprint under all conditions (**Figure 3.4E**) and increased number of networks in most conditions. In PC3 cells, glucose and O₂ levels had few effects in the absence of RES (**Figure 3.5**), though the mitochondrial footprint was consistently higher in low glucose media (main effect of glucose – $F_{1,138}=13.11$, $p=0.0004$) (**Figure 3.5E**). RES increased mitochondrial footprint under all conditions tested ($F_{1,138}=63.78$, $p<0.0001$). In 5% O₂ and low glucose, RES had no effect on the number of individual structures (rods and puncta) ($p=0.8068$) (**Figure 3.5B**), or the number of networks ($p=0.6064$) (**Figure 3.5C**) but increased mean network size (number of branches) ($p=0.0129$) (**Figure 3.5D**) in PC3 cells. Thus, under the most physiologically relevant conditions,

RES promoted the production of larger and more highly branched networks in both C2C12 and PC3 cells.

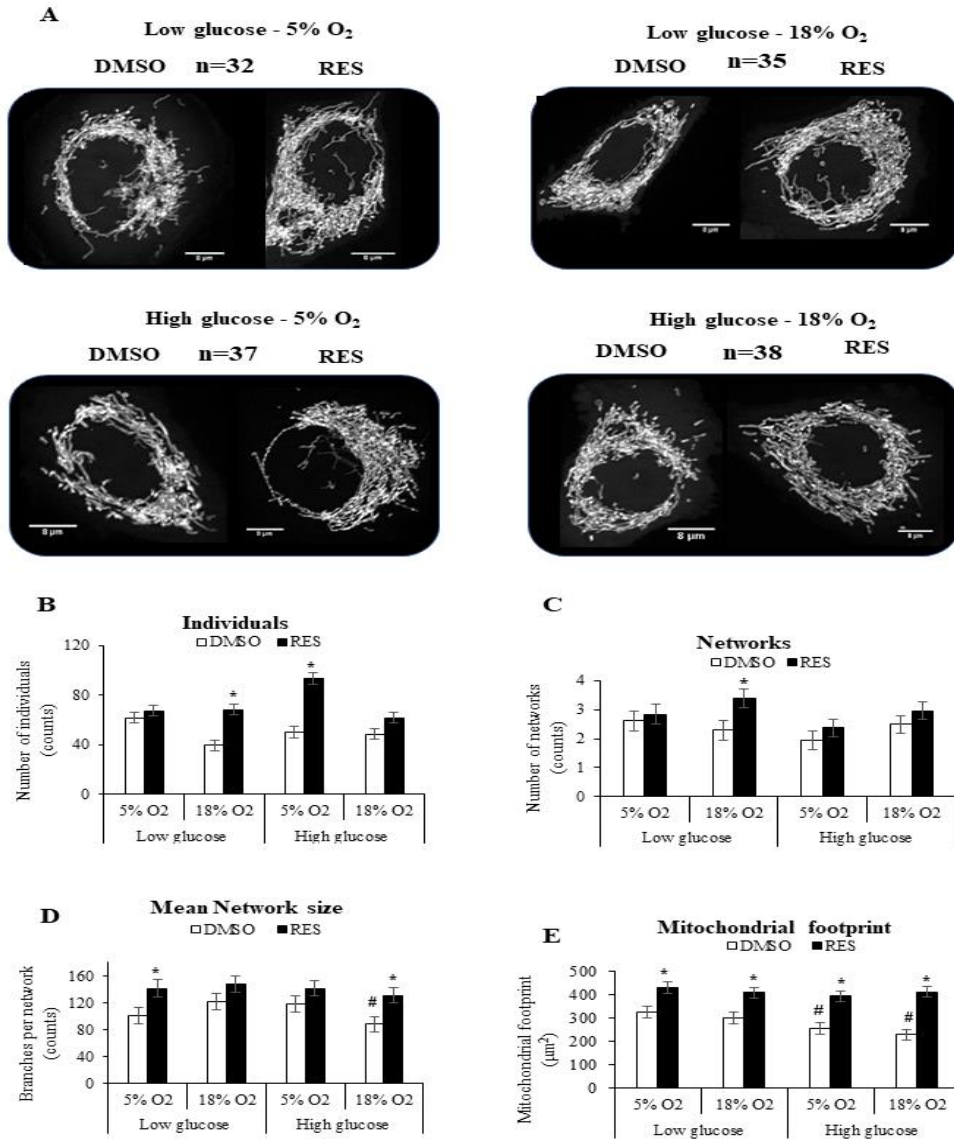


Figure 3.5. RES effects on mitochondrial network parameters are mostly unaffected by media glucose and O₂ levels in PC3 cells. Representative images of PC3 cells' mitochondrial network parameters (A). There was a main effect of RES on the number of individuals (B), networks (C), mean network size (branches per network) (D) and mitochondrial footprint (E). RES-treated cells showed an increase in all of these mitochondrial network parameters. An interaction between glucose and O₂ was also observed for mean network size (branches per network) (C). Main effect of glucose was observed in mitochondrial footprint (D). At low glucose levels mitochondrial footprint was increased. Total magnification in all experiments was 630×. Cells were treated for 48h with 10 μM RES (filled bars) or an equal volume of vehicle control (DMSO; open bars). Data shown are means ± SEM. Randomly selected individual cells were analyzed with MiNA. ‘*’ represents differences between RES-treated and DMSO-treated cells. ‘#’ represents differences between low and high glucose levels. ‘\$’ represents differences between low and high O₂ levels. P values were calculated by ANOVA followed by post-hoc analysis.

Finally, due to the important role that RES has on ROS metabolism, I set out to determine whether some ROS-producing enzymes such as NOX (major ROS contributors at 18% O₂) and nitric oxide synthase (NOS) (more specifically its uncoupling) mediated RES effects on H₂O₂ production. As shown in **appendix S2** RES effects on H₂O₂ production seem to be modulated by NOX4 and NOX1 (**Figure S2.1-S2.4**) but not by NOS (**Figure S2.5**). Most important these effects were determined by O₂ and glucose levels in cell culture (**Figure S2.1-S2.5**).

3.6 Discussion

Most studies of RES's molecular interactions within mammalian cells have been performed in cell culture inside humidified incubators at 37 °C with CO₂ regulated at 5% but no control over O₂ levels, which are 18–19% under these conditions. Many cell culture media contain glucose at concentrations 2–5 times those found in normal human blood. Here I have demonstrated that these non-physiological conditions in cell culture can substantially affect the outcomes of these experiments.

The effects of RES on cell growth were strongly influenced by media glucose levels in both C2C12 cells and PC3 cells, with more subtle effects of RES observed in media with physiological glucose levels. Interestingly, the least effective inhibition of growth in both cell lines was observed in physiological O₂ and glucose levels. This may be an important observation: although RES robustly inhibits growth of a wide variety of cancer cell lines in vitro (Feng et al., 2016; Wu et al., 2015; Yu et al., 2016), its effects on cancer growth in vivo are far less straightforward. This discrepancy has typically been attributed to low RES bioavailability in vivo, (Sergides et al., 2016; Tomé-Carneiro et al., 2013) but our results suggest that an additional difference might be important: RES may simply be a less effective inhibitor of growth in physiologically normal O₂ and glucose levels. This could relate to RES's ability to switch cellular metabolism away from glucose fermentation and toward oxidative phosphorylation, and this switching can inhibit cancer cell growth (Le et al., 2010; Lu et al., 2015). Low glucose conditions already promote increased reliance on oxidative phosphorylation (Elkalaf et al., 2013), so there may be limited further scope for RES to further affect this. In general, our results suggest that more attention should be paid to O₂ and glucose levels during in vitro studies of cancer cell growth.

RES has multiple effects on cellular ROS metabolism, with chemical antioxidant and pro-oxidant activities, as well as effects on ROS production and ROS removal. We have found that high O₂ levels in culture increase cellular H₂O₂ production (Maddalena et al., 2017). This increased ROS production at high O₂ might not create an ideal baseline from which to determine how RES affects ROS metabolism, since these conditions may not occur in vivo. Indeed, I found that, although both O₂ and glucose interacted with RES in affecting cellular H₂O₂ production in C2C12 and PC3 cells, RES had essentially no effect when cells were growing in physiological O₂ and glucose levels. Again, this emphasizes how these two parameters can determine experimental outcomes, which indicates the importance of maintaining both at physiologically appropriate values. If the antioxidant effect of RES is not observable in vivo, it may be because the effect is simply minimal or absent in the absence of high O₂ or glucose.

We have previously shown that RES promotes fusion of the mitochondrial network (Robb et al., 2017). However, mitochondrial dynamics are sensitive to redox state (Shutt et al., 2012) and exposure to bolus H₂O₂ addition causes extensive fragmentation. It was therefore possible that the RES stimulation of mitochondrial fusion was simply reversing fragmentation caused by high O₂. Our results did not support this, however; the effects of RES on mitochondrial network parameters seemed relatively independent of media glucose and O₂. I found a main effect of RES on mitochondrial footprint, network size (number of branches), number of networks, and number of individual structures in both cell lines. The ability of RES to increase mitochondrial footprint and network size was observed even in low O₂, low glucose media.

Overall, our results demonstrate the importance of O₂ and glucose as determinants of RES's effects on cell growth, ROS production, and mitochondrial network characteristics. Although I

included only one cancer cell line here (PC3 cells), it will be important to determine whether the widespread observation that RES inhibits cancer cell growth in vitro can be replicated in more physiologically representative media. If not, this could offer a partial explanation for the failure of RES to achieve the same anti-cancer outcomes in vivo as have been seen in vitro. Similarly, I suggest that experiments to determine how RES affects cellular ROS metabolism should also be done in low O₂ and low glucose media to ensure that outcomes properly represent what would occur in vivo.

Chapter 4 General Discussion and Conclusions

Metabolic reprogramming is an important cancer hallmark (Hanahan and Weinberg, 2011; Pavlova and Thompson, 2016) and a key player involved in this metabolic reprogramming is the transcription factor HIF-1 (Masson and Ratcliffe, 2014). It is well established that hypoxia is a defining feature of solid tumors (Eales et al., 2016; Schito and Semenza, 2016), and several reports have shown that tumors with a higher proportion of hypoxic cells have a poorer prognosis (Muz et al., 2015). Therefore, strategies aimed at preventing HIF-1 stabilization and/or shifting glucose catabolism toward complete mitochondrial oxidation can be of great therapeutic value (Luengo et al., 2017).

4.1 Cancer therapy

Many cancer cells are characterized by their reliance in on aerobic glycolysis. This cellular metabolic reorganization supports cancer cells' increased need for rapid proliferation (Vander Heiden and DeBerardinis, 2017). Strategies to revert cancer cells metabolic reliance on aerobic glycolysis towards OXPHOS are associated with slowed cancer cell growth (Lu et al., 2015). Interestingly, RES antiproliferative effects involve a metabolic reprogramming (i.e. a switch between glycolytic and oxidative metabolism) mediated by HIF-1 α . This supports previous research showing that RES decreased cell proliferation in HeLa (cervical cancer), MCF-7 (breast cancer) and HepG2 (hepatocellular carcinoma) cell lines by inhibiting glucose metabolism (Iqbal and Bamezai, 2012). Similarly (Jung et al., 2013) showed that RES anti-cancer effects both *in vitro* and *in vivo* were dependent on RES ability to suppress cancer cell glucose uptake by inhibiting

intracellular ROS, and by decreasing HIF-1 α levels. Having this in mind, it would be of practical value to assess whether the antiproliferative properties of RES are more prominent in cell lines that express high levels of HIF-1 α .

Due to poor vascularization, most tumors experience low levels of O₂ at some stages of their development (McKeown, 2014b; Muz et al., 2015), which is associated with an increased risk of mortality (Muz et al., 2015; Semenza, 2011). Given the importance of the HIF-1 pathway in RES's antiproliferative effects, I hypothesized that RES would be a particularly effective inhibitor of cell growth under hypoxic conditions. Indeed, under near anoxic conditions ($\leq 0.4\%$ O₂), RES's cell growth inhibitory effects were enhanced. In this thesis, I have also showed that RES concentrations as low as 1 μ M could inhibit PC3 cell growth. This is an important observation. One of the unresolved issues in RES research is the difference between the concentration of RES required to generate *in vitro* effects versus the measured *in vivo* levels. It is possible that the supraphysiological O₂ levels of 18-19% in cell culture are one of the causes of this discrepancy. Nevertheless, the important role that hypoxia has in tumor development opens a therapeutic window for RES by targeting hypoxic tumor cells *in vivo*.

RES antiproliferative effects have been well described (reviewed in (Stuart and Robb, 2013)). However, the exact molecular mechanisms by which they are exerted is still unknown. Previously in our lab we have shown that RES's antiproliferative effects are dependent on an interaction with ER β , and consequent increase in MnSOD expression (Robb and Stuart, 2011). Furthermore, mitochondrial dynamics (i.e. increased in Mfn2 expression) was also proposed to be an important target that may account for RES' growth inhibitory effects (Robb et al., 2017). In this thesis I demonstrate that RES antiproliferative effects involve a decrease in HIF-1 α expression

concomitant with a metabolic shift towards OXPHOS. A possible mechanism by which RES can exert these effects is through modulation of ER signaling. Indeed, ER β is known to interact with HIF-1 α under hypoxia and its overexpression in PC3 cells (which express endogenous ER β) inhibits HIF-1 transactivation (Park and Lee, 2014). Of note, a varying intracellular ER α /ER β might be one of the reasons for the observed variability of RES effects in different cell lines (Thomas and Gustafsson, 2011). Furthermore, Kaewpila et al., 2008 demonstrated that upregulation of MnSOD suppresses HIF-1 α induction under hypoxic conditions. Lastly, several studies have shown that ER β activation and consequent interaction with NRF and TFAM promotes OXPHOS and mitochondrial biogenesis (reviewed in (Liao et al., 2015)). These findings show a promising therapeutic approach, since strategies that promote oxidative metabolism have been shown to slow cancer cell growth (Kuo et al., 2017).

4.2 Mitochondria as a resveratrol target

RES effects on mitochondria function have been well described (Lagouge et al., 2006; De Oliveira et al., 2016). However, most of those studies use a qualitative method to evaluate mitochondrial abundance and morphology. On the other hand, to ensure a more objective analysis of mitochondrial morphology I have used a novel open source tool, named MiNA (Valente et al., 2017). In this way it was possible to assess accurately not only mitochondria biogenesis but also mitochondria morphology an important feature of mitochondrial function.

Mitochondria respond to environmental changes through several mechanisms, such as mitochondrial dynamics (Archer, 2013). Regulation of mitochondrial dynamics is important to

maintenance of proper cell physiology (Willems et al., 2015), as well as stress adaptation (Eisner et al., 2018). A well studied mitochondrial stressor is the oversupply of nutrients (e.g. glucose). Cells exposed to a rich-nutrient environment tend to develop an impaired balance between fusion and fission events, with a shift towards a more fragmented mitochondrial state (reviewed in (Liesa and Shirihai, 2013)), which is usually associated with the development of several metabolic disorders (e.g. cancer, type 2 diabetes) (Liesa and Shirihai, 2013; Maycotte et al., 2017). On the other hand, mitochondrial fusion is usually associated with a more efficient mitochondria, and improved cellular function (Detmer and Chan, 2007). Due to the importance of mitochondrial dynamics in maintaining mitochondrial and cellular functions, the use of small molecules like RES, which have the capacity to promote mitochondrial fusion are therefore of great interest for their therapeutic potential (De Paepe and Van Coster, 2017).

4.3 Cell culture caveats

RES's bioavailability has been widely regarded as the main factor that accounts for the discrepancies observed between RES's *in vitro* and *in vivo* effects (Vitaglione et al., 2005; Walle et al., 2004; Wenzel and Somoza, 2005). Indeed, several *in vitro* studies report doses of RES that are not achievable *in vivo* (Madreiter-Sokolowski et al., 2017). However, cell culture non-physiological conditions (e.g. glucose and O₂ levels) have not received the deserved attention.

In vitro culture is performed in CO₂ incubators, which provide control over key factors such as CO₂ (5%; maintaining proper pH levels), temperature (37°C) and humidity (95%; prevents medium evaporation). The main goal of these incubators is to mimic *in vivo* conditions; however, they do not consider one significant factor – O₂. Indeed, standard cell culture is usually performed

under hyperoxic conditions, which can influence several oxygen-dependent reactions (reviewed in (Stuart et al., 2018)). Furthermore, recently in our lab we have showed that H₂O₂ production is influenced by oxygen levels in cell culture, more specifically, cells growing at 18% O₂ had a higher H₂O₂ production when compared to cells growing under 5% O₂ (Maddalena et al., 2017). Having this in mind and given the important role that RES has on cellular ROS metabolism, by both regulating the expression and/or activity of antioxidant and pro-oxidant enzymes, it might be necessary to reconsider some of RES *in vitro* results found in the literature.

Another important caveat of cell culture is medium composition. Commercial culture media, such as DMEM, contains a disproportionate metabolite composition, which do not represent the normal physiological environment. For example, while glucose (25mM), glutamine (4mM) and pyruvate (1.2mM) account for over three-quarters of the entire pool of nutrients in DMEM formulation, their contribution to the whole pool of nutrients in a normal adult serum is comparatively lower (<50%; 5mM for glucose, 600μM for glutamine and 34.5μM for pyruvate) (Psychogios et al., 2011). Most importantly, this limitation in cell culture may interfere with some signaling pathways. Interestingly, HIF-1α expression has been shown to be influenced by both oxygen-dependent (Kaelin and Ratcliffe, 2008) and O₂-independent mechanisms (Lu et al., 2005). In the presence of O₂, HIF-1α is usually sent for degradation by the proteasome in a process that requires the post-translational modification of proline residues 402 and 564 within the HIF-1α O₂ dependent (ODD) domain (Kaelin and Ratcliffe, 2008). On the other hand, some glucose metabolites such as pyruvate and oxaloacetate can also prevent HIF-1α degradation (Lu et al., 2005). Indeed, in a recent study it was observed that supraphysiological pyruvate concentrations promoted a chronic pseudohypoxia even under hyperoxic conditions (~18% O₂) (Vande Voorde et al., 2019). This mechanism of chronic pseudohypoxia induction is thought to be promoted by

pyruvate effects on PHD activity (Lu et al., 2005). HIF-1 plays an important role in several cellular functions including cell growth, proliferation and metabolic adaptation (Kumar and Choi, 2015). Therefore, to improve *in vitro* models' reliability, special attention needs to be given to potential artifacts in cell culture, especially when studying pathways that are directly or indirectly affected by HIF-1 levels.

Besides pyruvate, commercial media also contain supraphysiological levels of glucose (~5 times higher than normal glucose levels observed in a healthy human). Nutrient availability is known to influence mitochondrial morphology (Liesa and Shirihai, 2013). For example, cells that are exposed to a rich-nutrient environment usually possess a more fragmented mitochondria, while under starvation mitochondria tend to be more fused. In this thesis, I have shown that the *in vitro* antiproliferative effects of RES are highly dependent on a metabolic reprogramming characterized by a higher reliance on OXPHOS (these results were obtained in cells growing under hyperoxia and hyperglycemic conditions). More importantly, these same effects were diminished or even abolished when cells were grown in a more relevant physiological condition (eg. 5% O₂ and 5mM glucose). This observation is relevant when delineating *in vitro* models that study molecules that affect mitochondria morphology and function.

4.4 Study limitations and future work

Tissue oxygenation heterogeneity in both health and disease tissues is well documented (Harrison and Vaupel, 2014), and therefore the use of a single O₂ concentration to represent normoxia is potentially a limiting factor in the present study. *In vivo* oxygenation is heterogeneous

in both space and time, which means that depending on the cell type, normoxia values will change accordingly. Therefore, future *in vitro* investigations may benefit from studying a range of physiological relevant O₂ concentrations that better represent the conditions experienced in the tissue of origin.

In this thesis, normoxia was defined as 5% O₂. This value refers to ambient O₂ levels, which depending on cell density, cell type and cell metabolism, can be quite variable (Pettersen et al., 2005). For example, in our lab we showed that when growing PC3 cells and C2C12 cells at 5% incubator O₂ levels, pericellular O₂ levels are often lower (near anoxia for PC3 cells growing for 72h) and variable (Maddalena et al., 2017). The observed variability can lead to reproducibility issues, especially when studying intracellular signaling pathways that are O₂ regulated (e.g. HIF-1). Another important reason to report the exact pericellular O₂ levels is the relationship between O₂ and ROS production, which has mentioned previously affect a myriad of cellular processes. Therefore, to ensure better reproducibility across different studies, pericellular and not ambient O₂ levels should be reported.

Another important consideration to ensure results reproducibility is the metric used to report O₂ levels. Some studies have stated that reporting O₂ levels in % is a more physiological meaningful metric (McKeown, 2014a). On the other hand, other studies defend that this is a less than perfect metric for measuring the amount of O₂ present in culture, because it does not account for altitude or differences of humidity (Wenger et al., 2015). Instead, the use of the partial pressure of O₂ (measured in millimeter mercury (mmHg)), is the most reliable metric and as the only one that should be used to define O₂ levels in culture (Wenger et al., 2015).

O₂ and glucose levels are important cell culture parameters that define the outcomes of RES *in vitro* effects. However, these are only two variables in a broader context. For example, as mentioned before, supraphysiological concentrations of pyruvate in cell culture are known to stabilize HIF-1 α even under normoxia (Vande Voorde et al., 2019). Having this in mind, it is expected that other components present in standard commercial media (e.g. glutamine) may affect *in vitro* studies outcomes. Therefore, it would be relevant to assess whether RES *in vitro* effects in commercial media can be reproduced in culture medium that better recapitulates the physiological cellular environment.

Finally, although this thesis only focuses on RES, other stilbenes such as pterostilbene and piceid should also be studied. Pterostilbene and piceid are produced via the same stilbene biosynthesis routes and are structural analogues to RES. Most importantly, they are known to exert similar *in vitro* effects to RES (i.e. inhibit mammalian cells' growth through a mitochondrial response) (Robb and Stuart, 2014). Therefore, it would be interesting to observe whether the antiproliferative effects of pterostilbene and piceid are also affected by the *in vitro* non-physiological environment.

4.5 Conclusion

In vitro O₂ and glucose levels influence key cellular processes (e.g. cell metabolism, cell growth and differentiation). Recent studies have shown the impact that cell culture artifacts may have in normal physiological processes (Keeley and Mann, 2019; Vande Voorde et al., 2019). Therefore, in order to improve the reliability of *in vitro* results, cell culture conditions should try to mimic as much as possible the *in vivo* environment. On the bright side, there has been an increase

in awareness about cell culture caveats, with some laboratories making efforts to regulate *in vitro* conditions. For example, by simply regulating the O₂ levels of incubators and formulating specific media compositions (e.g. Plasmax) (Vande Voorde et al., 2019) that better reproduce the *in vivo* environment, it is possible to circumvent some of cell culture downfalls.

Current cell biology research relies heavily on results obtained using cell culture. Therefore, its important not only to be aware of its limitations, but also to implement cell culture conditions that best mimic physiological environment. Achieving this will ultimately improve the results obtained *in vitro* (i.e. improve *in vitro* reproducibility), which could reduce the use of animal models.

Appendix

S.1 Supplementary information to chapter 2

I. Intracellular H₂O₂ detection

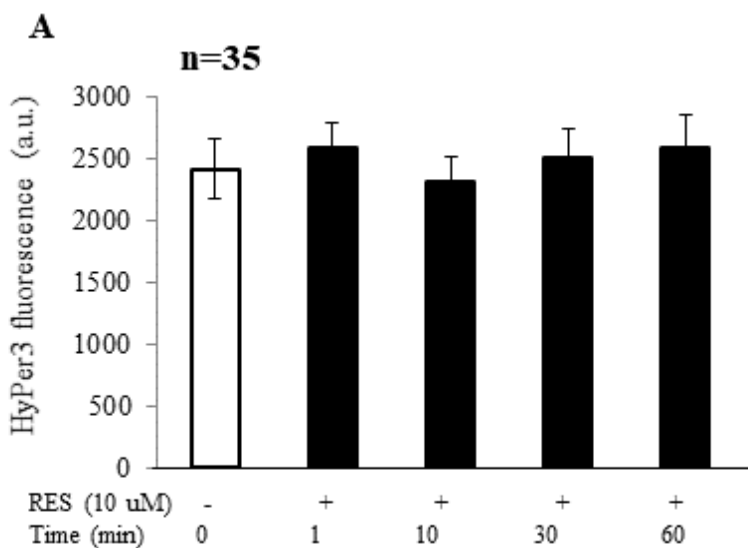


Figure S.1.1 A) Acute addition of 10 μ M RES did not affect PC3 cytosolic H₂O₂ levels. RES had no acute effects on intracellular H₂O₂ levels as measured with Hyper 3 ($F_{3,102} = 0.85$, $p=0.4710$). At the same time a pH control was performed (data not shown). PC3 cells were cultured on Matek 35mm poly-D-lysine-coated glass bottom culture dishes for 24 before transfection. Transfections were performed with Lipofectamine 2000. 24h after transfection cells were imaged using a Carl Zeiss Axio Observer Z1 inverted light/epifluorescence microscope. Green fluorescence was detected using a fluorescence channel possessing excitation and emission wavelength filter sets of 450nm-490nm and 500-550 nm, respectively. Cells were treated with 10 μ M RES for an hour and images of live cells were taken at 1min, 10min, 30min and 60min after treatment. Exogenous H₂O₂ and DTT were added as positives control to drive the probes to its fully oxidized and reduced states, respectively. eGFP intensity was measured using the Zeiss software. At least 30 cells per condition were selected randomly from at least three separate experiments. pC1-Hyper-3 (Addgene plasmid no. 42131) and pC1-Hyper-C199S were a gift from Vsevolod Belousov (Belousov et al., 2006; Bilan et al., 2013). P values were calculated by repeated measures ANOVA.

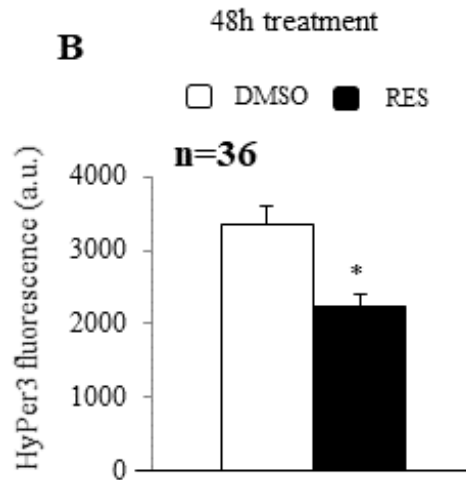


Figure S1.1 B) Chronic treatments (48h) with 10 μ M RES reduced cytosolic H₂O₂ levels in PC3 cells. 48h treatment with RES decreased intracellular H₂O₂ levels in PC3 cells as measured with Hyper 3 (**p=0.0002**). PC3 cells were cultured on Matek 35mm poly-D-lysine-coated glass bottom culture dishes. RES and vehicle control treatments were added to PC3 cells every day for 48h. After treatments, PC3 cells were transfected with pC1-Hyper-3 by using the Lipofectamine 2000 reagent. 24h after transfection cells were imaged using a Carl Zeiss Axio Observer Z1 inverted light/epifluorescence microscope. Green fluorescence was detected using a fluorescence channel possessing excitation and emission wavelength filter sets of 450nm-490nm and 500-550 nm, respectively. Exogenous H₂O₂ and DTT were added as positives control to drive the probes to its fully oxidized and reduced states, respectively. eGFP intensity was measured using the Zeiss software. At least 30 cells per condition were selected randomly from at least three separate experiments. pC1-Hyper-3 (Addgene plasmid no. 42131) was a gift from Vsevolov Belousov (Bilan et al., 2013). ‘*’ represent differences between RES-treated and DMSO-treated. P values were calculated by t-test (unpaired, two-tailed).

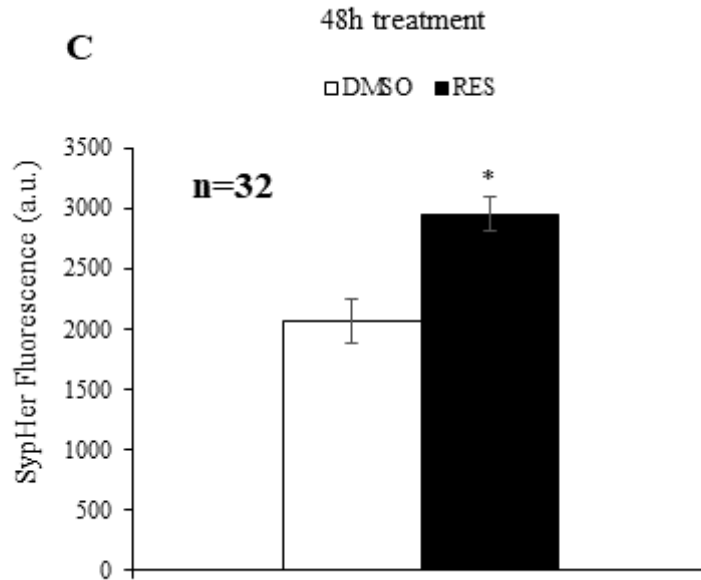


Figure S1.1 C) Chronic treatments (48h) with 10 μ M RES RES increased intracellular pH (pHi) PC3 cells. RES promoted an alkalization of the intracellular environment ($p < 0.0001$). PC3 cells were cultured on Matek 35mm poly-D-lysine-coated glass bottom culture dishes. RES and vehicle control treatments were added to PC3 cells every day for 48h. After treatments, PC3 cells were transfected with pC1-Hyper-C199S by using the Lipofectamine 2000 reagent. 24h after transfection cells were imaged using a Carl Zeiss Axio Observer Z1 inverted light/epifluorescence microscope. Green fluorescence was detected using a fluorescence channel possessing excitation and emission wavelength filter sets of 450nm-490nm and 500-550 nm, respectively. Exogenous H₂O₂ and DTT were added as positives control to drive the probes to its fully oxidized and reduced states, respectively. eGFP intensity was measured using the Zeiss software. At least 30 cells per condition were selected randomly from at least three separate experiments. pC1-Hyper-C199S was a gift from Vsevolov Belousov (Belousov et al., 2006). ‘*’ represent differences between RES-treated and DMSO-treated cells. P values were calculated by t-test (unpaired, two-tailed).

II. HIF-1

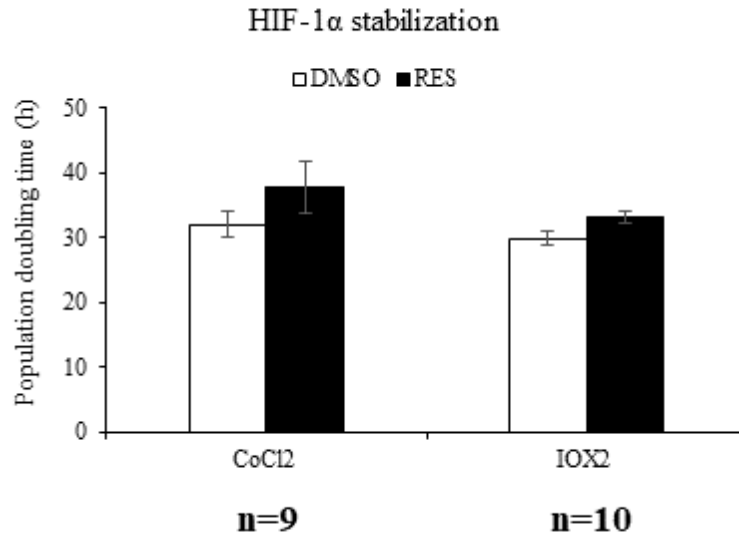


Figure S1.2. RES effects on cell doubling time were abolished when HIF-1 α is stabilized both with cobalt chloride (CoCl₂) and IOX₂. When HIF-1 α is stabilized by pharmacological (IOX₂, **p=0.0693**) or chemical inhibition (CoCl₂, **p=0.2423**) of PHD activity, RES slowed growth effects were not observed. Cells were cultured in high glucose DMEM at 37°C in humidified 5% CO₂ and 18% O₂ atmosphere. ‘Pseudo-hypoxia’ was induced through chemical means via treatment with the PHD inhibitors, CoCl₂ (100 μ M) and IOX₂ (25 μ M). Cells were incubated overnight with CoCl₂ and IOX₂ prior to commencing the treatments with vehicle control (DMSO) and RES. Treatments were added directly to the culture media for 48h. Media and treatments were refreshed every day. Cell population doubling time was determined by trypan blue exclusion assay. P values were calculated by t-test (unpaired, two-tailed).

III. Pentose phosphate pathway

Glucose-6-phosphate dehydrogenase (G6PDH) is a cytosolic enzyme expressed in all cells of the body, that catalyzes the first reaction and rate-limiting step in the pentose phosphate pathway (PPP). G6PDH catalyzes the oxidation of glucose 6-phosphate (G6P) to 6-phosphoglucono- δ -lactone and in the process reducing NADP^+ to $\text{NADPH} + \text{H}^+$. This reaction is the rate-determining step of the PPP and is dependent on the $\text{NADP}^+/\text{NADPH}$ ratio. PPP is crucial in the nucleotide biosynthesis pathway, as well as in redox homeostasis maintenance through NADPH formation (reviewed in (Salati and Amir-Ahmady, 2001)). Due to its role in nucleic acid synthesis and NADPH formation (required for fatty acids synthesis), PPP is of major importance in rapidly dividing cells, such as cancer cells (reviewed in (Patra and Hay, 2014)). Most importantly, under hypoxia, cancer cells redirect glucose metabolism into the PPP by induction of G6PDH gene expression (Gao et al., 2004), a process that involves HIF-1 α activation (Osada-Oka et al., 2010). Because of that the PPP and more specifically the G6PDH enzyme, has been suggested as a potential therapeutic target in cancer (Cho et al., 2018).

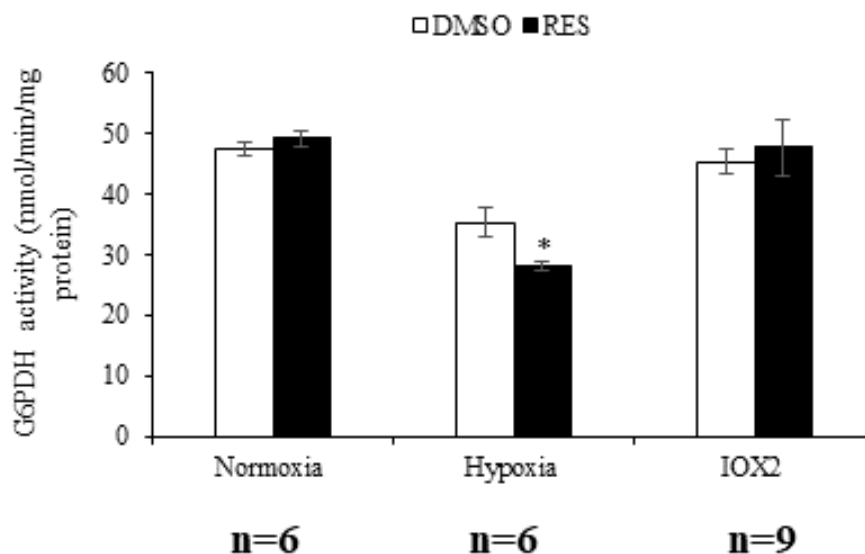


Figure S1.3. RES decreased G6PDH activity in PC3 cells growing at hypoxic conditions (≤ 0.4 % O_2 , but had no effect when cells were grown at normoxic (18% O_2) conditions or treated with IOX2. RES-treated cells growing under hypoxic conditions showed a decrease in G6PDH activity when compared to the vehicle control ($p=0.0271$). That effect was abolished when cells were grown at normoxia (18% O_2) ($p=0.3562$) or treated with the specific PHD inhibitor IOX2 ($p=0.0701$). Surprisingly, cells growing at 18% O_2 showed a higher activity when compared to cells that were grown under hypoxic conditions ($p=0.0030$). An interaction between normoxia/hypoxia/IOX2 and G6PDH was observed ($F_{2,36} = 13.71$, $p < 0.0001$). Hypoxic conditions were performed as described in (Fonseca et al., 2019). Cells were treated for 48h with RES or the vehicle control and treatments were refreshed daily. G6PDH activity was measured in a solution containing 55mM Tris buffer (pH7.8), 3mM magnesium chloride, 2mM $NADP^+$, 33mM G6P and 15 μ g. The conversion of $NADP^+$ to NADPH after G6P addition was followed spectrophotometrically (340nm) using a Varian Cary 100 UV-visible spectrophotometer. Background rate of $NADP^+$ reduction was monitored for 2 minutes before G6P was added to initiate the reaction. Assays were performed at 30°C. ‘*’ represent differences between RES-treated and DMSO-treated cells. P values were calculated by ANOVA followed by post-hoc analysis.

IV. Cell doubling time (hypoxia vs normoxia)

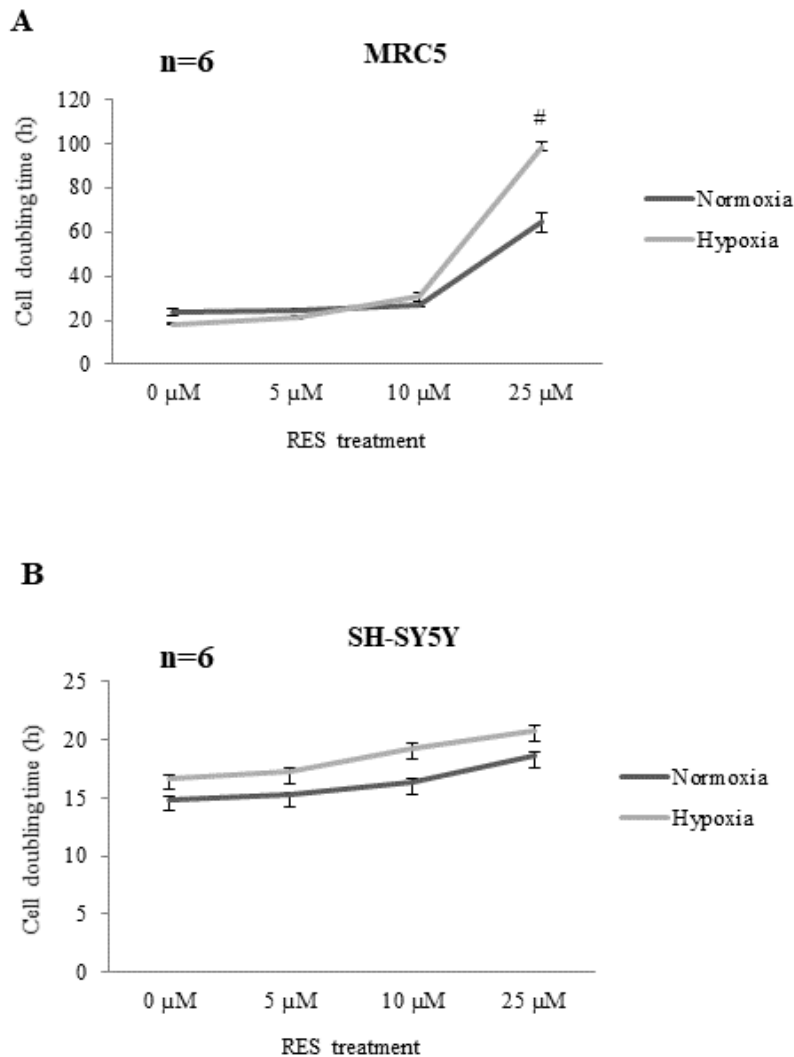


Figure S1.4. RES cell growth inhibitory effects under hypoxic conditions are cell type dependent. As seen in chapter 2, **figure 2.6E**, RES inhibitory effects in PC3 cells were strongly enhanced under hypoxic conditions, even for low RES concentrations such as 1 μM. However, this was not observed in MRC5 (**A**) and SH-SY5Y ($F_{3,40} = 0.67$, $p = 0.5763$) (**B**) cells. Indeed, while for SH-SY5Y there was no correlation between oxygen levels and RES treatment for any of the RES concentrations used, in MRC5 a correlation between oxygen levels and RES treatment was only observed for the highest concentration of RES used (25 μM; $F_{3,40} = 51.74$, $p < 0.0001$). Hypoxic conditions were performed as described in (Fonseca et al., 2019). Cell population doubling time was determined by trypan blue exclusion assay. ‘#’ represent differences between hypoxia and normoxia. P values were calculated by ANOVA followed by post-hoc analysis.

V. Mitochondrial ROS

RES effects on cell doubling time were enhanced under hypoxic conditions, a process dependent on HIF-1 α expression. Previous data has shown that RES cell growth inhibitory effects are dependent on MnSOD induction (Robb and Stuart, 2011). Furthermore, compelling data suggests that a decrease in MnSOD expression under hypoxic conditions leads to an increased HIF-1 α expression, through a significant increase in the level of superoxide (Kaewpila et al., 2008). Indeed, some studies have implied the involvement of ROS in HIF-1 α stabilization in various types of cancer cells (reviewed in (Galanis et al., 2008)).

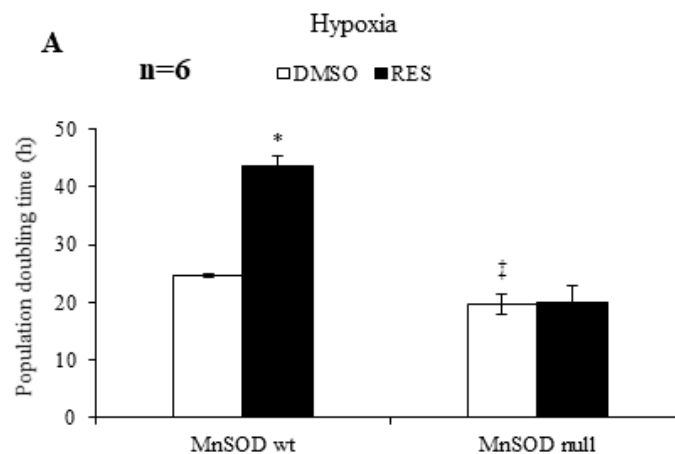


Figure S1.5 A) RES cell growth inhibitory effects under hypoxic conditions are dependent on MnSOD expression. An interaction between cell line and treatment was observed ($F_{1,20} = 21.89$, $p=0.0001$). RES slowed cell growth in MnSOD wt MEFs cells ($p<0.0001$). On the other hand, RES effects on cell growth were abolished in MnSOD null MEFs cells ($p=0.9471$). Interestingly, MnSOD null cells have a lower population doubling time, when compared to MnSOD wt ($p=0.0377$). Hypoxic conditions were performed as described in (Fonseca et al., 2019). MnSOD null and wild-type MEFs were generously provided by Dr. Prabhat Goswami of the University of Iowa. Treatments were added directly to the culture media for 48h. Media and treatments were refreshed every day. Cell population doubling time was determined by trypan blue exclusion assay. '*' represent differences between RES-treated and DMSO-treated cells. '‡' represents differences between MnSOD wt and MnSOD null. P values were calculated by ANOVA followed by post-hoc analysis.

A wide range of antioxidants can be targeted to mitochondria by conjugation to a lipophilic cation, such as the triphenylphosphonium (TPP) moiety. A typical TPP-based mitochondrial-targeted antioxidant is composed of a targeting moiety (i.e. TPP⁺), a linker alkyl chain (typically n=2-10) and a functional moiety (e.g. a nitroxide group that exhibits a superoxide dismutase mimetic activity). Mitochondrial-targeted antioxidants take advantage of the negative membrane potential of the mitochondrial inner membrane, which accumulate in the mitochondrial matrix against their concentration gradient (Smith et al., 1999; Zielonka et al., 2017).

One of the most used mitochondria-targeted antioxidants is MitoQ, a mitochondria-targeted derivative of ubiquinone (Murphy and Smith, 2007). Inside the mitochondria MitoQ is reduced to the active antioxidant ubiquinol by complex II. Ubiquinol can be oxidized to the ubiquinone form, which is then rapidly reduced by complex II. MitoQ recycling is of major importance for its efficacy as ROS scavenger (James et al., 2005). MitoQ mainly reacts with mitochondrial O₂^{•-}, with negligible reactivity against H₂O₂ (James et al., 2005). While most of the work on mitochondria-targeted antioxidants has been on MitoQ, other mitochondria-targeted antioxidants have also been developed. A promising specific mitochondrial O₂^{•-} scavenger is MitoSOD, a SOD mimetic (Salvemini et al., 1999). Of note, mitochondria-targeted antioxidants have been proposed as promising chemotherapeutic molecules (Kalyanaraman et al., 2018).

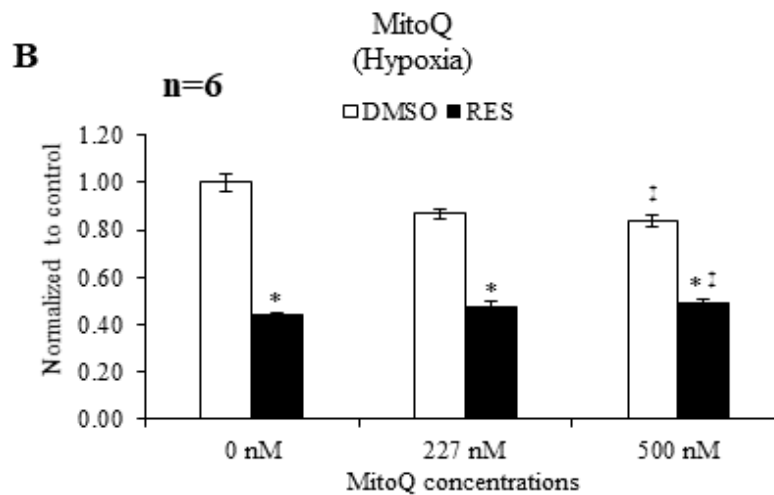


Figure S1.5 B) RES cell growth inhibitory effects were diminished in the presence of a specific mitochondrial $O_2^{\cdot-}$ scavenger (MitoQ). MitoQ (500nM) decreased cell growth in PC3 cells ($p=0.0006$). However, the inhibitor effect was not exacerbated in the presence of RES. Indeed, the combination of MitoQ (500nM) with RES treatment had a lower inhibitor effect than just RES alone (0nM) ($p=0.0427$). Finally, there was a strong interaction between MitoQ concentrations and treatments (DMSO and RES) ($F_{2,30} = 14.02$, $p<0.0001$). PC3 cells were either treated with RES or vehicle control in the presence (227nM and 500nM) or not of MitoQ for 48h. Hypoxic conditions were performed as described in (Fonseca et al., 2019). Cell population doubling time was determined by trypan blue exclusion assay. ‘*’ represent differences between RES-treated and DMSO-treated cells. ‘‡’ represents differences between MitoQ concentrations. All the data was normalized to vehicle control. P values were calculated by ANOVA followed by post-hoc analysis.

S.2 Supplementary information to chapter 3

I. NADPH oxidases

As previously mentioned, a wide range of cell lines showed a consistent increase in H₂O₂ efflux when grown at 18% O₂ compared to 5% O₂ (Maddalena et al., 2017), and NOX isoforms 1 and/or 4 seem to be the major contributors to this difference (Maddalena et al., 2017). Furthermore, NADPH oxidase protein levels are increased and are considered to be major ROS contributors under hyperglycemic conditions (Manea et al., 2015; Mustapha et al., 2010; Yao et al., 2017). Having that in mind, and given that RES is able to modulate NOXs expression/activity (Chen et al., 2013; He et al., 2016; Schilder et al., 2009; Zhang et al., 2012) I set out to determine whether RES effects on H₂O₂ production in C2C12 cells were NOX1/NOX4 dependent.

25mM glucose

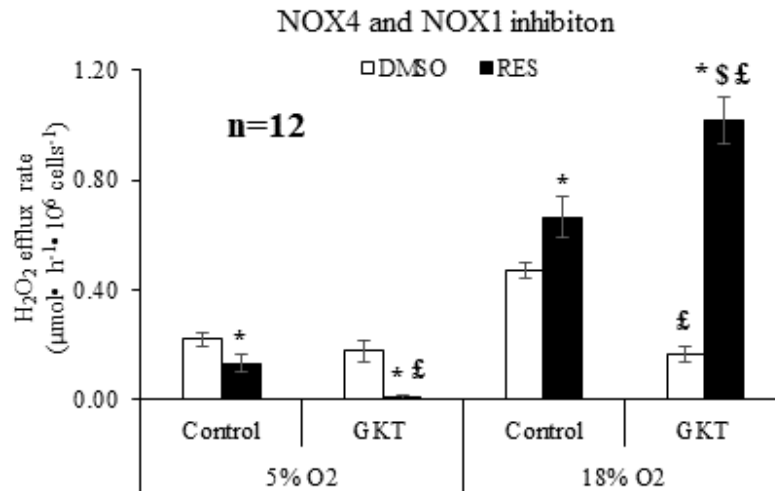


Figure S2.1. NOX 1 and 4 inhibition by GKT137831 modulates RES effects on H₂O₂ production in C2C12 cells. Cells produce more H₂O₂ at 18% O₂ versus 5% O₂. This increment in H₂O₂ production at 18% O₂ was prevented by selective NADPH oxidase 1 and 4 inhibitor, GKT137831. RES modulates H₂O₂ efflux in an O₂-dependent manner ($F_{1,88} = 27.73$, $p < 0.0001$). Briefly, in C2C12 mouse myoblasts RES acts as antioxidant at 5% O₂ ($p = 0.0356$) and as a prooxidant at 18% O₂ ($p = 0.0216$). Furthermore, RES effects were mostly exacerbated with GKT137831 (5% O₂ – $p = 0.0004$; 18% O₂ – $p < 0.0001$). H₂O₂ efflux from cells was measured using the Amplex Red reagent. During the experiment, cells were incubated in the presence of 5µM GKT137831 or vehicle control. Data were analyzed using JASP version 9 software and consisted of analyses of variance (ANOVA). Between-subject factors were O₂, (5% O₂, 18% O₂) and treatment (DMSO, RES). Bars represent the mean \pm SEM. ‘*’ represent differences between RES-treated and DMSO-treated cells. ‘\$’ represents differences between 5% O₂ and 18% O₂. ‘£’ represent differences between control and GKT137831.

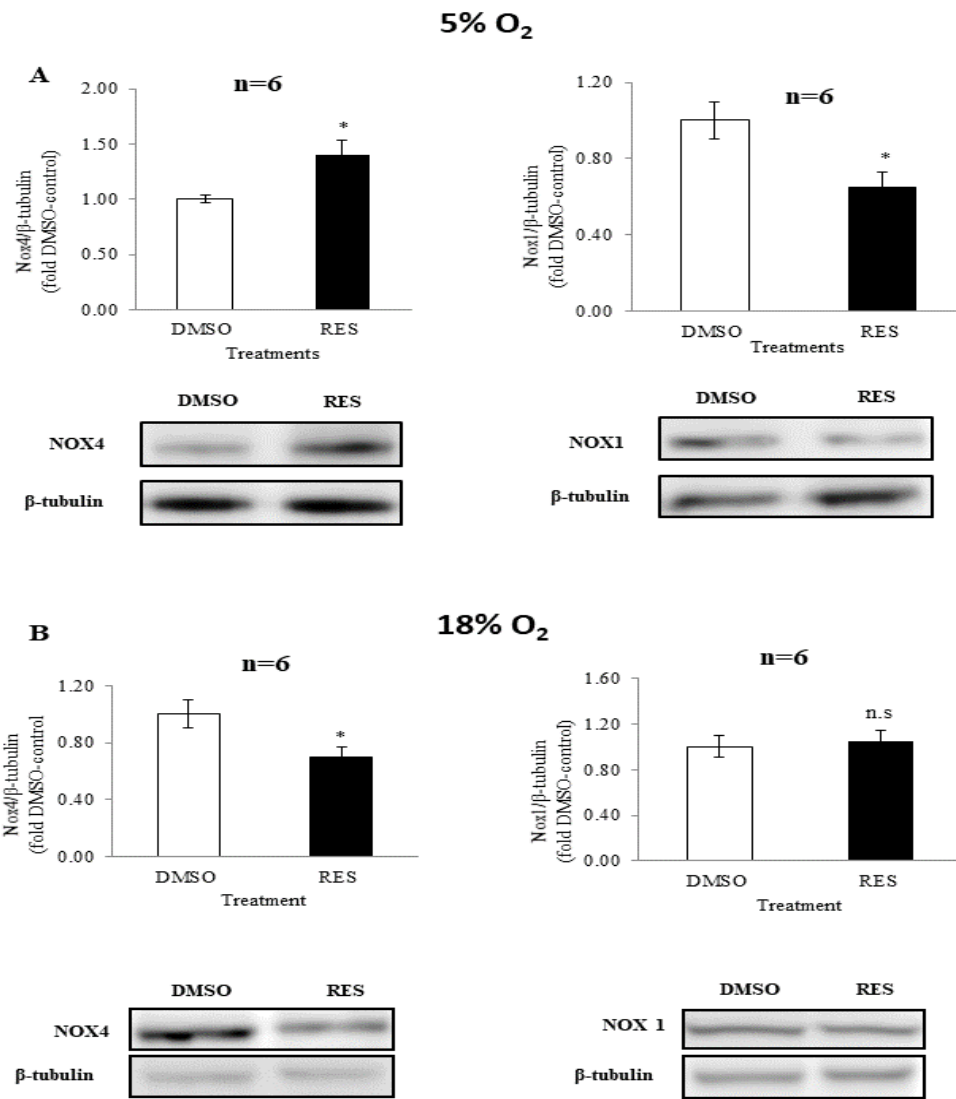


Figure S2.2. RES effects on NOX 1 and 4 protein expression in C2C12 cells were different at 5% O₂ versus 18% O₂ (C2C12 cells). RES had opposite effects on NOX4 expression at 18% O₂ and 5% O₂, with a decrease ($p= 0.0163$) and increase ($p= 0.0175$) in NOX4 expression, respectively. In relation to NOX1 expression, RES had no effect or decreased its expression at 5% O₂ and 18% O₂, respectively. Representative Western blots showing NOX4 and NOX1 in C2C12 cells, at 18% O₂ (A) and 5% O₂ (B). Nox1 and Nox4 signal was standardized to β-tubulin. Western Blots were performed as in (Stuart et al., 2018). Briefly, equal amounts of total protein (15μg per sample) were resolved on 10% SDS-PAGE, transferred to a PVDF membrane, and probed overnight for Nox1 or Nox4. β-tubulin was incubated for 2h room temperature and was used as an internal loading and transfer control. All antibodies were purchased from Novus Biologicals; Nox1 (NBP1-31546), Nox4 (NB110-5858), β-tubulin (NB600-936). Bars represent means ±SEM. ‘*’ represent differences between RES-treated and DMSO-treated cells. P values were calculated by t-test (unpaired, two-tailed).

5mM glucose

NOX4 and NOX1 inhibition

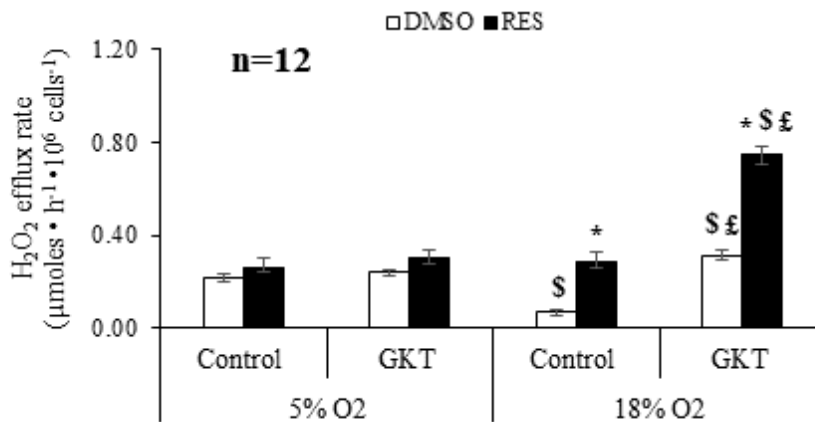


Figure S2.3. At the most physiological conditions (5% O₂ and 5mM glucose) NOX1/4 specific inhibition does not influence RES effects on C2C12 cells' H₂O₂ production. An interaction between glucose, O₂ and treatment was observed ($F_{1,88} = 7.84$, $p=0.0063$). RES effects on H₂O₂ efflux rate were abolished when cells were grown at 5% O₂ and in 5mM glucose media ($p=0.0849$). In contrast with what was observed for high glucose media (**Figure S2.1**), cells growing in a 5mM glucose media showed an increase in H₂O₂ efflux rate at 5% O₂ versus 18% O₂ ($p<0.0001$). Furthermore, while GKT137831 has no effect at 5% O₂ ($p=0.2917$; like what was observed in high glucose), selective inhibition of NADPH oxidase 1 and 4 at 18% O₂, showed an increase in H₂O₂ efflux rate ($p<0.0001$). Finally, RES effects in H₂O₂ efflux rate were exacerbated at 18% O₂ ($p<0.0001$). H₂O₂ efflux from cells was measured using the Amplex Red reagent. During the experiment, cells were incubated in the presence of 5µM GKT137831 or vehicle control. Data were analyzed using JASP version 9 software and consisted of analyses of variance (ANOVA). Between-subject factors were O₂, (5% O₂, 18% O₂) and treatment (DMSO, RES). Bars represent the mean \pm SEM. '*' represent differences between RES-treated and DMSO-treated cells. '\$' represents differences between 5% O₂ and 18% O₂. '£' represent differences between control and GKT137831.

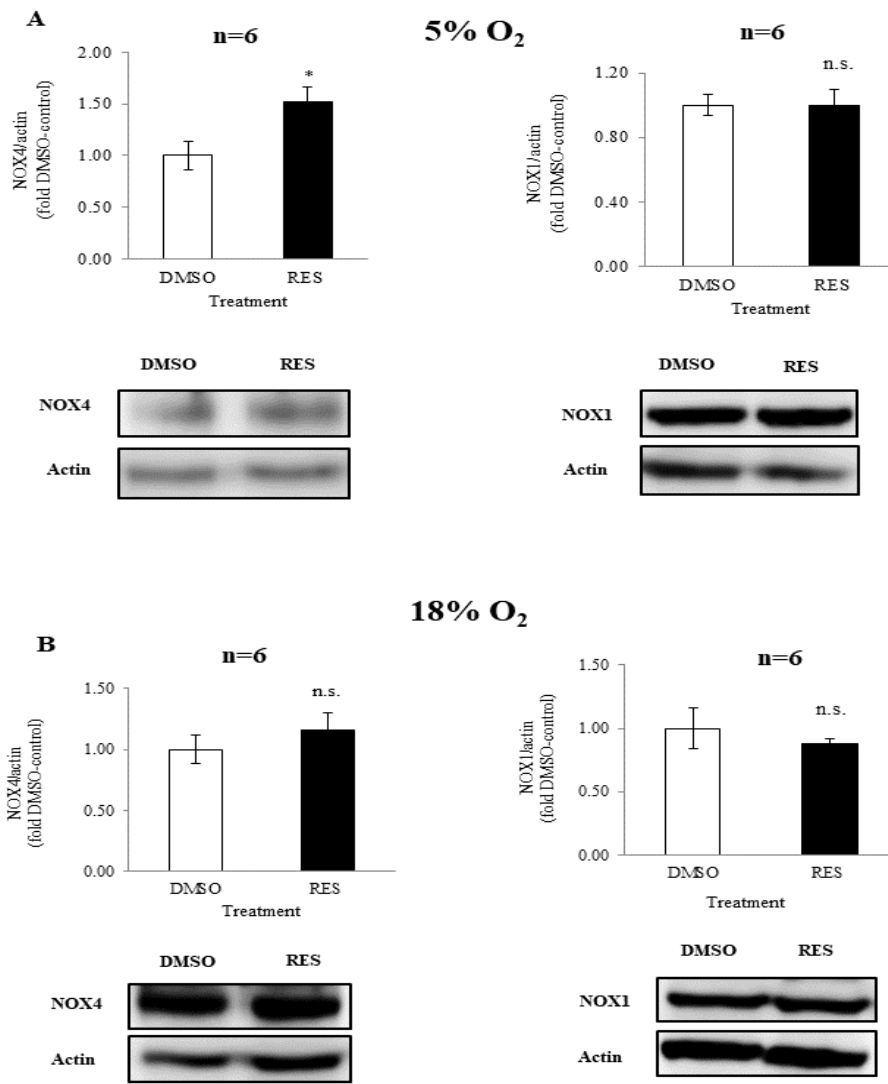


Figure S2.4. In low glucose media [5mM glucose], RES effects on NOX4 protein expression in C2C12 cells were O₂-dependent. RES effects on NOX1 expression were not influenced by O₂ levels. At 5% O₂ RES increased NOX4 expression ($p=0.0172$). However, at 18% O₂ NOX4 protein levels were not altered by RES treatment. RES treatment had no effect in NOX1 expression at both 5% O₂ and 18% O₂. Representative Western blots showing NOX4 and NOX1 in C2C12 cells, at 5% O₂ (A) and 18% O₂ (B). Nox1 and Nox4 signal was standardized to β -tubulin. Western Blots were performed as in (Stuart et al., 2018). Briefly, equal amounts of total protein (15 μ g per sample) were resolved on 10% SDS-PAGE, transferred to a PVDF membrane, and probed overnight for Nox1 or Nox4. Actin was incubated for 2h room temperature and was used as an internal loading and transfer control. Nox1 (NBP1-31546), Nox4 (NB110-5858) antibodies were purchased from Novus Biologicals; Actin (I-19: Sc-1616) antibody was purchase from Santa Cruz Biotechnology. Bars represent means \pm SEM from at least 4 independent experiments. ‘*’. P values were calculated by t-test (unpaired, two-tailed).

The study of NOXs enzymes is not without some difficulties, mostly because of the lack of reliable tools. Firstly, most of the available commercial antibodies generated against NOX1 and NOX4 are polyclonal, which possess low sensitivity, as well as low specificity (Altenhöfer et al., 2012; Meitzler et al., 2017). Secondly, despite recent advances in the design of pharmacological NOX inhibitors (Altenhöfer et al., 2015), some of them still possess off-target effects, with some studies also reporting direct antioxidant effects (Altenhöfer et al., 2012). The inhibitor used in this study (GKT137831) is one of the best characterized NOX inhibitors currently available and is known to possess high selectivity for NOX1 ($IC_{50}=0.14\mu M$) and NOX4 ($IC_{50}=0.11\mu M$) (Altenhöfer et al., 2015). Furthermore, GKT137831 is the first NOX inhibitor in clinical development (Jiang et al., 2012). Despite this, NOX research translational needs to be approached carefully.

II. Nitric oxide synthases

Nitric oxide synthases (NOS) enzymes catalyze the conversion of L-arginine and molecular O₂ to L-citrulline and nitric oxide (NO), using NADPH, FMN, FAD, calmodulin, heme, and tetrahydrobiopterin (BH₄) as cofactors (Marletta, 1993). This small cell signaling molecule is produced by three isoforms of NO synthase, endothelial NOS (eNOS), neuronal NOS (nNOS), and inducible NOS (iNOS) (Alderton et al., 2001). Under certain conditions, NOS loses its ability to convert L-arginine to L-citrulline producing superoxide instead of NO (Xia et al., 1998). This phenomenon is called NOS uncoupling (i.e. uncoupling of O₂ reduction from NO synthesis).

All NOS isoforms possess a wide range of O₂ affinities, with K_m (O₂) values varying from as low as 0.3 to as high as 39.8 (Stuart et al., 2018). Therefore, it is expected that NOS isoforms are sensitive to changes in O₂ levels between physioxia and 18% O₂. This can lead to changes in NO and/or superoxide production between *in vitro* and *in vivo* conditions, especially in cell lines with higher NOS isoforms expression.

RES increases NO production by upregulating NOS expression, stimulating NOS enzymatic activity as well as reversal of NOS uncoupling (reviewed in (Xia et al., 2014)).

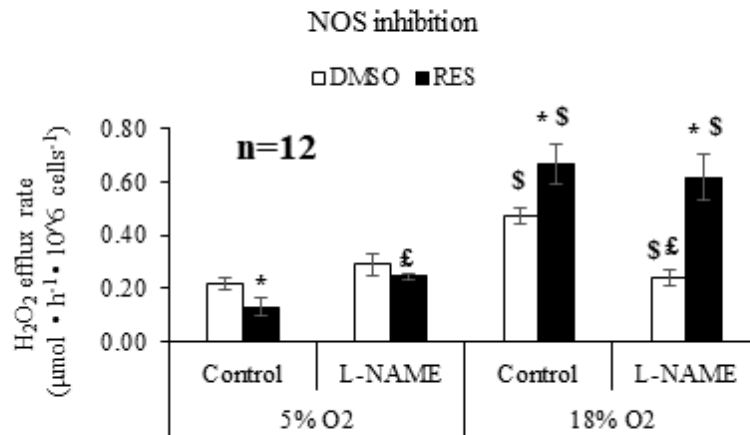


Figure S2.5. RES effects on C2C12 cells' H₂O₂ production are independent of NOS inhibition with L-NAME. There was no interaction between L-NAME, O₂ and treatment ($F_{1,88} = 0.72$, $p=0.3975$). Treatment with L-Nitroarginine-methyl-ester (L-NAME), an established NOS inhibitor that blocks both NO and superoxide formation, decreased H₂O₂ efflux at 18% O₂ ($p=0.0002$). However, no effect was observed at 5% O₂ ($p=0.1219$). At 18% O₂ RES reverted L-NAME inhibition and promoted an increase in H₂O₂ efflux rate ($p<0.0001$). H₂O₂ efflux from cells was measured using the Amplex Red reagent. During the experiment, cells were incubated in the presence of 5µM GKT137831 or vehicle control. Data were analyzed using JASP version 9 software and consisted of analyses of variance (ANOVA). Between-subject factors were O₂, (5% O₂, 18% O₂) and treatment (DMSO, RES). Bars represent the mean \pm SEM. '*' represent differences between RES-treated and DMSO-treated cells. '\$' represents differences between 5% O₂ and 18% O₂. '£' represent differences between control and L-NAME.

References

- Aguer, C., Gambarotta, D., Mailloux, R.J., Moffat, C., Dent, R., McPherson, R., and Harper, M.-E. (2011). Galactose enhances oxidative metabolism and reveals mitochondrial dysfunction in human primary muscle cells. *PLoS One* 6, e28536.
- Al-Ani, A., Toms, D., Kondro, D., Thundathil, J., Yu, Y., and Ungrin, M. (2018). Oxygenation in cell culture: Critical parameters for reproducibility are routinely not reported. *PLoS One* 13, e0204269.
- Alderton, W.K., Cooper, C.E., and Knowles, R.G. (2001). Nitric oxide synthases: structure, function and inhibition. *Biochem. J.* 357, 593–615.
- Altenhöfer, S., Kleikers, P.W.M., Radermacher, K.A., Scheurer, P., Hermans, J.J.R., Schiffers, P., Ho, H., Wingler, K., and Schmidt, H.H.H.W. (2012). The NOX toolbox: Validating the role of NADPH oxidases in physiology and disease. *Cell. Mol. Life Sci.* 69, 2327–2343.
- Altenhöfer, S., Radermacher, K.A., Kleikers, P.W.M., Wingler, K., and Schmidt, H.H.H.W. (2015). Evolution of NADPH Oxidase Inhibitors: Selectivity and Mechanisms for Target Engagement. *Antioxid. Redox Signal.* 23, 406–427.
- Altman, B.J., Stine, Z.E., and Dang, C. V. (2016). From Krebs to clinic: glutamine metabolism to cancer therapy. *Nat. Rev. Cancer* 16, 619–634.
- Amoedo, N.D., Obre, E., and Rossignol, R. (2017). Drug discovery strategies in the field of tumor energy metabolism: Limitations by metabolic flexibility and metabolic resistance to chemotherapy. *Biochim. Biophys. Acta. Bioenerg.* 1858, 674–685.
- Aquilano, K., Vigilanza, P., Baldelli, S., Pagliei, B., Rotilio, G., and Ciriolo, M.R. (2010). Peroxisome proliferator-activated receptor gamma co-activator 1alpha (PGC-1alpha) and sirtuin 1 (SIRT1) reside in mitochondria: possible direct function in mitochondrial biogenesis. *J. Biol. Chem.* 285, 21590–21599.
- Archer, S.L. (2013). Mitochondrial dynamics--mitochondrial fission and fusion in human diseases. *N. Engl. J. Med.* 369, 2236–2251.
- Ascenzi, P., Bocedi, A., and Marino, M. (2006). Structure-function relationship of estrogen receptor alpha and beta: impact on human health. *Mol. Aspects Med.* 27, 299–402.

Ashrafi, G., and Schwarz, T.L. (2013). The pathways of mitophagy for quality control and clearance of mitochondria. *Cell Death Differ.* 20, 31–42.

Athar, M., Back, J.H., Tang, X., Kim, K.H., Kopelovich, L., Bickers, D.R., and Kim, A.L. (2007). Resveratrol: a review of preclinical studies for human cancer prevention. *Toxicol. Appl. Pharmacol.* 224, 274–283.

Babbar, M., and Sheikh, M.S. (2013). Metabolic Stress and Disorders Related to Alterations in Mitochondrial Fission or Fusion. *Mol. Cell. Pharmacol.* 5, 109–133.

Ban, T., Ishihara, T., Kohno, H., Saita, S., Ichimura, A., Maenaka, K., Oka, T., Mihara, K., and Ishihara, N. (2017). Molecular basis of selective mitochondrial fusion by heterotypic action between OPA1 and cardiolipin. *Nat. Cell Biol.* 19, 856–863.

Bánfi, B., Molnár, G., Maturana, A., Steger, K., Hegedűs, B., Demaurex, N., and Krause, K.H. (2001). A Ca²⁺-activated NADPH Oxidase in Testis, Spleen, and Lymph Nodes. *J. Biol. Chem.* 276, 37594–37601.

Baur, J.A., and Sinclair, D.A. (2006). Therapeutic potential of resveratrol: The in vivo evidence. *Nat. Rev. Drug Discov.* 5, 493–506.

Bayeva, M., Gheorghiade, M., and Ardehali, H. (2013). Mitochondria as a therapeutic target in heart failure. *J. Am. Coll. Cardiol.* 61, 599–610.

Bedard, K., and Krause, K.-H. (2007). The NOX family of ROS-generating NADPH oxidases: physiology and pathophysiology. *Physiol. Rev.* 87, 245–313.

Belousov, V. V., Fradkov, A.F., Lukyanov, K.A., Staroverov, D.B., Shakhbazov, K.S., Terskikh, A. V., and Lukyanov, S. (2006). Genetically encoded fluorescent indicator for intracellular hydrogen peroxide. *Nat. Methods* 3, 281–286.

Bienert, G.P., and Chaumont, F. (2014). Aquaporin-facilitated transmembrane diffusion of hydrogen peroxide. *Biochim. Biophys. Acta* 1840, 1596–1604.

Bienert, G.P., Møller, A.L.B., Kristiansen, K.A., Schulz, A., Møller, I.M., Schjoerring, J.K., and Jahn, T.P. (2007). Specific aquaporins facilitate the diffusion of hydrogen peroxide across membranes. *J. Biol. Chem.* 282, 1183–1192.

Bilan, D.S., Pase, L., Joosen, L., Gorokhovatsky, A.Y., Ermakova, Y.G., Gadella, T.W.J., Grabher,

- C., Schultz, C., Lukyanov, S., and Belousov, V. V. (2013). HyPer-3: a genetically encoded H₂O₂ probe with improved performance for ratiometric and fluorescence lifetime imaging. *ACS Chem. Biol.* 8, 535–542.
- Blake, R., and Trounce, I.A. (2014). Mitochondrial dysfunction and complications associated with diabetes. *Biochim. Biophys. Acta - Gen. Subj.* 1840, 1404–1412.
- Blanquer-Rosselló, M. del M., Hernández-López, R., Roca, P., Oliver, J., and Valle, A. (2017). Resveratrol induces mitochondrial respiration and apoptosis in SW620 colon cancer cells. *Biochim. Biophys. Acta. Gen. Subj.* 1861, 431–440.
- Block, K., and Gorin, Y. (2012). Aiding and abetting roles of NOX oxidases in cellular transformation. *Nat. Rev. Cancer* 12, 627–637.
- Block, K., Gorin, Y., and Abboud, H.E. (2009). Subcellular localization of Nox4 and regulation in diabetes. *Proc. Natl. Acad. Sci. U. S. A.* 106, 14385–14390.
- Boroughs, L.K., and DeBerardinis, R.J. (2015). Metabolic pathways promoting cancer cell survival and growth. *Nat. Cell Biol.* 17, 351–359.
- Bouhabel, H., Durán, R. V., and Gottlieb, E. (2009). Prolyl hydroxylases as regulators of cell metabolism. *Biochem. Soc. Trans.* 37, 291–294.
- Brigelius-Flohé, R., and Maiorino, M. (2013). Glutathione peroxidases. *Biochim. Biophys. Acta* 1830, 3289–3303.
- Brown, D.I., and Griendling, K.K. (2009). Nox proteins in signal transduction. *Free Radic. Biol. Med.* 47, 1239–1253.
- Brown, G.C., and Borutaite, V. (2012). There is no evidence that mitochondria are the main source of reactive oxygen species in mammalian cells. *Mitochondrion* 12, 1–4.
- Van Buul, J.D., Fernandez-Borja, M., Anthony, E.C., and Hordijk, P.L. (2005). Expression and localization of NOX2 and NOX4 in primary human endothelial cells. *Antioxid. Redox Signal.* 7, 308–317.
- Calabrese, G., Morgan, B., and Riemer, J. (2017). Mitochondrial Glutathione: Regulation and Functions. *Antioxid. Redox Signal.* 27, 1162–1177.
- Cannino, G., Ciscato, F., Masgras, I., Sánchez-Martín, C., and Rasola, A. (2018). Metabolic

Plasticity of Tumor Cell Mitochondria. *Front. Oncol.* 8, 333.

Cantó, C., Gerhart-Hines, Z., Feige, J.N., Lagouge, M., Noriega, L., Milne, J.C., Elliott, P.J., Puigserver, P., and Auwerx, J. (2009). AMPK regulates energy expenditure by modulating NAD⁺ metabolism and SIRT1 activity. *Nature* 458, 1056–1060.

Cantor, J.R., and Sabatini, D.M. (2012). Cancer cell metabolism: One hallmark, many faces. *Cancer Discov.* 2, 881–898.

Carreau, A., Hafny-Rahbi, B. El, Matejuk, A., Grillon, C., and Kieda, C. (2011). Why is the partial oxygen pressure of human tissues a crucial parameter? Small molecules and hypoxia. *J. Cell. Mol. Med.* 15, 1239–1253.

Carter, L.G., D’Orazio, J.A., and Pearson, K.J. (2014). Resveratrol and cancer: focus on in vivo evidence. *Endocr. Relat. Cancer* 21, R209-25.

Chalal, M., Klinguer, A., Echairi, A., Meunier, P., Vervandier-Fasseur, D., and Adrian, M. (2014). Antimicrobial activity of resveratrol analogues. *Molecules* 19, 7679–7688.

Chen, F., Qian, L.-H., Deng, B., Liu, Z.-M., Zhao, Y., and Le, Y.-Y. (2013). Resveratrol protects vascular endothelial cells from high glucose-induced apoptosis through inhibition of NADPH oxidase activation-driven oxidative stress. *CNS Neurosci. Ther.* 19, 675–681.

Chen, H., Vermulst, M., Wang, Y.E., Chomyn, A., Prolla, T.A., McCaffery, J.M., and Chan, D.C. (2010). Mitochondrial fusion is required for mtDNA stability in skeletal muscle and tolerance of mtDNA mutations. *Cell* 141, 280–289.

Chen, L., Shi, Y., Yuan, J., Han, Y., Qin, R., Wu, Q., Jia, B., Wei, B., Wei, L., Dai, G., et al. (2014). HIF-1 alpha overexpression correlates with poor overall survival and disease-free survival in gastric cancer patients post-gastrectomy. *PLoS One* 9, e90678.

Chen, N., Rinner, O., Czernik, D., Nytko, K.J., Zheng, D., Stiehl, D.P., Zamboni, N., Gstaiger, M., and Frei, C. (2011). The oxygen sensor PHD3 limits glycolysis under hypoxia via direct binding to pyruvate kinase. *Cell Res.* 21, 983–986.

Cho, E.S., Cha, Y.H., Kim, H.S., Kim, N.H., and Yook, J.I. (2018). The Pentose Phosphate Pathway as a Potential Target for Cancer Therapy. *Biomol. Ther. (Seoul)*. 26, 29–38.

Choi, H., Kim, S., Mukhopadhyay, P., Cho, S., Woo, J., Storz, G., and Ryu, S.E. (2001). Structural

basis of the redox switch in the OxyR transcription factor. *Cell* 105, 103–113.

Cioffi, C.L., Liu, X.Q., Kosinski, P.A., Garay, M., and Bowen, B.R. (2003). Differential regulation of HIF-1 alpha prolyl-4-hydroxylase genes by hypoxia in human cardiovascular cells. *Biochem. Biophys. Res. Commun.* 303, 947–953.

Cipolletti, M., Solar Fernandez, V., Montalesi, E., Marino, M., and Fiocchetti, M. (2018). Beyond the antioxidant activity of dietary polyphenols in cancer: the modulation of estrogen receptors (ers) signaling. *Int. J. Mol. Sci.* 19, 2624.

Circu, M.L., and Aw, T.Y. (2010). Reactive oxygen species, cellular redox systems, and apoptosis. *Free Radic. Biol. Med.* 48, 749–762.

Cottart, C.H., Nivet-Antoine, V., Laguillier-Morizot, C., and Beaudoux, J.L. (2010). Resveratrol bioavailability and toxicity in humans. *Mol. Nutr. Food Res.* 54, 7–16.

Courtney, R., Ngo, D.C., Malik, N., Ververis, K., Tortorella, S.M., and Karagiannis, T.C. (2015). Cancer metabolism and the Warburg effect: the role of HIF-1 and PI3K. *Mol. Biol. Rep.* 42, 841–851.

Cox, A.G., Winterbourn, C.C., and Hampton, M.B. (2009). Mitochondrial peroxiredoxin involvement in antioxidant defence and redox signalling. *Biochem. J.* 425, 313–325.

Csiszar, A., Labinskyy, N., Pinto, J.T., Ballabh, P., Zhang, H., Losonczy, G., Pearson, K., de Cabo, R., Pacher, P., Zhang, C., et al. (2009). Resveratrol induces mitochondrial biogenesis in endothelial cells. *Am. J. Physiol. Heart Circ. Physiol.* 297, H13-20.

D'Autréaux, B., and Toledano, M.B. (2007). ROS as signalling molecules: Mechanisms that generate specificity in ROS homeostasis. *Nat. Rev. Mol. Cell Biol.* 8, 813–824.

Dan Dunn, J., Alvarez, L.A.J., Zhang, X., and Soldati, T. (2015). Reactive oxygen species and mitochondria: A nexus of cellular homeostasis. *Redox Biol.* 6, 472–485.

Davinelli, S., Sapere, N., Visentin, M., Zella, D., and Scapagnini, G. (2013). Enhancement of mitochondrial biogenesis with polyphenols: combined effects of resveratrol and equol in human endothelial cells. *Immun. Ageing* 10, 28.

DeBerardinis, R.J., and Chandel, N.S. (2016). Fundamentals of cancer metabolism. *Sci. Adv.* 2, e1600200.

- DeBerardinis, R.J., Mancuso, A., Daikhin, E., Nissim, I., Yudkoff, M., Wehrli, S., and Thompson, C.B. (2007). Beyond aerobic glycolysis: transformed cells can engage in glutamine metabolism that exceeds the requirement for protein and nucleotide synthesis. *Proc. Natl. Acad. Sci. U. S. A.* *104*, 19345–19350.
- Detmer, S.A., and Chan, D.C. (2007). Functions and dysfunctions of mitochondrial dynamics. *Nat. Rev. Mol. Cell Biol.* *8*, 870–879.
- Diaz-Ruiz, R., Rigoulet, M., and Devin, A. (2011). The Warburg and Crabtree effects: On the origin of cancer cell energy metabolism and of yeast glucose repression. *Biochim. Biophys. Acta* *1807*, 568–576.
- Diebold, I., Petry, A., Hess, J., and Görlach, A. (2010). The NADPH oxidase subunit NOX4 is a new target gene of the hypoxia-inducible factor-1. *Mol. Biol. Cell* *21*, 2087–2096.
- Dinkova-Kostova, A.T., and Abramov, A.Y. (2015). The emerging role of Nrf2 in mitochondrial function. *Free Radic. Biol. Med.* *88*, 179–188.
- Durán, R. V., MacKenzie, E.D., Boulahbel, H., Frezza, C., Heiserich, L., Tardito, S., Bussolati, O., Rocha, S., Hall, M.N., and Gottlieb, E. (2013). HIF-independent role of prolyl hydroxylases in the cellular response to amino acids. *Oncogene* *32*, 4549–4556.
- Eagle, H. (1955). Nutrition needs of mammalian cells in tissue culture. *Science* *122*, 501–514.
- Eales, K.L., Hollinshead, K.E.R., and Tennant, D.A. (2016). Hypoxia and metabolic adaptation of cancer cells. *Oncogenesis* *5*, e190.
- Earle, W.R., Schilling, E.L., Stark, T.H., Straus, N.P., Brown, M.F., and Shelton, E. (1943). Production of Malignancy in Vitro. IV. The Mouse Fibroblast Cultures and Changes Seen in the Living Cells. *JNCI J. Natl. Cancer Inst.* *4*, 165–212.
- Ehrismann, D., Flashman, E., Genn, D.N., Mathioudakis, N., Hewitson, K.S., Ratcliffe, P.J., and Schofield, C.J. (2007). Studies on the activity of the hypoxia-inducible-factor hydroxylases using an oxygen consumption assay. *Biochem. J.* *401*, 227–234.
- Eisner, V., Picard, M., and Hajnóczky, G. (2018). Mitochondrial dynamics in adaptive and maladaptive cellular stress responses. *Nat. Cell Biol.* *20*, 755–765.
- Eiyama, A., and Okamoto, K. (2015). PINK1/Parkin-mediated mitophagy in mammalian cells.

Curr. Opin. Cell Biol. 33, 95–101.

Elkalaf, M., Anděl, M., and Trnka, J. (2013). Low glucose but not galactose enhances oxidative mitochondrial metabolism in C2C12 myoblasts and myotubes. *PLoS One* 8, e70772.

Ermakova, Y.G., Bilan, D.S., Matlashov, M.E., Mishina, N.M., Markvicheva, K.N., Subach, O.M., Subach, F. V., Bogeski, I., Hoth, M., Enikolopov, G., et al. (2014). Red fluorescent genetically encoded indicator for intracellular hydrogen peroxide. *Nat. Commun.* 5, 5222.

Evans, M.D., Dizdaroglu, M., and Cooke, M.S. (2004). Oxidative DNA damage and disease: induction, repair and significance. *Mutat. Res.* 567, 1–61.

Fantin, V.R., St-Pierre, J., and Leder, P. (2006). Attenuation of LDH-A expression uncovers a link between glycolysis, mitochondrial physiology, and tumor maintenance. *Cancer Cell* 9, 425–434.

Federico, A., Cardaioli, E., Da Pozzo, P., Formichi, P., Gallus, G.N., and Radi, E. (2012). Mitochondria, oxidative stress and neurodegeneration. *J. Neurol. Sci.* 322, 254–262.

Feng, M., Zhong, L.-X., Zhan, Z.-Y., Huang, Z.-H., and Xiong, J.-P. (2016). Resveratrol Treatment Inhibits Proliferation of and Induces Apoptosis in Human Colon Cancer Cells. *Med. Sci. Monit.* 22, 1101–1108.

Fernandez-Marcos, P.J., and Auwerx, J. (2011). Regulation of PGC-1 α , a nodal regulator of mitochondrial biogenesis. *Am. J. Clin. Nutr.* 93, 884S – 90.

Finkel, T. (2011). Signal transduction by reactive oxygen species. *J. Cell Biol.* 194, 7–15.

Fonseca, J., Moradi, F., Maddalena, L.A., Ferreira-Tollstadius, B., Selim, S., and Stuart, J.A. (2019). Resveratrol integrates metabolic and growth effects in PC3 prostate cancer cells- involvement of prolyl hydroxylase and hypoxia inducible factor-1. *Oncol. Lett.* 17, 697–705.

Franco, A., Kitsis, R.N., Fleischer, J.A., Gavathiotis, E., Kornfeld, O.S., Gong, G., Biris, N., Benz, A., Qvit, N., Donnelly, S.K., et al. (2016). Correcting mitochondrial fusion by manipulating mitofusin conformations. *Nature* 540, 74–79.

Fukuhara, K., Nagakawa, M., Nakanishi, I., Ohkubo, K., Imai, K., Urano, S., Fukuzumi, S., Ozawa, T., Ikota, N., Mochizuki, M., et al. (2006). Structural basis for DNA-cleaving activity of resveratrol in the presence of Cu(II). *Bioorg. Med. Chem.* 14, 1437–1443.

Galanis, A., Pappa, A., Giannakakis, A., Lanitis, E., Dangaj, D., and Sandaltzopoulos, R. (2008).

Reactive oxygen species and HIF-1 signalling in cancer. *Cancer Lett.* 266, 12–20.

Gao, L., Mejías, R., Echevarría, M., and López-Barneo, J. (2004). Induction of the glucose-6-phosphate dehydrogenase gene expression by chronic hypoxia in PC12 cells. *FEBS Lett.* 569, 256–260.

García-Santamarina, S., Boronat, S., and Hidalgo, E. (2014). Reversible cysteine oxidation in hydrogen peroxide sensing and signal transduction. *Biochemistry* 53, 2560–2580.

Garvalov, B.K., Foss, F., Henze, A.-T., Bethani, I., Gräf-Höchst, S., Singh, D., Filatova, A., Dopeso, H., Seidel, S., Damm, M., et al. (2014). PHD3 regulates EGFR internalization and signalling in tumours. *Nat. Commun.* 5, 5577.

Gegg, M.E., Cooper, J.M., Chau, K.-Y., Rojo, M., Schapira, A.H. V, and Taanman, J.-W. (2010). Mitofusin 1 and mitofusin 2 are ubiquitinated in a PINK1/parkin-dependent manner upon induction of mitophagy. *Hum. Mol. Genet.* 19, 4861–4870.

Geiszt, M., Kopp, J.B., Várnai, P., and Leto, T.L. (2000). Identification of renox, an NAD(P)H oxidase in kidney. *Proc. Natl. Acad. Sci. U. S. A.* 97, 8010–8014.

Giorgio, M., Migliaccio, E., Orsini, F., Paolucci, D., Moroni, M., Contursi, C., Pelliccia, G., Luzi, L., Minucci, S., Marcaccio, M., et al. (2005). Electron transfer between cytochrome c and p66Shc generates reactive oxygen species that trigger mitochondrial apoptosis. *Cell* 122, 221–233.

Giorgio, M., Trinei, M., Migliaccio, E., and Pelicci, P.G. (2007). Hydrogen peroxide: a metabolic by-product or a common mediator of ageing signals? *Nat. Rev. Mol. Cell Biol.* 8, 722–728.

Gnaiger, E. (2001). Bioenergetics at low oxygen: dependence of respiration and phosphorylation on oxygen and adenosine diphosphate supply. *Respir. Physiol.* 128, 277–297.

Gomez, L.S., Zancan, P., Marcondes, M.C., Ramos-Santos, L., Meyer-Fernandes, J.R., Sola-Penna, M., and Da Silva, D. (2013). Resveratrol decreases breast cancer cell viability and glucose metabolism by inhibiting 6-phosphofructo-1-kinase. *Biochimie* 95, 1336–1343.

Goncalves, R.L.S., Quinlan, C.L., Perevoshchikova, I. V., Hey-Mogensen, M., and Brand, M.D. (2015). Sites of superoxide and hydrogen peroxide production by muscle mitochondria assessed ex vivo under conditions mimicking rest and exercise. *J. Biol. Chem.* 290, 209–227.

Goyal, P., Weissmann, N., Grimminger, F., Hegel, C., Bader, L., Rose, F., Fink, L., Ghofrani,

H.A., Schermuly, R.T., Schmidt, H.H.H.W.H.W., et al. (2004). Upregulation of NAD(P)H oxidase 1 in hypoxia activates hypoxia-inducible factor 1 via increase in reactive oxygen species. *Free Radic. Biol. Med.* *36*, 1279–1288.

Graham, K.A., Kulawiec, M., Owens, K.M., Li, X., Desouki, M.M., Chandra, D., and Singh, K.K. (2010). NADPH oxidase 4 is an oncoprotein localized to mitochondria. *Cancer Biol. Ther.* *10*, 223–231.

Greer, S.N., Metcalf, J.L., Wang, Y., and Ohh, M. (2012). The updated biology of hypoxia-inducible factor. *EMBO J.* *31*, 2448–2460.

Gregg, J.L., Turner, R.M., Chang, G., Joshi, D., Zhan, Y., Chen, L., and Maranchie, J.K. (2014). NADPH oxidase nox4 supports renal tumorigenesis by promoting the expression and nuclear accumulation of hif2a. *Cancer Res.* *74*, 3501–3511.

Grek, C.L., Zhang, J., Manevich, Y., Townsend, D.M., and Tew, K.D. (2013). Causes and consequences of cysteine s-glutathionylation. *J. Biol. Chem.* *288*, 26497–26504.

Gülçin, İ. (2010). Antioxidant properties of resveratrol: A structure–activity insight. *Innov. Food Sci. Emerg. Technol.* *11*, 210–218.

Habler, O.P., and Messmer, K.F. (1997). The physiology of oxygen transport. *Transfus. Sci.* *18*, 425–435.

Halliwell, B. (2003). Oxidative stress in cell culture: An under-appreciated problem? *FEBS Lett.* *540*, 3–6.

Hamanaka, R.B., and Chandel, N.S. (2011). Cell biology. Warburg effect and redox balance. *Science* *334*, 1219–1220.

Hamm, A., Veschini, L., Takeda, Y., Costa, S., Delamarre, E., Squadrito, M.L., Henze, A.-T., Wenes, M., Serneels, J., Pucci, F., et al. (2013). PHD2 regulates arteriogenic macrophages through TIE2 signalling. *EMBO Mol. Med.* *5*, 843–857.

Han, G., Xia, J., Gao, J., Inagaki, Y., Tang, W., and Kokudo, N. (2015). Anti-tumor effects and cellular mechanisms of resveratrol. *Drug Discov. Ther.* *9*, 1–12.

Hanahan, D., and Weinberg, R.A. (2011). Hallmarks of cancer: the next generation. *Cell* *144*, 646–674.

- Handy, D.E., and Loscalzo, J. (2012). Redox regulation of mitochondrial function. *Antioxid. Redox Signal.* *16*, 1323–1367.
- Harrison, D.K., and Vaupel, P. (2014). Heterogeneity in tissue oxygenation: from physiological variability in normal tissues to pathophysiological chaos in malignant tumours. *Adv. Exp. Med. Biol.* *812*, 25–31.
- Hayflick, L., and Moorhead, P.S. (1961). The serial cultivation of human diploid cell strains. *Exp. Cell Res.* *25*, 585–621.
- He, T., Guan, X., Wang, S., Xiao, T., Yang, K., Xu, X., Wang, J., and Zhao, J. (2015). Resveratrol prevents high glucose-induced epithelial-mesenchymal transition in renal tubular epithelial cells by inhibiting NADPH oxidase/ROS/ERK pathway. *Mol. Cell. Endocrinol.* *402*, 13–20.
- He, T., Xiong, J., Nie, L., Yu, Y., Guan, X., Xu, X., Xiao, T., Yang, K., Liu, L., Zhang, D., et al. (2016). Resveratrol inhibits renal interstitial fibrosis in diabetic nephropathy by regulating AMPK/NOX4/ROS pathway. *J. Mol. Med.* *94*, 1359–1371.
- Vander Heiden, M.G., and DeBerardinis, R.J. (2017). Understanding the Intersections between Metabolism and Cancer Biology. *Cell* *168*, 657–669.
- Vander Heiden, M.G., Cantley, L.C., and Thompson, C.B. (2009). Understanding the Warburg effect: the metabolic requirements of cell proliferation. *Science* *324*, 1029–1033.
- Hertweck, K.L., and Dasgupta, S. (2017). The Landscape of mtDNA Modifications in Cancer: A Tale of Two Cities. *Front. Oncol.* *7*, 1–12.
- Hilenski, L.L., Clempus, R.E., Quinn, M.T., Lambeth, J.D., and Griendling, K.K. (2004). Distinct subcellular localizations of Nox1 and Nox4 in vascular smooth muscle cells. *Arterioscler. Thromb. Vasc. Biol.* *24*, 677–683.
- Hirschey, M.D., DeBerardinis, R.J., Diehl, A.M.E., Drew, J.E., Frezza, C., Green, M.F., Jones, L.W., Ko, Y.H., Le, A., Lea, M.A., et al. (2015). Dysregulated metabolism contributes to oncogenesis. *Semin. Cancer Biol.* *35 Suppl*, S129–S150.
- Hirsilä, M., Koivunen, P., Günzler, V., Kivirikko, K.I., and Myllyharju, J. (2003). Characterization of the human prolyl 4-hydroxylases that modify the hypoxia-inducible factor. *J. Biol. Chem.* *278*, 30772–30780.

- Hock, M.B., and Kralli, A. (2009). Transcriptional control of mitochondrial biogenesis and function. *Annu. Rev. Physiol.* *71*, 177–203.
- Hoffman, D.L., and Brookes, P.S. (2009). Oxygen sensitivity of mitochondrial reactive oxygen species generation depends on metabolic conditions. *J. Biol. Chem.* *284*, 16236–16245.
- Hoffman, D.L., Salter, J.D., and Brookes, P.S. (2007). Response of mitochondrial reactive oxygen species generation to steady-state oxygen tension: implications for hypoxic cell signaling. *Am. J. Physiol. Heart Circ. Physiol.* *292*, H101-8.
- Holden, H.M., Rayment, I., and Thoden, J.B. (2003). Structure and function of enzymes of the Leloir pathway for galactose metabolism. *J. Biol. Chem.* *278*, 43885–43888.
- Holmström, K.M., and Finkel, T. (2014). Cellular mechanisms and physiological consequences of redox-dependent signalling. *Nat. Rev. Mol. Cell Biol.* *15*, 411–421.
- Horbay, R., and Bilyy, R. (2016). Mitochondrial dynamics during cell cycling. *Apoptosis* *21*, 1327–1335.
- Huang, H., Benzonana, L.L., Zhao, H., Watts, H.R., Perry, N.J.S., Bevan, C., Brown, R., and Ma, D. (2014a). Prostate cancer cell malignancy via modulation of HIF-1 α pathway with isoflurane and propofol alone and in combination. *Br. J. Cancer* *111*, 1338–1349.
- Huang, X., Zhou, J., Liu, J., Tang, B., Zhao, F., and Qu, Y. (2014b). Biological characteristics of prostate cancer cells are regulated by hypoxia-inducible factor 1 α . *Oncol. Lett.* *8*, 1217–1221.
- Imlay, J.A. (2003). Pathways of oxidative damage. *Annu. Rev. Microbiol.* *57*, 395–418.
- Imlay, J.A. (2008). Cellular defenses against superoxide and hydrogen peroxide. *Annu. Rev. Biochem.* *77*, 755–776.
- Iqbal, M.A., and Bamezai, R.N.K. (2012). Resveratrol inhibits cancer cell metabolism by down regulating pyruvate kinase M2 via inhibition of mammalian target of rapamycin. *PLoS One* *7*, e36764.
- James, A.M., Cochemé, H.M., Smith, R.A.J., and Murphy, M.P. (2005). Interactions of mitochondria-targeted and untargeted ubiquinones with the mitochondrial respiratory chain and reactive oxygen species. Implications for the use of exogenous ubiquinones as therapies and experimental tools. *J. Biol. Chem.* *280*, 21295–21312.

Jang, M., Cai, L., Udeani, G.O., Slowing, K. V, Thomas, C.F., Beecher, C.W., Fong, H.H., Farnsworth, N.R., Kinghorn, A.D., Mehta, R.G., et al. (1997). Cancer chemopreventive activity of resveratrol, a natural product derived from grapes. *Science* 275, 218–220.

Jiang, J.X., Chen, X., Serizawa, N., Szyndralewicz, C., Page, P., Schröder, K., Brandes, R.P., Devaraj, S., and Török, N.J. (2012). Liver fibrosis and hepatocyte apoptosis are attenuated by GKT137831, a novel NOX4/NOX1 inhibitor in vivo. *Free Radic. Biol. Med.* 53, 289–296.

Jokilehto, T., and Jaakkola, P.M. (2010). The role of HIF prolyl hydroxylases in tumour growth. *J. Cell. Mol. Med.* 14, 758–770.

Jones, D.P. (2008). Radical-free biology of oxidative stress. *Am. J. Physiol. Cell Physiol.* 295, C849–68.

Jones, D.P., and Sies, H. (2015). The Redox Code. *Antioxid. Redox Signal.* 23, 734–746.

Jung, K.-H., Lee, J.H., Thien Quach, C.H., Paik, J.-Y., Oh, H., Park, J.W., Lee, E.J., Moon, S.-H., and Lee, K.-H. (2013). Resveratrol suppresses cancer cell glucose uptake by targeting reactive oxygen species-mediated hypoxia-inducible factor-1 α activation. *J. Nucl. Med.* 54, 2161–2167.

Kaelin, W.G. (2005). ROS: really involved in oxygen sensing. *Cell Metab.* 1, 357–358.

Kaelin, W.G., and Ratcliffe, P.J. (2008). Oxygen Sensing by Metazoans: The Central Role of the HIF Hydroxylase Pathway. *Mol. Cell* 30, 393–402.

Kaewpila, S., Venkataraman, S., Buettner, G.R., and Oberley, L.W. (2008). Manganese superoxide dismutase modulates hypoxia-inducible factor-1 alpha induction via superoxide. *Cancer Res.* 68, 2781–2788.

Kalyanaraman, B., Cheng, G., Hardy, M., Ouari, O., Bennett, B., and Zielonka, J. (2018). Teaching the basics of reactive oxygen species and their relevance to cancer biology: Mitochondrial reactive oxygen species detection, redox signaling, and targeted therapies. *Redox Biol.* 15, 347–362.

Kamata, T. (2009). Roles of Nox1 and other Nox isoforms in cancer development. *Cancer Sci.* 100, 1382–1388.

Kanki, T., Ohgaki, K., Gaspari, M., Gustafsson, C.M., Fukuoh, A., Sasaki, N., Hamasaki, N., and Kang, D. (2004). Architectural role of mitochondrial transcription factor A in maintenance of human mitochondrial DNA. *Mol. Cell. Biol.* 24, 9823–9834.

Kankotia, S., and Stacpoole, P.W. (2014). Dichloroacetate and cancer: new home for an orphan drug? *Biochim. Biophys. Acta* *1846*, 617–629.

Kasiotis, K.M., Pratsinis, H., Kletsas, D., and Haroutounian, S.A. (2013). Resveratrol and related stilbenes: Their anti-aging and anti-angiogenic properties. *Food Chem. Toxicol.* *61*, 112–120.

Keeley, T.P., and Mann, G.E. (2019). Defining Physiological Normoxia for Improved Translation of Cell Physiology to Animal Models and Humans. *Physiol. Rev.* *99*, 161–234.

Kehrer, J.P. (2000). The Haber-Weiss reaction and mechanisms of toxicity. *Toxicology* *149*, 43–50.

Kelley, E.E., Khoo, N.K.H., Hundley, N.J., Malik, U.Z., Freeman, B.A., and Tarpey, M.M. (2010). Hydrogen peroxide is the major oxidant product of xanthine oxidase. *Free Radic. Biol. Med.* *48*, 493–498.

Khan, H.Y., Zubair, H., Faisal, M., Ullah, M.F., Farhan, M., Sarkar, F.H., Ahmad, A., and Hadi, S.M. (2014). Plant polyphenol induced cell death in human cancer cells involves mobilization of intracellular copper ions and reactive oxygen species generation: a mechanism for cancer chemopreventive action. *Mol. Nutr. Food Res.* *58*, 437–446.

Kikuchi, D., Minamishima, Y.A., and Nakayama, K. (2014). Prolyl-hydroxylase PHD3 interacts with pyruvate dehydrogenase (PDH)-E1 β and regulates the cellular PDH activity. *Biochem. Biophys. Res. Commun.* *451*, 288–294.

Kim, J.W., Tchernyshyov, I., Semenza, G.L., and Dang, C. V. (2006). HIF-1-mediated expression of pyruvate dehydrogenase kinase: A metabolic switch required for cellular adaptation to hypoxia. *Cell Metab.* *3*, 177–185.

Klimova, T., and Chandel, N.S. (2008). Mitochondrial complex III regulates hypoxic activation of HIF. *Cell Death Differ.* *15*, 660–666.

Koppenol, W.H., Bounds, P.L., and Dang, C. V (2011). Otto Warburg's contributions to current concepts of cancer metabolism. *Nat. Rev. Cancer* *11*, 325–337.

Korshunov, S.S., Skulachev, V.P., and Starkov, A.A. (1997). High protonic potential actuates a mechanism of production of reactive oxygen species in mitochondria. *FEBS Lett.* *416*, 15–18.

Kumar, H., and Choi, D.-K. (2015). Hypoxia Inducible Factor Pathway and Physiological

Adaptation: A Cell Survival Pathway? *Mediators Inflamm.* 2015, 584758.

Kuo, C.-W., Tsai, M.-H., Lin, T.-K., Tiao, M.-M., Wang, P.-W., Chuang, J.-H., Chen, S.-D., and Liou, C.-W. (2017). mtDNA as a Mediator for Expression of Hypoxia-Inducible Factor 1 α and ROS in Hypoxic Neuroblastoma Cells. *Int. J. Mol. Sci.* 18, 1–16.

Kuroda, J., Nakagawa, K., Yamasaki, T., Nakamura, K., Takeya, R., Kuribayashi, F., Imajoh-Ohmi, S., Igarashi, K., Shibata, Y., Sueishi, K., et al. (2005). The superoxide-producing NAD(P)H oxidase Nox4 in the nucleus of human vascular endothelial cells. *Genes Cells* 10, 1139–1151.

Kussmaul, L., and Hirst, J. (2006). The mechanism of superoxide production by NADH:ubiquinone oxidoreductase (complex I) from bovine heart mitochondria. *Proc. Natl. Acad. Sci. U. S. A.* 103, 7607–7612.

de la Lastra, C.A., and Villegas, I. (2007). Resveratrol as an antioxidant and pro-oxidant agent: mechanisms and clinical implications. *Biochem. Soc. Trans.* 35, 1156–1160.

LaGory, E.L., and Giaccia, A.J. (2016). The ever-expanding role of HIF in tumour and stromal biology. *Nat. Cell Biol.* 18, 356–365.

Lagouge, M., Argmann, C., Gerhart-Hines, Z., Meziane, H., Lerin, C., Daussin, F., Messadeq, N., Milne, J., Lambert, P., Elliott, P., et al. (2006). Resveratrol improves mitochondrial function and protects against metabolic disease by activating SIRT1 and PGC-1 α . *Cell* 127, 1109–1122.

Le, A., Cooper, C.R., Gouw, A.M., Dinavahi, R., Maitra, A., Deck, L.M., Royer, R.E., Vander Jagt, D.L., Semenza, G.L., and Dang, C. V. (2010). Inhibition of lactate dehydrogenase A induces oxidative stress and inhibits tumor progression. *Proc. Natl. Acad. Sci. U. S. A.* 107, 2037–2042.

Lebovitz, R.M., Zhang, H., Vogel, H., Cartwright, J., Dionne, L., Lu, N., Huang, S., and Matzuk, M.M. (1996). Neurodegeneration, myocardial injury, and perinatal death in mitochondrial superoxide dismutase-deficient mice. *Proc. Natl. Acad. Sci. U. S. A.* 93, 9782–9787.

Lecomte, S., Demay, F., Ferrière, F., and Pakdel, F. (2017). Phytochemicals Targeting Estrogen Receptors: Beneficial Rather Than Adverse Effects? *Int. J. Mol. Sci.* 18, 1–19.

Lehuédé, C., Dupuy, F., Rabinovitch, R., Jones, R.G., and Siegel, P.M. (2016). Metabolic Plasticity as a Determinant of Tumor Growth and Metastasis. *Cancer Res.* 76, 5201–5208.

Leitman, D.C., Paruthiyil, S., Vivar, O.I., Saunier, E.F., Herber, C.B., Cohen, I., Tagliaferri, M.,

- and Speed, T.P. (2010). Regulation of specific target genes and biological responses by estrogen receptor subtype agonists. *Curr. Opin. Pharmacol.* *10*, 629–636.
- Lemasters, J.J. (2005). Selective mitochondrial autophagy, or mitophagy, as a targeted defense against oxidative stress, mitochondrial dysfunction, and aging. *Rejuvenation Res.* *8*, 3–5.
- León-González, A.J., Auger, C., and Schini-Kerth, V.B. (2015). Pro-oxidant activity of polyphenols and its implication on cancer chemoprevention and chemotherapy. *Biochem. Pharmacol.* *98*, 371–380.
- Leonard, S.S., Xia, C., Jiang, B.H., Stinefelt, B., Klandorf, H., Harris, G.K., and Shi, X. (2003). Resveratrol scavenges reactive oxygen species and effects radical-induced cellular responses. *Biochem. Biophys. Res. Commun.* *309*, 1017–1026.
- Li, G., Rivas, P., Bedolla, R., Thapa, D., Reddick, R.L., Ghosh, R., and Kumar, A.P. (2013). Dietary resveratrol prevents development of high-grade prostatic intraepithelial neoplastic lesions: involvement of SIRT1/S6K axis. *Cancer Prev. Res. (Phila.)* *6*, 27–39.
- Li, Y., Huang, T.T., Carlson, E.J., Melov, S., Ursell, P.C., Olson, J.L., Noble, L.J., Yoshimura, M.P., Berger, C., Chan, P.H., et al. (1995). Dilated cardiomyopathy and neonatal lethality in mutant mice lacking manganese superoxide dismutase. *Nat. Genet.* *11*, 376–381.
- Liao, T.-L., Tzeng, C.-R., Yu, C.-L., Wang, Y.-P., and Kao, S.-H. (2015). Estrogen receptor- β in mitochondria: implications for mitochondrial bioenergetics and tumorigenesis. *Ann. N. Y. Acad. Sci.* *1350*, 52–60.
- Liesa, M., and Shirihai, O.S. (2013). Mitochondrial dynamics in the regulation of nutrient utilization and energy expenditure. *Cell Metab.* *17*, 491–506.
- Lu, H., Dalgard, C.L., Mohyeldin, A., McFate, T., Tait, A.S., and Verma, A. (2005). Reversible inactivation of HIF-1 prolyl hydroxylases allows cell metabolism to control basal HIF-1. *J. Biol. Chem.* *280*, 41928–41939.
- Lu, J., Tan, M., and Cai, Q. (2015). The Warburg effect in tumor progression: mitochondrial oxidative metabolism as an anti-metastasis mechanism. *Cancer Lett.* *356*, 156–164.
- Lucey, B.P., Nelson-Rees, W.A., and Hutchins, G.M. (2009). Henrietta Lacks, HeLa cells, and cell culture contamination. *Arch. Pathol. Lab. Med.* *133*, 1463–1467.

- Luengo, A., Gui, D.Y., and Vander Heiden, M.G. (2017). Targeting Metabolism for Cancer Therapy. *Cell Chem. Biol.* *24*, 1161–1180.
- Lukyanov, K.A., and Belousov, V. V. (2014). Genetically encoded fluorescent redox sensors. *Biochim. Biophys. Acta* *1840*, 745–756.
- Lunt, S.Y., and Vander Heiden, M.G. (2011). Aerobic glycolysis: meeting the metabolic requirements of cell proliferation. *Annu. Rev. Cell Dev. Biol.* *27*, 441–464.
- Maddalena, L.A., Selim, S.M., Fonseca, J., Messner, H., McGowan, S., and Stuart, J.A. (2017). Hydrogen peroxide production is affected by oxygen levels in mammalian cell culture. *Biochem. Biophys. Res. Commun.* *493*, 246–251.
- Madreiter-Sokolowski, C.T., Gottschalk, B., Parichatikanond, W., Eroglu, E., Klec, C., Waldeck-Weiermair, M., Malli, R., and Graier, W.F. (2016). Resveratrol Specifically Kills Cancer Cells by a Devastating Increase in the Ca²⁺Coupling between the Greatly Tethered Endoplasmic Reticulum and Mitochondria. *Cell. Physiol. Biochem.* *39*, 1404–1420.
- Madreiter-Sokolowski, C.T., Sokolowski, A.A., and Graier, W.F. (2017). Dosis facit sanitatem—Concentration-dependent effects of resveratrol on mitochondria. *Nutrients* *9*, 1–19.
- Malinouski, M., Zhou, Y., Belousov, V. V., Hatfield, D.L., and Gladyshev, V.N. (2011). Hydrogen peroxide probes directed to different cellular compartments. *PLoS One* *6*, e14564.
- Manea, A., Manea, S.-A., Todirita, A., Albulescu, I.C., Raicu, M., Sasson, S., and Simionescu, M. (2015). High-glucose-increased expression and activation of NADPH oxidase in human vascular smooth muscle cells is mediated by 4-hydroxynonenal-activated PPAR α and PPAR β/δ . *Cell Tissue Res.* *361*, 593–604.
- Marcinek, D.J., Ciesielski, W.A., Conley, K.E., and Schenkman, K.A. (2003). Oxygen regulation and limitation to cellular respiration in mouse skeletal muscle in vivo. *Am. J. Physiol. Heart Circ. Physiol.* *285*, H1900-8.
- Marí, M., Morales, A., Colell, A., García-Ruiz, C., and Fernández-Checa, J.C. (2009). Mitochondrial glutathione, a key survival antioxidant. *Antioxid. Redox Signal.* *11*, 2685–2700.
- Marino, S.M., and Gladyshev, V.N. (2010). Cysteine function governs its conservation and degeneration and restricts its utilization on protein surfaces. *J. Mol. Biol.* *404*, 902–916.

- Markvicheva, K.N., Bilan, D.S., Mishina, N.M., Gorokhovatsky, A.Y., Vinokurov, L.M., Lukyanov, S., and Belousov, V. V. (2011). A genetically encoded sensor for H₂O₂ with expanded dynamic range. *Bioorg. Med. Chem.* 19, 1079–1084.
- Marletta, M.A. (1993). Nitric oxide synthase structure and mechanism. *J. Biol. Chem.* 268, 12231–12234.
- Marroquin, L.D., Hynes, J., Dykens, J.A., Jamieson, J.D., and Will, Y. (2007). Circumventing the Crabtree effect: replacing media glucose with galactose increases susceptibility of HepG2 cells to mitochondrial toxicants. *Toxicol. Sci.* 97, 539–547.
- Masoud, G.N., and Li, W. (2015). HIF-1 α pathway: role, regulation and intervention for cancer therapy. *Acta Pharm. Sin. B* 5, 378–389.
- Masson, N., and Ratcliffe, P.J. (2014). Hypoxia signaling pathways in cancer metabolism: the importance of co-selecting interconnected physiological pathways. *Cancer Metab.* 2, 3.
- Maycotte, P., Marín-Hernández, A., Goyri-Aguirre, M., Anaya-Ruiz, M., Reyes-Leyva, J., and Cortés-Hernández, P. (2017). Mitochondrial dynamics and cancer. *Tumour Biol.* 39, 1010428317698391.
- McBride, H.M., Neuspiel, M., and Wasiak, S. (2006). Mitochondria: more than just a powerhouse. *Curr. Biol.* 16, R551-60.
- McKee, T.J., and Komarova, S. V. (2017). Is it time to reinvent basic cell culture medium? *Am. J. Physiol. Cell Physiol.* 312, C624–C626.
- McKeown, S.R. (2014a). Defining normoxia, physoxia and hypoxia in tumours-implications for treatment response. *Br. J. Radiol.* 87, 20130676.
- McKeown, S.R. (2014b). Defining normoxia, physoxia and hypoxia in tumours - Implications for treatment response. *Br. J. Radiol.* 87, 1–12.
- Meira Martins, L.A., Vieira, M.Q., Ilha, M., de Vasconcelos, M., Biehl, H.B., Lima, D.B., Schein, V., Barbé-Tuana, F., Borojevic, R., and Guma, F.C.R. (2014). The interplay between apoptosis, mitophagy and mitochondrial biogenesis induced by resveratrol can determine activated hepatic stellate cells death or survival. *Cell Biochem. Biophys.* 71, 657–672.
- Meitzler, J.L., Antony, S., Wu, Y., Juhasz, A., Liu, H., Jiang, G., Lu, J., Roy, K., and Doroshov,

J.H. (2014). NADPH oxidases: a perspective on reactive oxygen species production in tumor biology. *Antioxid. Redox Signal.* *20*, 2873–2889.

Meitzler, J.L., Makhlouf, H.R., Antony, S., Wu, Y., Butcher, D., Jiang, G., Juhasz, A., Lu, J., Dahan, I., Jansen-Dürr, P., et al. (2017). Decoding NADPH oxidase 4 expression in human tumors. *Redox Biol.* *13*, 182–195.

Menzies, K.J., Singh, K., Saleem, A., and Hood, D.A. (2013). Sirtuin 1-mediated effects of exercise and resveratrol on mitochondrial biogenesis. *J. Biol. Chem.* *288*, 6968–6979.

Mitra, K., Wunder, C., Roysam, B., Lin, G., and Lippincott-Schwartz, J. (2009). A hyperfused mitochondrial state achieved at G1-S regulates cyclin E buildup and entry into S phase. *Proc. Natl. Acad. Sci. U. S. A.* *106*, 11960–11965.

Murphy, M.P. (2009). How mitochondria produce reactive oxygen species. *Biochem. J.* *417*, 1–13.

Murphy, M.P., and Smith, R.A.J. (2007). Targeting antioxidants to mitochondria by conjugation to lipophilic cations. *Annu. Rev. Pharmacol. Toxicol.* *47*, 629–656.

Mustapha, N.M., Tarr, J.M., Kohner, E.M., and Chibber, R. (2010). NADPH Oxidase versus Mitochondria-Derived ROS in Glucose-Induced Apoptosis of Pericytes in Early Diabetic Retinopathy. *J. Ophthalmol.* *2010*, 746978.

Muz, B., de la Puente, P., Azab, F., and Azab, A.K. (2015). The role of hypoxia in cancer progression, angiogenesis, metastasis, and resistance to therapy. *Hypoxia (Auckland, N.Z.)* *3*, 83–92.

Narendra, D., Tanaka, A., Suen, D.-F., and Youle, R.J. (2008). Parkin is recruited selectively to impaired mitochondria and promotes their autophagy. *J. Cell Biol.* *183*, 795–803.

Nguyen, T.L., and Durán, R. V. (2016). Prolyl hydroxylase domain enzymes and their role in cell signaling and cancer metabolism. *Int. J. Biochem. Cell Biol.* *80*, 71–80.

Nisimoto, Y., Diebold, B.A., Constantino-Gomes, D., and Lambeth, J.D. (2014). Nox4: A hydrogen peroxide-generating oxygen sensor. *Biochemistry* *53*, 5111–5120.

Nowicki, S., and Gottlieb, E. (2015). Oncometabolites: tailoring our genes. *FEBS J.* *282*, 2796–2805.

O'Hagan, K.A., Cocchiglia, S., Zhdanov, A. V., Tambuwala, M.M., Tambawala, M.M., Cummins, E.P., Monfared, M., Agbor, T.A., Garvey, J.F., Papkovsky, D.B., et al. (2009). PGC-1alpha is coupled to HIF-1alpha-dependent gene expression by increasing mitochondrial oxygen consumption in skeletal muscle cells. *Proc. Natl. Acad. Sci. U. S. A.* *106*, 2188–2193.

De Oliveira, M.R., Nabavi, S.M.F., Manayi, A., Daglia, M., Hajheydari, Z., and Nabavi, S.M.F. (2016). Resveratrol and the mitochondria: From triggering the intrinsic apoptotic pathway to inducing mitochondrial biogenesis, a mechanistic view. *Biochim. Biophys. Acta - Gen. Subj.* *1860*, 727–745.

Orr, A.L., Vargas, L., Turk, C.N., Baaten, J.E., Matzen, J.T., Dardov, V.J., Attle, S.J., Li, J., Quackenbush, D.C., Goncalves, R.L.S., et al. (2015). Suppressors of superoxide production from mitochondrial complex III. *Nat. Chem. Biol.* *11*, 834–836.

Osada-Oka, M., Hashiba, Y., Akiba, S., Imaoka, S., and Sato, T. (2010). Glucose is necessary for stabilization of hypoxia-inducible factor-1alpha under hypoxia: contribution of the pentose phosphate pathway to this stabilization. *FEBS Lett.* *584*, 3073–3079.

De Paepe, B., and Van Coster, R. (2017). A critical assessment of the therapeutic potential of resveratrol supplements for treating mitochondrial disorders. *Nutrients* *9*, 1–10.

Panday, A., Sahoo, M.K., Osorio, D., and Batra, S. (2015). NADPH oxidases: An overview from structure to innate immunity-associated pathologies. *Cell. Mol. Immunol.* *12*, 5–23.

Park, C., and Lee, Y. (2014). Overexpression of ER β is sufficient to inhibit hypoxia-inducible factor-1 transactivation. *Biochem. Biophys. Res. Commun.* *450*, 261–266.

Parrinello, S., Samper, E., Krtolica, A., Goldstein, J., Melov, S., and Campisi, J. (2003). Oxygen sensitivity severely limits the replicative lifespan of murine fibroblasts. *Nat. Cell Biol.* *5*, 741–747.

Patra, K.C., and Hay, N. (2014). The pentose phosphate pathway and cancer. *Trends Biochem. Sci.* *39*, 347–354.

Pavlova, N.N., and Thompson, C.B. (2016). The Emerging Hallmarks of Cancer Metabolism. *Cell Metab.* *23*, 27–47.

Peinado, J.R., Diaz-Ruiz, A., Frühbeck, G., and Malagon, M.M. (2014). Mitochondria in metabolic disease: Getting clues from proteomic studies. *Proteomics* *14*, 452–466.

Pernas, L., and Scorrano, L. (2016). Mito-Morphosis: Mitochondrial Fusion, Fission, and Cristae Remodeling as Key Mediators of Cellular Function. *Annu. Rev. Physiol.* 78, 505–531.

Pettersen, E.O., Larsen, L.H., Ramsing, N.B., and Ebbesen, P. (2005). Pericellular oxygen depletion during ordinary tissue culturing, measured with oxygen microsensors. *Cell Prolif.* 38, 257–267.

Pham, A.N., Xing, G., Miller, C.J., and Waite, T.D. (2013). Fenton-like copper redox chemistry revisited: Hydrogen peroxide and superoxide mediation of copper-catalyzed oxidant production. *J. Catal.* 301, 54–64.

Plauth, A., Geikowski, A., Cichon, S., Wowro, S.J., Liedgens, L., Rousseau, M., Weidner, C., Fuhr, L., Kliem, M., Jenkins, G., et al. (2016). Hormetic shifting of redox environment by pro-oxidative resveratrol protects cells against stress. *Free Radic. Biol. Med.* 99, 608–622.

Poburko, D., Santo-Domingo, J., and Demaurex, N. (2011). Dynamic regulation of the mitochondrial proton gradient during cytosolic calcium elevations. *J. Biol. Chem.* 286, 11672–11684.

Pollard, P.J., Brière, J.J., Alam, N.A., Barwell, J., Barclay, E., Wortham, N.C., Hunt, T., Mitchell, M., Olpin, S., Moat, S.J., et al. (2005). Accumulation of Krebs cycle intermediates and over-expression of HIF1alpha in tumours which result from germline FH and SDH mutations. *Hum. Mol. Genet.* 14, 2231–2239.

Procházková, D., Boušová, I., and Wilhelmová, N. (2011). Antioxidant and prooxidant properties of flavonoids. *Fitoterapia* 82, 513–523.

Psychogios, N., Hau, D.D., Peng, J., Guo, A.C., Mandal, R., Bouatra, S., Sinelnikov, I., Krishnamurthy, R., Eisner, R., Gautam, B., et al. (2011). The human serum metabolome. *PLoS One* 6, e16957.

Quinlan, C.L., Perevoshchikova, I. V., Hey-Mogensen, M., Orr, A.L., and Brand, M.D. (2013). Sites of reactive oxygen species generation by mitochondria oxidizing different substrates. *Redox Biol.* 1, 304–312.

Radi, R. (2013). Peroxynitrite, a stealthy biological oxidant. *J. Biol. Chem.* 288, 26464–26472.

Ray, P.D., Huang, B.-W.W., and Tsuji, Y. (2012). Reactive oxygen species (ROS) homeostasis

and redox regulation in cellular signaling. *Cell. Signal.* *24*, 981–990.

Reczek, C.R., and Chandel, N.S. (2015). ROS-dependent signal transduction. *Curr. Opin. Cell Biol.* *33*, 8–13.

Rezende, F., Brandes, R.P., and Schröder, K. (2018). Detection of Hydrogen Peroxide with Fluorescent Dyes. *Antioxid. Redox Signal.* *29*, 585–602.

Rhee, S.G., Bae, Y.S., Lee, S.R., and Kwon, J. (2000). Hydrogen peroxide: a key messenger that modulates protein phosphorylation through cysteine oxidation. *Sci. STKE* *2000*, pe1.

Rindler, P.M., Cacciola, A., Kinter, M., and Szweda, L.I. (2016). Catalase-dependent H₂O₂ consumption by cardiac mitochondria and redox-mediated loss in insulin signaling. *Am. J. Physiol. Heart Circ. Physiol.* *311*, H1091–H1096.

Robb, E.L., and Stuart, J.A. (2011). Resveratrol interacts with estrogen receptor- β to inhibit cell replicative growth and enhance stress resistance by upregulating mitochondrial superoxide dismutase. *Free Radic. Biol. Med.* *50*, 821–831.

Robb, E.L., and Stuart, J.A. (2014). The stilbenes resveratrol, pterostilbene and piceid affect growth and stress resistance in mammalian cells via a mechanism requiring estrogen receptor beta and the induction of Mn-superoxide dismutase. *Phytochemistry* *98*, 164–173.

Robb, E.L., Winkelmoen, L., Visanji, N., Brotchie, J., and Stuart, J.A. (2008). Dietary resveratrol administration increases MnSOD expression and activity in mouse brain. *Biochem. Biophys. Res. Commun.* *372*, 254–259.

Robb, E.L., Moradi, F., Maddalena, L.A., Valente, A.J.F.F., Fonseca, J., and Stuart, J.A. (2017). Resveratrol stimulates mitochondrial fusion by a mechanism requiring mitofusin-2. *Biochem. Biophys. Res. Commun.* *485*, 249–254.

Rossignol, R., Gilkerson, R., Aggeler, R., Yamagata, K., Remington, S.J., and Capaldi, R.A. (2004a). Energy substrate modulates mitochondrial structures and oxidative capacity in cancer cells. *Cancer Res.* *64*, 985–993.

Rossignol, R., Gilkerson, R., Aggeler, R., Yamagata, K., Remington, S.J., and Capaldi, R.A. (2004b). Energy substrate modulates mitochondrial structure and oxidative capacity in cancer cells. *Cancer Res.* *64*, 985–993.

- Salati, L.M., and Amir-Ahmady, B. (2001). Dietary regulation of expression of glucose-6-phosphate dehydrogenase. *Annu. Rev. Nutr.* 21, 121–140.
- Salvemini, D., Wang, Z.Q., Zweier, J.L., Samouilov, A., Macarthur, H., Misko, T.P., Currie, M.G., Cuzzocrea, S., Sikorski, J.A., and Riley, D.P. (1999). A nonpeptidyl mimic of superoxide dismutase with therapeutic activity in rats. *Science* 286, 304–306.
- Sarsour, E.H., Kalen, A.L., and Goswami, P.C. (2014). Manganese superoxide dismutase regulates a redox cycle within the cell cycle. *Antioxid. Redox Signal.* 20, 1618–1627.
- Saunier, E., Antonio, S., Regazzetti, A., Auzeil, N., Lapr evote, O., Shay, J.W., Coumoul, X., Barouki, R., Benelli, C., Huc, L., et al. (2017). Resveratrol reverses the Warburg effect by targeting the pyruvate dehydrogenase complex in colon cancer cells. *Sci. Rep.* 7, 6945.
- Scarpulla, R.C. (2011). Metabolic control of mitochondrial biogenesis through the PGC-1 family regulatory network. *Biochim. Biophys. Acta* 1813, 1269–1278.
- Schieber, M., and Chandel, N.S. (2014). ROS function in redox signaling and oxidative stress. *Curr. Biol.* 24, R453-62.
- Schilder, Y.D.C., Heiss, E.H., Schachner, D., Ziegler, J., Reznicek, G., Sorescu, D., and Dirsch, V.M. (2009). NADPH oxidases 1 and 4 mediate cellular senescence induced by resveratrol in human endothelial cells. *Free Radic. Biol. Med.* 46, 1598–1606.
- Schito, L., and Semenza, G.L. (2016). Hypoxia-Inducible Factors: Master Regulators of Cancer Progression. *Trends in Cancer* 2, 758–770.
- Schwarzl ander, M., Logan, D.C., Fricker, M.D., and Sweetlove, L.J. (2011). The circularly permuted yellow fluorescent protein cpYFP that has been used as a superoxide probe is highly responsive to pH but not superoxide in mitochondria: implications for the existence of superoxide “flashes”. *Biochem. J.* 437, 381–387.
- Semenza, G.L. (2007). Hypoxia-inducible factor 1 (HIF-1) pathway. *Sci. STKE* 2007, cm8.
- Semenza, G.L. (2011). Regulation of metabolism by hypoxia-inducible factor 1. *Cold Spring Harb. Symp. Quant. Biol.* 76, 347–353.
- Semenza, G.L. (2012). Hypoxia-inducible factors in physiology and medicine. *Cell* 148, 399–408.
- Sen, A., Ren, S., Lerchenm uller, C., Sun, J., Weiss, N., Most, P., and Peppel, K. (2013).

MicroRNA-138 regulates hypoxia-induced endothelial cell dysfunction by targeting S100A1. *PLoS One* 8, e78684.

Sena, L.A., and Chandel, N.S. (2012). Physiological roles of mitochondrial reactive oxygen species. *Mol. Cell* 48, 158–167.

Sergides, C., Chirilă, M., Silvestro, L., Pitta, D., and Pittas, A. (2016). Bioavailability and safety study of resveratrol 500 mg tablets in healthy male and female volunteers. *Exp. Ther. Med.* 11, 164–170.

Shirmanova, M. V., Druzhkova, I.N., Lukina, M.M., Matlashov, M.E., Belousov, V. V., Snopova, L.B., Prodanetz, N.N., Dudenkova, V. V., Lukyanov, S.A., and Zagaynova, E. V. (2015). Intracellular pH imaging in cancer cells in vitro and tumors in vivo using the new genetically encoded sensor SypHer2. *Biochim. Biophys. Acta* 1850, 1905–1911.

Shutt, T., Geoffrion, M., Milne, R., and McBride, H.M. (2012). The intracellular redox state is a core determinant of mitochondrial fusion. *EMBO Rep.* 13, 909–915.

Sies, H. (2017). Hydrogen peroxide as a central redox signaling molecule in physiological oxidative stress: Oxidative eustress. *Redox Biol.* 11, 613–619.

Slade, L., Chalker, J., Kuksal, N., Young, A., Gardiner, D., and Mailloux, R.J. (2017). Examination of the superoxide/hydrogen peroxide forming and quenching potential of mouse liver mitochondria. *Biochim. Biophys. Acta. Gen. Subj.* 1861, 1960–1969.

Smith, R.A., Porteous, C.M., Coulter, C. V, and Murphy, M.P. (1999). Selective targeting of an antioxidant to mitochondria. *Eur. J. Biochem.* 263, 709–716.

Stadtman, E.R., and Levine, R.L. (2000). Protein oxidation. *Ann. N. Y. Acad. Sci.* 899, 191–208.

Stöcker, S., Van Laer, K., Mijuskovic, A., and Dick, T.P. (2018). The Conundrum of Hydrogen Peroxide Signaling and the Emerging Role of Peroxiredoxins as Redox Relay Hubs. *Antioxid. Redox Signal.* 28, 558–573.

Stuart, J.A., and Robb, E.L. (2013). *Bioactive Polyphenols from Wine Grapes* (New York, NY: Springer New York).

Stuart, J.A., Fonseca, J., Moradi, F., Cunningham, C., Seliman, B., Worsfold, C.R., Dolan, S., Abando, J., and Maddalena, L.A. (2018). How Supraphysiological Oxygen Levels in Standard

Cell Culture Affect Oxygen-Consuming Reactions. *Oxid. Med. Cell. Longev.* 2018, 1–13.

Suen, D.-F., Norris, K.L., and Youle, R.J. (2008). Mitochondrial dynamics and apoptosis. *Genes Dev.* 22, 1577–1590.

Sugiyama, N., Barros, R.P.A., Warner, M., and Gustafsson, J.-A. (2010). ERbeta: recent understanding of estrogen signaling. *Trends Endocrinol. Metab.* 21, 545–552.

Suh, Y.A., Arnold, R.S., Lassegue, B., Shi, J., Xu, X., Sorescu, D., Chung, A.B., Griendling, K.K., and Lambeth, J.D. (1999). Cell transformation by the superoxide-generating oxidase Mox1. *Nature* 401, 79–82.

Sundaresan, M., Yu, Z.X., Ferrans, V.J., Irani, K., and Finkel, T. (1995). Requirement for generation of H₂O₂ for platelet-derived growth factor signal transduction. *Science* 270, 296–299.

Szkudelska, K., and Szkudelski, T. (2010). Resveratrol, obesity and diabetes. *Eur. J. Pharmacol.* 635, 1–8.

Taguchi, N., Ishihara, N., Jofuku, A., Oka, T., and Mihara, K. (2007). Mitotic phosphorylation of dynamin-related GTPase Drp1 participates in mitochondrial fission. *J. Biol. Chem.* 282, 11521–11529.

Takac, I., Schröder, K., Zhang, L., Lardy, B., Anilkumar, N., Lambeth, J.D., Shah, A.M., Morel, F., and Brandes, R.P. (2011). The E-loop is involved in hydrogen peroxide formation by the NADPH oxidase Nox4. *J. Biol. Chem.* 286, 13304–13313.

Teshima, Y., Takahashi, N., Nishio, S., Saito, S., Kondo, H., Fukui, A., Aoki, K., Yufu, K., Nakagawa, M., and Saikawa, T. (2014). Production of reactive oxygen species in the diabetic heart. Roles of mitochondria and NADPH oxidase. *Circ. J.* 78, 300–306.

Thomas, C., and Gustafsson, J.-Å. (2011). The different roles of ER subtypes in cancer biology and therapy. *Nat. Rev. Cancer* 11, 597–608.

Timpano, S., Guild, B.D., Specker, E.J., Melanson, G., Medeiros, P.J., Sproul, S.L.J., and Uniacke, J. (2019). Physioxic human cell culture improves viability, metabolism, and mitochondrial morphology while reducing DNA damage. *FASEB J.* fj201802279R.

Tomé-Carneiro, J., Larrosa, M., González-Sarrías, A., Tomás-Barberán, F.A., García-Conesa, M.T., and Espín, J.C. (2013). Resveratrol and clinical trials: the crossroad from in vitro studies to

human evidence. *Curr. Pharm. Des.* 19, 6064–6093.

Tormos, K. V., Anso, E., Hamanaka, R.B., Eisenbart, J., Joseph, J., Kalyanaraman, B., and Chandel, N.S. (2011). Mitochondrial complex III ROS regulate adipocyte differentiation. *Cell Metab.* 14, 537–544.

Torrence, M.E., and Manning, B.D. (2018). Nutrient Sensing in Cancer. *Annu. Rev. Cancer Biol.* 2, 251–269.

Truong, V.-L., Jun, M., and Jeong, W.-S. (2018). Role of resveratrol in regulation of cellular defense systems against oxidative stress. *Biofactors* 44, 36–49.

Turrens, J.F., Alexandre, A., and Lehninger, A.L. (1985). Ubisemiquinone is the electron donor for superoxide formation by complex III of heart mitochondria. *Arch. Biochem. Biophys.* 237, 408–414.

Ungvari, Z., Bagi, Z., Feher, A., Recchia, F.A., Sonntag, W.E., Pearson, K., de Cabo, R., and Csiszar, A. (2010). Resveratrol confers endothelial protection via activation of the antioxidant transcription factor Nrf2. *Am. J. Physiol. Heart Circ. Physiol.* 299, H18-24.

Valente, A.J., Maddalena, L.A., Robb, E.L., Moradi, F., and Stuart, J.A. (2017). A simple ImageJ macro tool for analyzing mitochondrial network morphology in mammalian cell culture. *Acta Histochem.* 119, 315–326.

Venditti, P., Di Stefano, L., and Di Meo, S. (2013). Mitochondrial metabolism of reactive oxygen species. *Mitochondrion* 13, 71–82.

Vitaglione, P., Sforza, S., Galaverna, G., Ghidini, C., Caporaso, N., Vescovi, P.P., Fogliano, V., and Marchelli, R. (2005). Bioavailability of trans-resveratrol from red wine in humans. *Mol. Nutr. Food Res.* 49, 495–504.

Vande Voorde, J., Ackermann, T., Pfetzer, N., Sumpton, D., Mackay, G., Kalna, G., Nixon, C., Blyth, K., Gottlieb, E., and Tardito, S. (2019). Improving the metabolic fidelity of cancer models with a physiological cell culture medium. *Sci. Adv.* 5, eaau7314.

Votyakova, T. V., and Reynolds, I.J. (2004). Detection of hydrogen peroxide with Amplex Red: Interference by NADH and reduced glutathione auto-oxidation. *Arch. Biochem. Biophys.* 431, 138–144.

- Walle, T., Hsieh, F., Delegge, M.H., Oatis, J.E., and Walle, U.K. (2004). High absorption but very low bioavailability of oral resveratrol in humans. *Drug Metab. Dispos.* 32, 1377–1382.
- Warburg, O. (1956). On the origin of cancer cells. *Science* 123, 309–314.
- Ward, P.S., and Thompson, C.B. (2012). Metabolic reprogramming: a cancer hallmark even warburg did not anticipate. *Cancer Cell* 21, 297–308.
- Weidinger, A., and Kozlov, A. V. (2015). Biological Activities of Reactive Oxygen and Nitrogen Species: Oxidative Stress versus Signal Transduction. *Biomolecules* 5, 472–484.
- Wenger, R.H., Kurtcuoglu, V., Scholz, C.C., Marti, H.H., and Hoogewijs, D. (2015). Frequently asked questions in hypoxia research. *Hypoxia* 3, 35–43.
- Wenzel, E., and Somoza, V. (2005). Metabolism and bioavailability of trans-resveratrol. *Mol. Nutr. Food Res.* 49, 472–481.
- Weydert, C.J., and Cullen, J.J. (2010). Measurement of superoxide dismutase, catalase and glutathione peroxidase in cultured cells and tissue. *Nat. Protoc.* 5, 51–66.
- Willems, P.H.G.M., Rossignol, R., Dieteren, C.E.J., Murphy, M.P., and Koopman, W.J.H. (2015). Redox Homeostasis and Mitochondrial Dynamics. *Cell Metab.* 22, 207–218.
- Winterbourn, C.C. (1995). Toxicity of iron and hydrogen peroxide: the Fenton reaction. *Toxicol. Lett.* 82–83, 969–974.
- Winterbourn, C.C. (2013). The biological chemistry of hydrogen peroxide. *Methods Enzymol.* 528, 3–25.
- Wood, Z.A., Schröder, E., Robin Harris, J., and Poole, L.B. (2003). Structure, mechanism and regulation of peroxiredoxins. *Trends Biochem. Sci.* 28, 32–40.
- Wu, J.M., and Hsieh, T. (2011). Resveratrol: a cardioprotective substance. *Ann. N. Y. Acad. Sci.* 1215, 16–21.
- Wu, Z., Liu, B., E, C., Liu, J.J., Zhang, Q., Liu, J.J., Chen, N., Chen, R., and Zhu, R. (2015). Resveratrol inhibits the proliferation of human melanoma cells by inducing G1/S cell cycle arrest and apoptosis. *Mol. Med. Rep.* 11, 400–404.
- Xia, N., Förstermann, U., and Li, H. (2014). Resveratrol and endothelial nitric oxide. *Molecules* 19, 16102–16121.

- Xia, Y., Tsai, A.L., Berka, V., and Zweier, J.L. (1998). Superoxide generation from endothelial nitric-oxide synthase. A Ca²⁺/calmodulin-dependent and tetrahydrobiopterin regulatory process. *J. Biol. Chem.* *273*, 25804–25808.
- Xie, L., Pi, X., Mishra, A., Fong, G., Peng, J., and Patterson, C. (2012). PHD3-dependent hydroxylation of HCLK2 promotes the DNA damage response. *J. Clin. Invest.* *122*, 2827–2836.
- Yamaguchi, J., Nishiyama, S., Shimanuki, M., Ono, T., Sato, A., Nakada, K., Hayashi, J.-I., Yonekawa, H., and Shitara, H. (2012). Comprehensive application of an mtDsRed2-Tg mouse strain for mitochondrial imaging. *Transgenic Res.* *21*, 439–447.
- Yan, Q., Bartz, S., Mao, M., Li, L., and Kaelin, W.G. (2007). The hypoxia-inducible factor 2 α N-terminal and C-terminal transactivation domains cooperate to promote renal tumorigenesis in vivo. *Mol. Cell. Biol.* *27*, 2092–2102.
- Yang, Z.-F., Drumea, K., Mott, S., Wang, J., and Rosmarin, A.G. (2014). GABP transcription factor (nuclear respiratory factor 2) is required for mitochondrial biogenesis. *Mol. Cell. Biol.* *34*, 3194–3201.
- Yao, T., and Asayama, Y. (2017). Animal-cell culture media: History, characteristics, and current issues. *Reprod. Med. Biol.* *16*, 99–117.
- Yao, M., Gao, F., Wang, X., Shi, Y., Liu, S., and Duan, H. (2017). Nox4 is involved in high glucose-induced apoptosis in renal tubular epithelial cells via Notch pathway. *Mol. Med. Rep.* *15*, 4319–4325.
- Youle, R.J., and van der Bliek, A.M. (2012). Mitochondrial fission, fusion, and stress. *Science* *337*, 1062–1065.
- Yu, X.-D., Yang, J., Zhang, W.-L., and Liu, D.-X. (2016). Resveratrol inhibits oral squamous cell carcinoma through induction of apoptosis and G2/M phase cell cycle arrest. *Tumor Biol.* *37*, 2871–2877.
- Żamojć, K., Zdrowowicz, M., Jacewicz, D., Wyrzykowski, D., and Chmurzyński, L. (2016). Fluorescent Probes Used for Detection of Hydrogen Peroxide under Biological Conditions. *Crit. Rev. Anal. Chem.* *46*, 171–200.
- Zhang, J., Pavlova, N.N., and Thompson, C.B. (2017). Cancer cell metabolism: the essential role

of the nonessential amino acid, glutamine. *EMBO J.* 36, 1302–1315.

Zhang, L., Pang, S., Deng, B., Qian, L., Chen, J., Zou, J., Zheng, J., Yang, L., Zhang, C., Chen, X., et al. (2012). High glucose induces renal mesangial cell proliferation and fibronectin expression through JNK/NF- κ B/NADPH oxidase/ROS pathway, which is inhibited by resveratrol. *Int. J. Biochem. Cell Biol.* 44, 629–638.

Zhang, M., Li, W., Yu, L., and Wu, S. (2014). The suppressive effect of resveratrol on HIF-1 α and VEGF expression after warm ischemia and reperfusion in rat liver. *PLoS One* 9, e109589.

Zhang, Q., Tang, X., Lu, Q.Y., Zhang, Z.F., Brown, J., and Le, A.D. (2005). Resveratrol inhibits hypoxia-induced accumulation of hypoxia-inducible factor-1 α and VEGF expression in human tongue squamous cell carcinoma and hepatoma cells. *Mol. Cancer Ther.* 4, 1465–1474.

Zhou, M., Diwu, Z., Panchuk-Voloshina, N., and Haugland, R.P. (1997). A stable nonfluorescent derivative of resorufin for the fluorometric determination of trace hydrogen peroxide: applications in detecting the activity of phagocyte NADPH oxidase and other oxidases. *Anal. Biochem.* 253, 162–168.

Zhou, X., Chen, M., Zeng, X., Yang, J., Deng, H., Yi, L., and Mi, M.T. (2014). Resveratrol regulates mitochondrial reactive oxygen species homeostasis through Sirt3 signaling pathway in human vascular endothelial cells. *Cell Death Dis.* 5, 1–13.

Zielonka, J., Hardy, M., Michalski, R., Sikora, A., Zielonka, M., Cheng, G., Ouari, O., Podsiadły, R., and Kalyanaraman, B. (2017). Recent Developments in the Probes and Assays for Measurement of the Activity of NADPH Oxidases. *Cell Biochem. Biophys.* 75, 335–349.

Züchner, S., Mersiyanova, I. V., Muglia, M., Bissar-Tadmouri, N., Rochelle, J., Dadali, E.L., Zappia, M., Nelis, E., Patitucci, A., Senderek, J., et al. (2004). Mutations in the mitochondrial GTPase mitofusin 2 cause Charcot-Marie-Tooth neuropathy type 2A. *Nat. Genet.* 36, 449–451.